

**NOVEL CARRIER PROTEIN FOR AN
ANTI-INFLUENZA THERAPEUTIC**

**DEVELOPMENT OF AN ELASTIN-LIKE POLYPEPTIDE
CARRIER FOR AN INFLUENZA VIRUS ANTIVIRAL
PEPTIDE**

By ZACHARIAH C. SCINOCCA, B.Sc.

A Thesis Submitted to the School of Graduate Studies in Partial
Fulfillment of the Requirements for the Degree Master of Science

DESCRIPTIVE NOTE

McMaster University MASTER OF SCIENCE (2017) Hamilton, Ontario (Medical Sciences)

TITLE: Development of an Elastin-Like Polypeptide Carrier for an Influenza Virus Antiviral Peptide

AUTHOR: Zachariah C. Scinocca, B.Sc. (University of Western Ontario)

SUPERVISOR: Dr. James Mahony

NUMBER OF PAGES: xx, 125

LAY ABSTRACT

The influenza virus causes seasonal outbreaks each year and can have life-threatening symptoms in the young and elderly. In addition, it can rapidly mutate through antigenic drift; therefore, a new vaccine is required each year. Pandemic influenza strains can enter the population when the virus undergoes genetic reassortment by antigenic shift. However, it can take a significant amount of time to formulate a vaccine against pandemic influenzas, which means antiviral drugs are often used as the first line of defense. New antivirals to treat influenza must be developed because resistance to the current influenza antivirals has steadily increased. In this work, we developed an antiviral peptide to disrupt a critical interaction in the influenza RNA-dependent RNA polymerase and inhibit virus replication. This peptide was previously conjugated to an *E. coli* MBP carrier protein, which would likely not be compatible *in vivo*. This thesis focused on attaching the antiviral peptide to an elastin-like polypeptide protein, which mimics human tropoelastin, and should be non-immunogenic in humans.

ABSTRACT

Background: Despite the availability of a yearly vaccine and antivirals, the incidence of influenza infections remains high. The genome of the influenza virus can mutate rapidly, therefore novel influenza strains that may be resistant to the current vaccine or antivirals frequently enter the population. Because of the long production time necessary to produce a vaccine, new antivirals must be created to combat early stages of influenza outbreaks. The most effective antivirals will target a highly conserved and essential stage of virus replication. The influenza RNA-dependent RNA polymerase is a heterotrimeric complex composed of three subunits: PA, PB1, and PB2. The three components of the polymerase interact through well-defined domains and are essential for viral replication. Previously, influenza replication has been inhibited using a small synthetic peptide that mimics the interaction domain between PA and PB1 and inhibits the formation of the heterotrimeric complex.

Problem and Hypothesis: Although the peptide could inhibit influenza replication, synthetic peptides are costly to produce and are not a viable option for large-scale production. This problem can often be overcome by attaching the peptide to a highly soluble carrier protein. We hypothesize that influenza replication can be inhibited by attaching a peptide, that mimics the binding domain between the PA and PB1 subunits, to a human elastin-like polypeptide (ELP) carrier protein.

Methods and Results: The peptide and a nuclear localization sequence was genetically linked to a maltose binding protein (MBP) or ELP carrier protein. The MBP construct was purified by affinity chromatography using FPLC. A high yield of the ELP

construct was obtained using inverse transition cycling, a method unique to ELPs because of their temperature-dependent solubility. The ELP construct was designed to be soluble at physiological temperature to limit cellular toxicity due to protein aggregation. The cytotoxicity of the ELP construct was assessed by monitoring the growth of A549 cells, a human lung epithelial cell line. The ELP construct did not have any adverse effects on A549 cell growth. Both constructs could localize to cell nuclei using their respective nuclear localization sequences and could also interact with the PA subunit, demonstrating their potential to inhibit influenza replication. Despite this, only the MBP construct was able to inhibit the replication of influenza. The MBP construct could inhibit the replication of both the H1N1 and H3N2 subtypes of influenza, indicating the recombinant protein had cross-strain activity.

Conclusion: Linking a small peptide to carrier protein can result in high protein yields, however a carrier protein must be chosen that will maintain the peptides' therapeutic activity. In this study, a small anti-influenza peptide inhibited influenza replication when attached to an MBP carrier protein, however was not able to inhibit influenza replication when attached to an ELP carrier protein. Although the peptide was ineffective when attached to this particular ELP carrier protein, different ELP proteins of various lengths and compositions may still be effective carrier proteins for an antiviral peptide.

ACKNOWLEDGMENTS

Firstly, I would like to thank my supervisor Dr. Mahony for his guidance and leadership throughout my time in his lab. You have provided me with a tremendous amount of mentorship and have aided me in my ability to critically analyze each and every situation. You have provided me with knowledge that will help me not only in my future academic endeavours, but in life as well. I would also like to thank my committee members, Dr. Ali Ashkar and Dr. Martin Stampfli. Your knowledgeable insights have allowed me to enhance my research abilities and you challenged me to strive to become a more curious and well-rounded scientist. Your diverse academic backgrounds have allowed me to think about the “bigger picture” and the possible meaning of every result.

Every member of the lab also helped me along the way, each of them with their own unique talents and knowledge base. Not only are you all extremely smart individuals, but you also provided a positive, fun, and unique environment for me to conduct my studies in. Dr. David Bulir’s method of teaching continually made me strive to increase my knowledge set and your passion for science is truly amazing. Dr. Christopher Stone has helped me tremendously throughout my project and has always seemed to have a good answer to any problem I had. I greatly appreciate Sylvia Chong always willing to chat about science, baseball, or our inability to inform her of any lab supplies running out. I would also like to thank fellow students Samantha Mihalco, Christopher Chiang, Steven Liang, and Jordan Nelson. We all shared many great laughs, coffee runs, and discussions about science and life. I would also like to thank all other members of the lab who have made my experience as enjoyable as it was: Jodi Gilchrist, Dan Jang, Kathy Luinstra, Lucas Penny, Steven

Zhang, Karanbir Brar, Kimberly Lau, Heather Gunter, and Albert Choe. You all have my deepest gratitude.

Finally, I would like to thank my family and friends who have believed in me throughout my degree. Everyone around me has shown me nothing but support and respect as I tried to reach my goals. My father and mother, Paul and Vicky, and my girlfriend, Cayla, have encouraged me and been extremely positive even when times were toughest. You are all role models and I am happy to have you all around me as I enter the next chapter in my life.

*This thesis is dedicated to my father and mother, Paul and Vicky, and my girlfriend,
Cayla*

TABLE OF CONTENTS

List of Abbreviations.....	XIV
List of Figures.....	XVII
List of Tables.....	XIX
Declaration of Academic Achievement.....	XX
Chapter 1 – Background and Objective.....	1
1.1 Influenza History and Overview.....	2
1.2 Clinical Presentation and Past Pandemics.....	3
1.3 Influenza Taxonomy and Nomenclature.....	7
1.4 Influenza Structure and Genome.....	8
1.5 Influenza Replication and Life Cycle.....	10
1.6.1 Current Preventative Influenza Measures – Vaccines.....	18
1.6.2 Current Preventative Influenza Measures – Antivirals.....	21
1.7 Immune Avoidance by Antigenic Drift and Shift.....	23
1.8 The Influenza RNA-Dependent RNA Polymerase Complex as a Drug Target.....	25
1.9 Small Peptides as Dominant Negatives Therapeutics.....	30
1.10 The Elastin Like Polypeptide Class of Protein Carriers.....	32
1.11 Thesis Objectives.....	35
Chapter 2 – Materials and Methods.....	37
2.1 Genetic Techniques	
2.1.1 Genetic Cloning and Design of Expression Constructs Using the Invitrogen Gateway Cloning System.....	38

2.1.2 Genetic Cloning and Design of Expression Constructs Using Recursive Directional Ligation.....	39
2.1.3 Primer Resuspension and Polymerase Chain Reaction.....	40
2.1.4 Quantification and Agarose Gel Electrophoresis of DNA.....	41
2.2 <i>Escherichia coli</i> Transformation	
2.2.1 Preparation of Chemically Competent <i>E. coli</i>	42
2.2.2 Transformation of Chemically Competent <i>E. coli</i>	42
2.3 Protein Purification Techniques	
2.3.1 Hexa-histidine Tagged Recombinant Protein Expression and Affinity Purification.....	43
2.3.2 Purification of Elastin-Like Polypeptide Fusion Constructs.....	45
2.4 Protein Analysis	
2.4.1 Gel Electrophoresis of Protein Samples.....	46
2.4.2 Assessment of Protein Purity Using Coomassie, Zinc Sulphate, and Ponceau S Red Staining.....	47
2.4.3 Western Blotting.....	48
2.4.4 Quantification of Protein Samples.....	49
2.4.5 Protein Sample Concentration using TCA Precipitation.....	49
2.4.6 Thermal Characterization of ELP Fusion Constructs.....	50
2.5 Cell Culture Techniques	
2.5.1 Cell Culture Seeding and Passaging.....	50
2.5.2 Cell Culture Cryopreservation and Thawing.....	51
2.6 Influenza Handling	
2.6.1 Influenza Propagation.....	52
2.6.2 Influenza Titering Using Plaque Assays.....	53

2.7 Recombinant Protein Analysis	
2.7.1 Assessing Protein Toxicity with a A549 Growth Assays.....	54
2.7.2 Assessing Protein Uptake Using Nuclear Localization Assays.....	55
2.7.3 Assessing Protein Interaction Using GST Pull-Down Assays.....	56
2.8 Viral Inhibition Assay Using Fluorescence Microscopy.....	57
2.9 Statistical Methods.....	58
Chapter 3 – Results.....	59
3.1 Recombinant Protein Design, Cloning, and Analysis	
3.1.1 Design of the Recombinant Proteins.....	60
3.1.2 Cloning of the PB1-Elastin-like Polypeptide Fusion Protein Using RDL.....	62
3.1.3 Expression and Purification of Hexahistidine Tagged Proteins	64
3.1.4 Expression and Purification of Elastin-like Polypeptide Fusion Proteins	65
3.1.5 Thermal Characterization of Elastin-like Polypeptide Fusion Proteins.....	68
3.2 The Elastin-like Polypeptide Fusion Protein Does Not Affect A549 Cell Replication.....	70
3.3 The ELP and HisMBP Fusion Proteins Localize Primarily into the Nucleus of Two Different Cell Types.....	72
3.4 The ELP and HisMBP Fusion Proteins Interact with the C-terminal Portion of the Influenza PA Protein.....	74
3.5.1 Inhibition of Influenza A H3N2 Replication by the HisMBP Fusion Protein but Not the ELP Fusion Protein.....	76

3.5.2 Inhibition of Influenza A H3N2 Replication by the HisMBP Fusion Protein but Not the ELP Fusion Protein	78
Chapter 4 – Discussion and Future Directions.....	81
4.1 Recombinant Protein Analysis	
4.1.1 Design, Synthesis, and Purification of Elastin-like Polypeptide Proteins.....	82
4.1.2 The Transition Temperature of the Recombinant Elastin-like Polypeptides.....	84
4.1.3 Assessing the Recombinant Elastin like Polypeptide Toxicity.....	85
4.2 Recombinant Protein Influenza Inhibition Potential	
4.2.1 Recombinant Proteins Mechanism of Inhibition - CPPs.....	87
4.2.2 Recombinant Proteins Mechanism of Inhibition – PA and PB1 Subunit Interaction.....	90
4.2.3 Influenza Inhibition Using the Recombinant Proteins.....	91
4.3 Future Directions	
4.3.1 Future Objective: Modification of the ELP Carrier.....	93
4.3.2 Future Objective: Subcellular Localization of the Recombinant Proteins.....	94
4.3.3 Future Objective: Other Human Specific Carriers.....	96
4.3.4 Future Objective: Delivery of the Recombinant Proteins.....	97
4.4 Influenza Global Burden, the Need for New Therapeutics, and Closing Remarks.....	99
Chapter 5 – References.....	100

Chapter 6 – Appendix	119
6.1 Supplementary Figures.....	120
6.2 Supplementary Tables.....	124

LIST OF ABBREVIATIONS

- APS** – Ammonium Persulfate
- BSA** – Bovine Serum Albumin
- CCP** – Clathrin-Coated Pit
- CPP** – Cell Penetrating Peptide
- cRNA** – Complementary RNA
- ddH₂O** – Double Distilled Water
- DMEM** – Dulbecco's Modified Eagle Medium
- DMSO** – Dimethyl Sulfoxide
- EDTA** – Ethylenediaminetetraacetic Acid
- ELP** – Elastin-like Polypeptide
- FBS** – Fetal Bovine Serum
- FITC** – Fluorescein Isothiocyanate
- GST** – Glutathione S-Transferase
- HA** – Hemagglutinin
- HELP** – Human Elastin-like Polymers
- HPAI** – Highly Pathogenic Avian Influenza
- HSA** – Human Serum Albumin
- hTrx** – Human Thioredoxin
- IFN- β** – Interferon Beta
- IPTG** – Isopropyl β -D-1-Thiogalactopyranoside
- ITC** – Inverse Transition Cycling
- iTEP** – Immune Tolerant Elastin-like Polypeptide
- LB** – Luria Bertani Media
- LDAO** – N,N-Dimethyldodecylamine N-Oxide
- M1** – Matrix Protein 1

M2 – Matrix Protein 2

MBP – Maltose-Binding Protein

MDCK – Madin-Darby Canine Kidney

mRNA – Messenger RNA

NA – Neuraminidase

NAI – Neuraminidase Inhibitor

NLS – Nuclear Localization Sequence

NP – Nucleoprotein

NS – Non-Structural Protein

OD – Optical Density

PA – Polymerase Acidic

PB1 – Polymerase Basic 1

PB2 – Polymerase Basic 2

PBS – Phosphate Buffered Saline

PMSF – Phenylmethylsulfonyl Fluoride

RDL – Recursive Directional Ligation

RdRp – RNA-Dependent RNA Polymerase

RNP – Ribonucleoprotein

RPM – Revolutions per Minute

SALP – Synthetic Anti-Lipopolysaccharide Peptide

SA α 2,6/3Gal – Sialic Acid α 2,6/3-Galactose

SDS – Sodium Dodecyl Sulfate

SDS-PAGE – Sodium Dodecyl Sulfate Polyacrylamide Gel Electrophoresis

SOC – Super Optimal Broth with Catabolite Repression

Tat – Transactivator of Transcription Cell Penetrating Peptide

TCA – Trichloroacetic acid

TEMED – Tetramethylethylenediamine

TPCK – N-Tosyl-L-Phenylalanylchloromethyl Ketone

T_t – Transition Temperature

vRNA – Viral RNA

x g – Centrifugal Force

LIST OF FIGURES

FIGURE 1.1 Influenza A Virus Structure

FIGURE 1.2 Influenza A Replication Cycle

FIGURE 1.3 Overview of the Influenza Heterotrimeric RNA-Dependent RNA Polymerase and Key Interactions

FIGURE 1.4 Interaction Between the RdRp PA C-terminus and the PB1 N-terminus

FIGURE 1.5 ClustalW Alignment of the First 50 Amino Acids of PB1 of Various Influenza A Strains

FIGURE 3.1 Structure of Recombinant Proteins Used in This Study

FIGURE 3.2 Library of ELP[A0.2] Containing 5, 10, 20, and 40 Repeats

FIGURE 3.3 Purification and Buffer Exchange Chromatogram for HisMBP-NLS-PB1

FIGURE 3.4 Precipitation of T6R-NLS-ELP[A0.2]₄₀ Using NaCl During Inverse Transition Cycling Purification

FIGURE 3.5 Purity of the T6R-NLS-ELP[A0.2]₄₀ After Each Round of Inverse Transition Cycling

FIGURE 3.6 Thermal Characterization of T6R-NLS-ELP[A0.2]₄₀ Using Temperature Regulated Turbidimetry

FIGURE 3.7 Growth of A549 cells in presence of T6R-NLS-ELP[A0.2]₄₀

FIGURE 3.8 Nuclear Localization of the HisMBP-NLS-PB1 and T6R-NLS-His-Tev-ELP[A0.2]₄₀ in LLC-MK2 Cells and MDCK Cells

FIGURE 3.9 The HisMBP-NLS-PB1 and T6R-NLS-His-Tev-NLS-ELP[A0.2]₄₀ Proteins Can Interact with the PA Portion of the Influenza Polymerase Complex

FIGURE 3.10 Inhibition of Influenza H3N2 Replication Using the HisMBP-NLS-PB1 and T6R-NLS-His-Tev-ELP[A0.2]₄₀ Proteins

FIGURE 3.11 Inhibition of Influenza H1N1 Replication Using the HisMBP-NLS-PB1 and T6R-NLS-His-Tev-ELP[A0.2]₄₀ Proteins

FIGURE 4.1 Proposed Models of the Interaction Between the Influenza RdRp

SUPPLEMENTARY FIGURE 6.1 Zhorov Molecular Modelling to Predict Low Energy Binding Mutants at PB1 Position Number 6

SUPPLEMENTARY FIGURE 6.2 Overview of the Recursive Directional Ligation Process

SUPPLEMENTARY FIGURE 6.3 Overview of the Inverse Transition Cycling Method to Purify ELP Proteins

SUPPLEMENTARY FIGURE 6.4 Growth of MDCK cells in presence of HisMBP-NLS-PB1

LIST OF TABLES

SUPPLEMENTARY TABLE 6.1 List of All Primers Used in This Study

SUPPLEMENTARY TABLE 6.2 Expression Strains Used in This Study

DECLARATION OF ACADEMIC ACHIEVEMENT

Zachariah C. Scinocca performed all experiments described in this thesis except for the following:

1. The ClustalW alignment of PB1 seen in **Figure 1.5** was performed by Kenneth Mwawasi
2. Cloning of the HisMBP-NLS-PB1 and GST-PA_{c(257-716)} constructs was performed by Kenneth Mwawasi. Cloning of the HisMBP-NLS-PB2 construct was performed by Steven Liang

Chapter 1 – Background and Objectives

BACKGROUND AND OBJECTIVES

1.1 Influenza History and Overview

Although the influenza virus has been extensively studied and vaccinations are available, it remains prevalent, affecting 3 to 5 million people each year (World Health Organization, 2016). Despite the influenza vaccine being free to most individuals in Canada, the virus still represents a significant economic burden. It was estimated that the seasonal strain of influenza in 2003 resulted in 610,660 years of life lost and cost 87.1 billion dollars, in the USA alone (Molinari et al., 2007). In addition to seasonal influenza, which rapidly changes its genetic makeup, sporadic outbreaks of highly pathogenic strains of influenza can emerge. The emergence of pathogenic influenza strains may lead to epidemics with increased mortality rates. Because influenza viruses also circulate in animal populations, some strains can be zoonotic and pose a threat to the population. Recently, there has been an increase in the incidence of highly pathogenic avian influenza (HPAI), likely due to growing numbers of livestock bred for consumption (Peiris, de Jong, & Guan, 2007). Although still infrequent, outbreaks of HPAI in humans have resulted in an estimated mortality rate of 15 – 60%; this is very high considering the mortality rates of previous human influenza pandemics ranged from 0.1 – 2.5% (Li et al. 2008). Although global surveillance programs have been put in place to track influenza progression (World Health Organization, 2014), novel strains still enter the population. Therefore, more effective therapeutics must be discovered to decrease mortality associated with influenza infection.

The influenza virus may have been reported as early as 412 BC, when symptoms consistent with influenza infections were described by Hippocrates (Ghendon, 1994). The name influenza is of Italian origin and is derived from the observation that symptoms were thought to be due to the “influence” of the stars and heavenly bodies (Fleming, Van Der Velden, & Paget, 2003). In 1892, the bacteria *Bacillus influenzae* (later renamed *Haemophilus influenzae*) was first isolated and it was widely believed to be responsible for all symptoms now associated with influenza virus infection (Turk, 1984). This bacteria was believed to cause influenza symptoms until 1921, when symptoms were instead associated with a non-filterable anaerobic organism (Olitsky & Gates, 1921). In 1933, human influenza was isolated, and after being filtered through a bacteria-impermeable membrane it was still able to cause influenza-like diseases in ferrets (Smith, Andrewes, & Laidlaw, 1933). This further established the viral origin of influenza symptoms. Influenza viruses had been previously isolated, when in 1901 a virus was determined to be the causative agent of fowl plague (HPAI) (Lupiani & Reddy, 2009). However, it was not until 1955 that the human and avian virus were determined to be of common *Influenza A* origin (Lupiani & Reddy, 2009). Soon after their isolation, it was discovered that influenza viruses could be passaged to high titres in chicken eggs. Based on this, work began on a vaccine in the late 1930s. The first vaccine for influenza was formulated by Jonas Salk and Thomas Francis and tested on WWII soldiers throughout the 1940s (Salk, Menke, & Francis, 1945).

1.2 Clinical Presentation and Past Pandemics

Influenza is an acute respiratory virus associated with symptoms similar to the common cold, including: fever, cough, muscle and joint pain, sore throat, malaise, and

runny nose (World Health Organization, 2016). Influenza can spread through direct-contact, large respiratory droplets that settle rapidly, and small droplet nuclei that are thought to remain aerosolized for long periods of time (Cowling et al., 2013). Aerosolized influenza is thought to account for up to 50% of the transmission events and therefore surface sterilization may not control its spread (Cowling et al., 2013). Influenza infects the epithelial cells of the respiratory tract, and its deposition in the upper or lower tract is directly related to the aerosol droplet size and presence of the correct sialic acid moiety on the alveolar epithelium (Tellier, 2006). The incubation period for influenza typically ranges from 1 to 4 days (with 2 being the most common) and virus shedding can begin before the onset of clinical symptoms; both these factors leads to the rapid spread of the virus (Carrat et al., 2008). Individuals infected with influenza may continue to shed virus beyond 7 days post infection (Leekha et al., 2007). Common complications of influenza infections include: sinus and ear infections, viral pneumonia, secondary bacterial pneumonia, severe inflammation, sepsis, and asthma attacks (Centers for Disease Control and Prevention, 2016a).

Seasonal influenza typically has the most severe impact on the young and the elderly; however, this is not always true of pandemic influenzas. This was evident during the second wave of the 1918 Spanish flu as the largest impact was on individuals aged 25-29 (Nguyen-Van-Tam, 2003). Outbreaks of potentially pathogenic influenza strains with will happen sporadically, which can result in major pandemics. There has been four major influenza pandemics in the past century: the Spanish flu (1918), the Asian flu (1957), the Hong Kong flu (1968), and most recently the H1N1 swine flu pandemic (2009). Major

pandemics of influenza have been reported for at least 500 years and there is often 3-4 pandemics each century (Taubenberger & Morens, 2010).

The most notable influenza pandemic is the 1918 H1N1 Spanish flu, which became widespread near the end of WWI. Recent evidence suggests it claimed over 50 million lives, which is more than the war itself, in the two years it was most prevalent (Johnson & Mueller, 2002). The origin of the influenza strain responsible for this pandemic has been greatly debated; however, many people agree that the pandemic did not start in Spain (Barry, 2004). It is widely believed the name likely originated because of the freedom of the Spanish press due to their neutrality in WWI, which led to their early coverage of the disease (Trilla, Trilla, & Daer, 2008). This virus had the highest mortality rate in young adults as the elderly likely had some cross-protection from being exposed to an H1N1 influenza strain during their childhood. (Worobey, Han, & Rambaut, 2014).

In 1957, a novel H2N2 influenza virus emerged in China and quickly spread throughout the rest of Asia. A human H1N1 virus had acquired the hemagglutinin (HA), neuraminidase (NA), and the polymerase basic 1 (PB1) genes from an avian H2N2 influenza strain through antigenic shift, resulting in the recombinant H2N2 virus (Lindstrom, Cox, & Klimov, 2004). The response to the H2N2 virus was rapid and a vaccine was being distributed by late 1957; however, the vaccine was only 53 – 60% effective and only limited amounts were available, with most doses being distributed after the peak of the pandemic (Henderson, Courtney, Inglesby, Toner, & Nuzzo, 2009). Shortly after the Asian flu outbreak, another genetic shift occurred between the circulating H2N2 virus and an avian H3 virus. The H2N2 virus received the avian HA and PB1 genes, which

resulted in a recombinant H3N2 virus (Lindstrom et al., 2004). The Hong Kong flu was generally believed to be milder than the Asian flu, likely due to some residual immunity to the NA subtype (Viboud, Grais, Lafont, Miller, & Simonsen, 2005). Overall, the death tolls of the Asian flu and Hong Kong flu were predicted to be approximately 1.5 million and 1 million respectively (Gatherer, 2009).

In 2009, an H1N1 strain of influenza arose from antigenic shift between swine and avian-like swine lineages of influenza virus. The swine virus was already a triple-reassortant virus containing genes of human, swine, and avian origin (Neumann, Noda, & Kawaoka, 2009). The high hospitalization rate and intensive care requirements needed for patients who contracted this virus suggested that the virus may be very severe (Kumar et al., 2009). Initially the 2009 H1N1 virus was also thought to be genetically similar to the 1918 Spanish flu. However, the virus was different in many ways including having a truncated PB1-F2 protein and no lysine present at position 627 of the polymerase basic 2 (PB2) protein, which are key determinants of host range and pathogenicity (Garten et al., 2009). Although the mortality attributed to this outbreak was fairly low (151,700 - 575,400), the impact of this virus was high due to an increased number of years of life lost (Centers for Disease Control and Prevention, 2012). The increase in years of life lost was due to the uncharacteristically low average age of patients who died due to the virus (Viboud, Miller, Olson, Osterholm, & Simonsen, 2010). The initial reports of the severity of the 2009 H1N1 virus were incorrect, however the threat of an influenza pandemic once again became the forefront of public knowledge.

1.3 Influenza Taxonomy and Nomenclature

Influenza viruses are negative-sense, single-stranded, segmented RNA viruses belonging to the family *Orthomyxoviridae* (Cox & Subbarao, 2000; Zambon, 2001). All members of the *Orthomyxoviridae* family contain host-derived lipid-envelopes (King, Adams, Carsten, & Lefkowitz, 2012). The *Orthomyxoviridae* family contains three genera of influenza viruses; namely, *Influenza A*, *Influenza B*, and *Influenza C*. Although each of these virus types can infect humans, it is believed that only *Influenza A* can cause serious pandemics because it has successfully established itself in animal reservoirs (Zambon, 2001). *Influenza B* and *C* have been isolated from other mammalian hosts, such as seals and swine; however, these hosts likely can not sustain influenza infection and therefore are not an animal reservoir. Influenza viruses are classified in to their respective genera based on antigenic variation in their nucleoproteins (NP) and matrix proteins (M1) (Noda, 2011).

Influenza A is typically classified based on two surface proteins, HA and NA, that are required for viral uptake and progeny release, respectively (Green et al., 1982; Gubareva, Kaiser, & Hayden, 2000). With the recent discovery of two unique *Influenza A* virus types in bats, there are now 18 known types of HA and 11 types of NA (Wu, Wu, Tefsen, Shi, & Gao, 2014). Excluding the two bat-specific HA and NA proteins, all HA and NA subtypes have been identified in aquatic birds (Alexander, 2007). Human influenza viruses most commonly have the H1, H2, H3, N1, and N2 subtypes. Nomenclature for the influenza viruses consists of the influenza genera, the species/object the influenza was isolated from (if non-human), location the virus was isolated from, the lineage number of the isolate, the year of isolation, and the antigenic type (when *Influenza A*) (World Health

Organization, 1980). As an example, the 2009 pandemic H1N1 was first isolated in California in 2009 and is written as Influenza A/California/04/2009(H1N1).

1.4 Influenza Structure and Genome

The structure of the influenza virus can be divided in-to three parts: the extracellular envelope and its associated proteins, the matrix layer, and the core (**Fig 1.1**). The Influenza virion is encapsulated by a host-derived lipid membrane and has three surface exposed proteins: HA, NA, and the Matrix Protein 2 (M2). Hemagglutinin is a homotrimer required for virus uptake, while NA is a homotetramer that plays a role in viral progeny release via budding (Gamblin & Skehel, 2010). The HA and NA proteins account for 80% and 17% of the extracellular protein, respectively, and are typically located in lipid rafts (Samji, 2009). The M2 protein is a homotetramer that functions as a pH-dependent H⁺ ion channel that is essential for virus release from the endosome (Holsinger, Nichani, Pinto, & Lamb, 1994). The M2 ion channel is the least abundant protein on the virus surface, with only 16 – 20 molecules of M2 on the entire virion (Samji, 2009). The influenza virion is most commonly spheroidal in shape with diameters ranging from approximately 80 – 120 nm; interestingly, the virus can also be filamentous, reaching lengths of up to 20 µm (Noda, 2011). What determines virus morphology remains unclear, however, clinical isolates are often filamentous while lab passaged strains are spherical. The polarity of the host cell and the genotype of the M2 and M1 proteins may also be important factors in determining the virion shape (Noda, 2011).

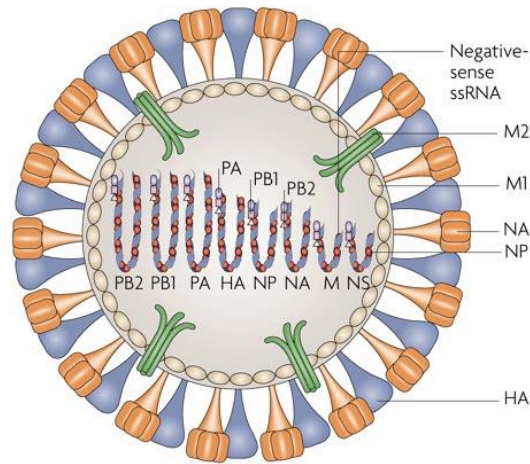


FIGURE 1.1 Influenza A Virus Structure

The influenza virus consists of extracellular proteins (HA, NA, M2) embedded in a host-derived lipid membrane, the matrix protein (M1) which bridges the envelope and viral core, and the core which consists of 8 negative sense RNA segments and associated proteins (NP, PB1, PB2, and PA). Figure taken from Nelson and Holmes (2007)

The matrix layer of the influenza virus is composed of the M1 protein, which is the most abundant protein in the influenza virion (Hilsch et al., 2014). The function of the matrix layer is to bridge the lipid membrane and the core of the virus. The M1 protein interacts with the cytoplasmic portion of the extracellular proteins HA, NA, and M2, and with the NP in the viral core (B. J. Chen, Leser, Jackson, & Lamb, 2008; Rossman & Lamb, 2011). In addition to the M1 protein likely having a role in virus morphology, it may also be required for endosomal release, virus budding, and nuclear import of vRNPs (Rossman & Lamb, 2011).

The nucleocapsid of the *Influenza A* virus contains eight negative-sense RNA strands that make up the viral genome. Each RNA segment is contained in a ribonucleoprotein (RNP) complex composed of an RNA strand, multiple copies of NP, and one heterotrimeric RNA-dependent RNA polymerase (RdRp) complex (PB1, PB2, and PA)

(Zheng & Tao, 2013). The RNA strands closely interact with NP to form a double stranded helix conformation (Arranz et al., 2012). Since each RNP complex folds back on itself, both ends of the RNA strand can interact with the RdRp complex (Arranz et al., 2012).

The eight RNA segments of the *Influenza A* virus genome may code for up to 17 proteins using a variety mechanisms (Dubois, Terrier, & Rosa-Calatrava, 2014). The RNA segments coding for the matrix proteins and non-structural proteins (segment 7 and 8) undergo alternative splicing, using the host cell splicesome, to produce multiple mRNA products (Dubois et al., 2014). Additionally, RNA segments coding for the PB1 protein and polymerase acidic (PA) protein (segments 2 and 3) can produce additional protein products through alternative sites for the initiation of translation (Dubois et al., 2014). Finally, the PA segment can code for the PA-X protein through ribosomal frameshifting (Firth et al., 2012). Each RNA segment also has 5' and 3' non-coding regions that are fairly-conserved and important for viral function. The non-coding regions are 12-13 nucleotides long and are important for RdRp binding, transcription regulation, polyadenylation, and packaging of nascent RNPs into a budding virion (de Wit et al., 2007). Although the influenza genome is relatively small, it can orchestrate the production of multiple proteins using a variety of mechanisms.

1.5 Influenza Replication and Life Cycle

The replication cycle of the influenza virus is dependent on host cell recognition, attachment, and entry (**Fig 1.2a**). The host specificity of influenza is dependent on the viral recognition of host cell surface receptors; specifically, the HA surface receptor on the influenza virus recognizes surface exposed sialic acid on cells. Human adapted influenza

strains typically bind to sialic acid α 2,6-galactose (SA α 2,6Gal), which can be found in the human upper respiratory tract (Connor, Kawaoka, Webster, & Paulson, 1994). In contrast, avian influenza strains preferentially bind to sialic acid α 2,3-galactose (SA α 2,3Gal) (Connor et al., 1994). The human respiratory tract has a low density of SA α 2,3Gal; thus zoonotic infections are not common (Glaser et al., 2005). Hemagglutinin binding preferences are dependent on the structural topography of the sialic acid receptors, which is determined by the sialic acid linkage type (Wilks, de Graaf, Smith, & Burke, 2012). Sialic acid receptors with an SA α 2,6Gal linkage have an umbrella-like shape, whereas those with a SA α 2,3Gal linkage adopt a cone-like confirmation (Wilks et al., 2012). Amino acid positions 190 and 225 of HA are important determinants of sialic acid receptor specificity for H1 viruses, whereas position 226 determines specificity for H2 and H3 viruses (Matrosovich et al., 2000). The HA protein is initially synthesized as precursor HA0 protein and must undergo proteolytic cleavage to HA1 (which is responsible for binding sialic acid) and HA2 (which is important for membrane fusion) (Das, Aramini, Ma, Krug, & Arnold, 2010). Proteolytic cleavage of HA is achieved primarily by human airway trypsin-like protease and transmembrane protease serine S1 member 2 (TMPRSS2), two airway resident proteases (Böttcher-Friebertshäuser et al., 2010).

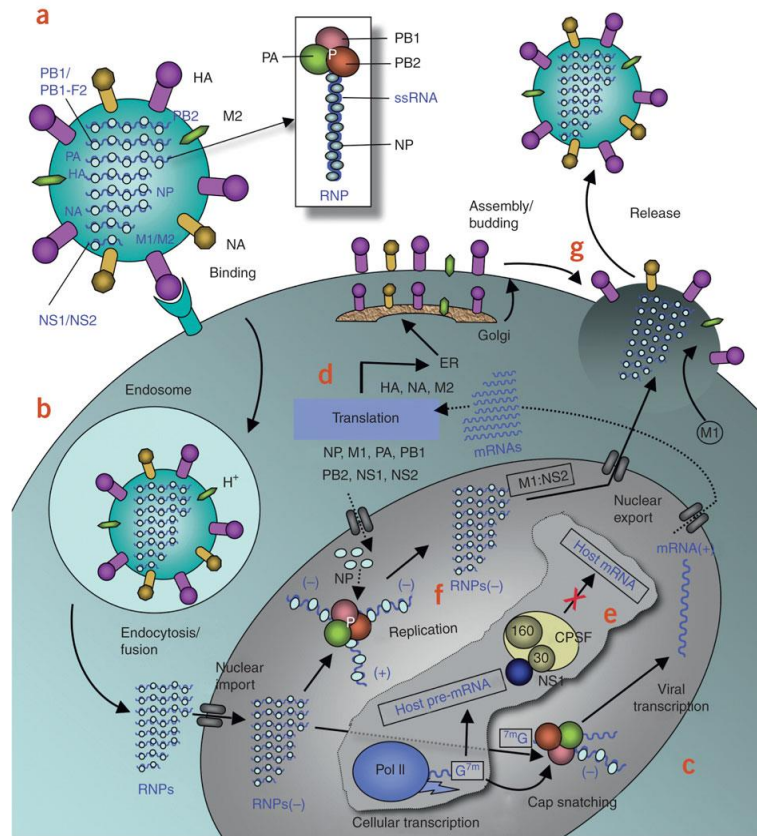


FIGURE 1.2 Influenza A Replication Cycle

See accompanying text for a detailed explanation of each step. (A) An influenza virion binds to host cell sialic acid using surface HA protein. (B) Virus is internalized in to a host cell through endocytosis. The viral membrane fuses with the endosomal membrane and the vRNP are released into the cytoplasm. (C) vRNP enters the host cell nucleus and transcription is initiated using the cap-snatching mechanism. (D) Newly synthesized viral transcripts are transported out of the nucleus and translated using host ribosomes. Transmembrane proteins are localized to lipid rafts through the golgi apparatus. (E) Cap-snatching decreases the amount of host mRNA slowing the production of host proteins. (F) To replicate the genome, negative-sense RNA is transcribed in to positive-sense RNA before being transcribed back in to negative-sense RNA. (G) all components needed inside a virion associate at subcellular locations, leading to viral budding and release. Figure taken from Das et al. (2010).

After binding to the cell, the virus is internalized into an endosome before being released into the cytoplasm. The bound virus is internalized primarily through receptor-mediated endocytosis using clathrin-coated pits (CCPs) (Rust, Lakadamyali, Zhang, & Zhuang, 2004). The majority of influenza internalization does not occur at pre-formed

CCPs, but relies on clathrin recruitment after the virus has bound to the host cell (Rust et al., 2004). Although CCPs appear to be the primary method of influenza internalization, influenza virus can be internalized through clathrin-independent mechanisms (Sieczkarski & Whittaker, 2002). Influenza morphology may also influence the endocytic route of the virus, as it has been suggested that filamentous viruses are believed to enter cells primarily through micropinocytosis (Rossman, Leser, & Lamb, 2012).

Once inside the cell, the virus must escape the endosome and enter the cell cytoplasm (**Fig 1.2b**). The acidic environment of the endosome results in a conformational change in the HA1 and HA2, which remain linked through a disulfide bond (Cross, Burleigh, & Steinhauer, 2001). Under the acidic environment, a previously buried fusion peptide sequence within HA2 is exposed; this sequence is a hydrophobic domain capable of insertion into the host endosomal membrane (Cross et al., 2001). For the viral membrane to fuse with the host endosome membrane, the two membranes must be brought within proximity of each other. The mechanism that brings the membranes together remains unclear, however, a popular theory is the “spring-loaded boomerang” model. This model suggests that the HA domain tilts after insertion into the host membrane, which brings the membranes into proximity (Tamm, 2003). When the two membranes are close enough, they will destabilize and fuse, allowing the virion to escape into the cytoplasm.

The M2 ion channel is required for acidification of the virus, which plays a role in viral uncoating (Pinto, Holsinger, & Lamb, 1992). The M2 protein is a small, 97 amino acid, transmembrane protein that forms a homotetramer in its active state (Sakaguchi, Tu, Pinto, & Lamb, 1997). Only 16 – 20 molecules of M2 are required to acidify the influenza

virion (Samji, 2009). Two residues are essential for proper function of the ion channel: His37, which acts as a sensor to pH levels, and Trp41, which acts as a gate for the ion channel (Schnell & Chou, 2008). At an elevated pH, His37 stabilizes the interaction between Trp41 and Asp44, which blocks the ion channel. When the pH decreases, His37 becomes protonated and the interaction between Trp41 and Asp44 is destabilized to allow for an influx of protons (Schnell & Chou, 2008). The resulting influx of hydrogen ions acidifies the interior of the influenza virion. This acidification of the virus results in the dissociation of the M1 protein from the RNPs due to weakened electrostatic interactions (Batishchev et al., 2015). Only RNPs that have dissociated from the M1 protein can enter the nucleus of infected cells (Bui, Whittaker, & Helenius, 1996). All proteins in the RNP complex contain a nuclear localization sequence (NLS); however the NP (which has three NLSs) is sufficient to traffic RNA to the nucleus (Cros & Palese, 2003). The process of membrane fusion and M1 dissociation is highly coordinated since non-infectious coagulates of RNP will form if M1 is released much prior to membrane fusion (Fontana, Cardone, Heymann, Winkler, & Steven, 2012).

Following the release of the viral RNPs into the cytoplasm, they must be transported to the nucleus to initiate transcription and replication (**Fig 1.2c**). Although the NP is sufficient to transport all necessary components of the RNP to the nucleus, each protein of the viral polymerase can independently localize to the nucleus through their respective NLS (Nieto, de la Luna, Bárcena, Portela, & Ortín, 1994). The PB1, PB2, and PA proteins associate to form the RdRp (Ohtsu, Honda, Sakata, Kato, & Toyoda, 2002). To initiate the transcription of positive sense mRNA, the influenza virus RdRp uses a process called “cap-

snatching” (Dias et al., 2009). The RdRp cleaves 10-13 nucleotides (the cap) off the 5’ end of host pre-mRNAs and uses these as primers to initiate elongation. The PB2 subunit is responsible for pre-mRNA recruitment while the endonuclease domain is located on the PA subunit of the RdRp (Dias et al., 2009; Guilligay et al., 2008). Using the 5’ cap as a primer, the PB1 subunit catalyzes the addition of nucleotides to the pre-mRNA (Braam, Ulmanen, & Krug, 1983). Cap-snatching also results in a decrease the host mRNA levels, which subsequently decreases the production of IFN- β (Goraya, Wang, Munir, & Chen, 2015) (**Fig 1.2e**). Termination of transcription takes place at a series of 5-7 uracil residues that are copied multiple times, due to polymerase stuttering, to produce a poly-A tail (Poon, Pritlove, Fodor, & Brownlee, 1999). Polymerase stuttering at the uracil-site may be due to the inability of vRNA to continue entering the polymerase since the templates 5’ end is bound to the RdRp (Reich et al., 2014).

Newly formed mRNA sequences are exported out of the nucleus where they are translated into protein (**Fig 1.2d**). Prior to being exported, the matrix and non-structural (NS) pre-mRNAs are spliced using the host spliceosome. Gene segment 7 of *Influenza A* generates up to 4 M mRNAs whereas segment 8 generates up to 3 NS mRNAs (Dubois, Terrier, & Rosa-Calatrava, 2014). The NS Pre-mRNA is spliced at a low rate with only 10 – 15% of the mRNA being spliced (Robb, Jackson, Vreede, & Fodor, 2010). Export of the mRNA products to the cytoplasm is achieved primarily through host cell machinery (Read & Digard, 2010). Once mRNA has been transported to the cytoplasm, they are translated using host cell machinery. The surface exposed proteins HA, NA, and M2 are processed in the endoplasmic reticulum and transported through the golgi apparatus before eventually

being transported to the cell surface (Das et al., 2010). Glycosylation of the surface proteins is accomplished in the endoplasmic reticulum and golgi network (Kim & Park, 2012). Hemagglutinin and NA tend to be localized in lipid rafts in the host membrane, while M2 localizes to non-lipid raft areas (Nayak, Balogun, Yamada, Zhou, & Barman, 2009). Localization of membrane proteins to lipid rafts may be important for viral budding (Nayak et al., 2009).

The RdRp is also required to replicate the viral genome, although this process is still not well understood (**Fig 1.2f**). To replicate the genome, the vRNA is copied into complementary RNA (cRNA) that is subsequently copied back into full length vRNA (Boivin, Cusack, Ruigrok, & Hart, 2010). Differentiation between genome transcription and replication is poorly understood; however, replication does not require cap-snatching and may rely on a second RdRp complex (Moeller, Kirchdoerfer, Potter, Carragher, & Wilson, 2012). The genome is replicated throughout the entire infectious cycle, whereas transcription is sharply reduced after 2.5 hours post-infection, indicating that these processes are highly coordinated (Shapiro, Gurney, & Krug, 1987). After its synthesis, the vRNP forms a complex with M1 and NS2, which contains a nuclear export signal (Shimizu, Takizawa, Watanabe, Nagata, & Kobayashi, 2011). The vRNP-M1-NS2 complex is required for nuclear export of the vRNP. The NS2 binding to M1 protein may sterically hinder the M1 protein NLS and prevent re-import of cytoplasmic vRNAs (Shimizu et al., 2011).

Once all necessary virus components are present in the cytoplasm or on the cell surface, new viruses are released from the cell through the process of budding (**Fig 1.2g**).

Although budding is an organized process it can be error prone since up to 90% of virions released from the cell surface may be non-infectious (Nayak et al., 2009). Progeny virions will bud off from host membrane lipid rafts, where the extracellular HA and NA are localized (Nayak et al., 2009). How the remaining viral components localize to the bud initiation site remains unclear; however, localization of vRNP to the lipid rafts may be M1-dependent (Nayak et al., 2009). Once all components are present at the budding initiation site, the budding process will take place.

Mechanisms controlling the initiation of virus budding are not well understood; however, lipid rafts and the accumulation of M1 protein underneath the host lipid bilayer, may cause a curvature of the membrane that could initiate the budding process (Nayak et al., 2009; Rossman & Lamb, 2011). The M2 ion channel may also assist bud initiation by inserting its amphipathic helix into the neck of the budding envelope and modifying the curvature of the membrane (Rossman & Lamb, 2011). After the bud has elongated the membrane will pinch off, completing virus formation. The NA protein cleaves nearby sialic acid residues, preventing the interaction between the newly-formed virions HA and host sialic acid receptors, allowing the virus to release from the host cell surface (Rossman & Lamb, 2011). Specifically, NA cleaves an α -ketosidic linkage between sialic acid and a linked sugar residue. (Shtyrya, Mochalova, & Bovin, 2009). Similar to HA, NA subtypes show specificity for certain sialic acid residues and their linkage type (Shtyrya et al., 2009). Once virus has been released from the cell surface, the virions will infect nearby cells and re-initiate the replication process.

1.6.1 Current Preventative Influenza Measures – Vaccines

Immediately following the discovery of the virus responsible for influenza symptoms in 1933, efforts were underway to develop a vaccine. Experiments with live attenuated vaccines began as early as 1936, when it was discovered that influenza passaged through ferrets elicited only minor symptoms in humans and had some protective immunity (Smorodintseff, Tushinsky, Drobyshevskaya, Korovin, & Osteroff, 1937). After the discovery of *Influenza B* and the development of an effective strategy to passage influenza virus in chicken embryos, the first formalin-inactivated vaccine was tested in 1944 (Salk et al., 1945). This vaccine was originally reported to be almost 80% effective and was first used in soldiers before eventually being administered to the general public (Salk et al., 1945). This vaccine was used until 1947, when the vaccine showed severely reduced protection (Kilbourne et al., 2002). The 1947 influenza epidemic was initially thought to be due to a new virus type; however, we now know the vaccines ineffectiveness could be attributed to antigenic drift (**discussed in detail in section 1.7**) of the circulating virus. In 1958, a new H2N2 virus emerged through antigenic shift (**discussed in detail in section 1.7**), which required a new bivalent vaccine (Hannoun, 2013). Based on these observations, it was clear that a new influenza vaccine formulation would be required each year depending on the circulating strains.

During the 1978 flu season, two types of *Influenza A* were circulating, leading to the formulation of a trivalent inactivated vaccine (Hannoun, 2013; Kendal et al., 1979). Trivalent and quadrivalent inactivated vaccines are still being used as seasonal influenza vaccines in most parts of the world. To generate the vaccine each year, the circulating

influenza strain is predicted using genetic surveillance in over 100 countries (Centers for Disease Control and Prevention, 2016c). The effectiveness of each year's vaccine can vary, with the 2016 vaccine only being 51% effective against influenza A (Centers for Disease Control and Prevention, 2016b). Although the influenza vaccine is free to most people in each province, vaccination rates remain fairly low; likely due to the need for yearly administration (Government of Canada, 2016). Live-attenuated vaccines have also been developed by adapting the virus to grow only at 25°C (Maassab & Bryant, 1999). Although the live-attenuated influenza vaccine is being used more commonly, reports have been mixed on its effectiveness compared to inactivated vaccine (Belshe et al., 2007; Monto et al., 2009).

There are several limitations with influenza vaccines including the yearly administration schedule, the need to predict the epidemic strain, and the long response time to new pandemic influenza strains. The current vaccine primarily induces an antibody response to the highly variable head portion of HA, which results in very low levels of cross protection (Eggink, Goff, & Palese, 2014). Recent studies have focused on developing a universal influenza vaccine that would be effective against all viral reassortants. These efforts primarily rely on eliciting a humoral or cell-mediated immune response to highly conserved regions of influenza.

Although the humoral response to influenza virus is fairly strain-specific, cell mediated immunity can result in more cross protection between influenza subtypes (McMichael, Gotch, Noble, & Beare, 1983). In addition to clearing virus infected cells, pre-formed T-cells can also inhibit the initiation of influenza infections (Wilkinson et al.,

2012). Francis et al. (2015) have developed a vaccine, known as FP-01.1 or flunisyn, that is designed to produce a T-cell response to highly conserved internal antigens. The vaccine is composed of six different 35-mer peptides from the NP, M1, PB1 and PB2 proteins of influenza. Early clinical trial data suggests the formulation is safe and can induce a CD4+ and CD8+ T-cell response.

Vaccine candidates that induce a humoral response to a more conserved epitope have also been explored. Although the head of the HA protein varies between influenza strains, the stalk domain is highly conserved as it is required for endosomal release of the virus (Krammer & Palese, 2013). Stalk specific antibodies delivered passively to mice have been shown to elicit a protective response (T. T. Wang et al., 2010). Based on this, Wang et al. (2010) developed a peptide based vaccine that generates stalk specific antibodies and seemingly protects mice from lethal doses of influenza. Similar results have also been observed using a viral vector vaccine containing chimeric HA, which resulted in delayed or non-existent replication of influenza in ferrets (Nachbagauer et al., 2016). Mutations in the stalk region of HA attenuates influenza, suggesting that resistance to stalk specific antibodies would develop slowly (Krammer & Palese, 2013).

Other attempts at producing a humoral immune response have focused on increasing the immunogenicity of the naturally low-immunogenic M2 protein. The peptide vaccine, M2e, is fairly non-immunogenic by itself; however, to increase its immunogenicity various groups have attached this protein to different carrier proteins. The M2e peptide vaccine has been attached to the hepatitis B core protein, flagellin, and a T-Helper cell epitope in an attempt to increase its immunogenicity (De Filette et al., 2005;

Huleatt et al., 2008; Ma et al., 2013). Since both humoral and cell mediated immunity appear important in the control of influenza, vaccines have been designed to induce both these response types. A vaccine candidate, Multimeric-001, combines nine different peptide sequences of internal and external antigens, and is currently being evaluated in clinical trials (Atsmon et al., 2014). Although new vaccines are being designed and tested, no single vaccine can control all influenza types, which leads to influenza persistence in the population.

1.6.2 Current Preventative Influenza Measures – Antivirals

When influenza vaccines fail to provide a rapid or effective response, antivirals are often used to treat the high-risk patients, such as the elderly, until an effective vaccine can be developed. Novel antivirals are required since there are limited antiviral options available and resistance to these treatments has emerged in the population. There is a reluctance to using stockpiled antivirals for fear of further influenza resistance due to increased antiviral exposure (A. Patel & Gorman, 2009)

Two antiviral classes have been used to treat influenza: the adamantane derivatives, amantadine and rimantadine, which are M2 ion channel inhibitors (Stouffer et al., 2008), and the neuraminidase inhibitors (NAI), oseltamivir and zanamivir (McKimm-Breschkin, 2013). Although the adamantanes are cheaper to produce, resistance towards these compounds has steadily increased, with most circulating strains of influenza now being resistant (Centers for Disease Control and Prevention, 2015; McKimm-Breschkin, 2013). The majority of adamantane resistance is achieved through a serine to asparagine substitution at amino acid 31 of the M2 ion channel (Pielak, Schnell, & Chou, 2009). This

mutation destabilizes the M2 ion channel and lowers its affinity for the drug (Pielak et al., 2009). Although the NAIs are still fairly effective and their binding site is more highly conserved, clinical isolates of influenza have spontaneously emerged that are resistant to oseltamivir (Centers for Disease Control and Prevention, 2009). Most mutations that result in resistance to oseltamivir also decrease viral fitness; however, additional permissive mutations may be able to restore viral fitness (Bloom, Gong, & Baltimore, 2010).

Many novel strategies to develop influenza antivirals focus on inhibiting viral entry or replication. To inhibit viral entry, drugs often bind to viral or host surface receptors and inhibit the interaction required for virus uptake. Peptide mimotopes are small synthetic peptides that can mimic carbohydrates (Matsubara, 2012). Matsubara et al. (2010) developed a peptide mimotope that mimics sialic acid and can bind to HA, inhibiting viral entry. This peptide binds to HA on the cell surface of both an H1N1 and H3N2 influenza virus. Another drug under investigation to inhibit influenza replication is synthetic anti-lipopolysaccharide peptides (SALPs). Synthetic anti-lipopolysaccharide peptides were initially designed to bind to lipopolysaccharides of Gram-negative bacteria, but have been shown to have anti-influenza activity (Hoffmann et al., 2014). To inhibit virus infection, SALPs can bind to host cell sialic acid and block receptor interaction. Interestingly, SALPs administered intranasally to mice showed low levels of toxicity and protected the mice from lethal doses of influenza (Hoffmann et al., 2014).

Since the viral RdRp is essential for influenza replication, antivirals have also been designed to inhibit its function. Ribavirin, which is a guanosine analog, has been approved for the treatment of respiratory syncytial virus (Krillov, 2011) and hepatitis C (Te, Randall,

& Jensen, 2007). Ribavirin also showed promise in treating influenza infections since it was effective *in vitro* (Browne, Moss, & Boyd, 1983); however, this success did not translate to clinical studies where ribavirin was ineffective (Chan-Tack, Murray, & Birnkrant, 2009). Other nucleotide analogs to treat viral infections have been investigated for the treatment of influenza infections as well. Favipiravir (T-705) and viramidine are nucleotide and nucleoside analogs, respectively, which are being evaluated in clinical trials (Furuta et al., 2013; Sidwell, Bailey, Wong, Barnard, & Smee, 2005). Favipiravir can protect mice against lethal doses of HPAI (Kiso et al., 2010) and had positive potential in phase II clinical trials for safety (MDVI & LLC, 2010). Novel antivirals are urgently required to combat the constant threat of a pandemic influenza strain entering the population. Due to antigenic drift, influenza can become resistant to our present antivirals, highlighting the need for novel tools to treat this infection.

1.7 Immune Avoidance by Antigenic Drift and Shift

Influenza can rapidly alter its genome through antigenic drift and antigenic shift, allowing it to evade previously established immune responses. Antigenic drift is the gradual change in the influenza genome over time through random mutations and selection. Influenza has a fairly high mutation rate, resulting in approximately 1 mutation per genome replication (Drake, 1993). Not surprisingly, surface exposed proteins have the highest selective pressures while internal proteins seem to have lower selective pressures and are less likely to tolerate mutations (Webster, Bean, Gorman, Chambers, & Kawaoka, 1992). Mutations to the surface exposed proteins can result in influenza escaping previously established humoral immune responses. Interestingly, antigenic drift can actually take place

at different rates in different influenza strains with H3 species evolving more rapidly than other influenza subtypes (Treanor, 2004). In general, as one influenza variant becomes increasingly dominant in the population, the species it evolved from becomes less common until its eventual extinction (Earn, Dushoff, & Levin, 2002).

Certain protein codons are more likely to undergo positive selection and mutation in influenza. Within the HA protein, there are 18 different codons that are commonly mutated in past seasonal influenza epidemics (Bush, Bender, Subbarao, Cox, & Fitch, 1999). These sites are all within antibody binding epitopes or in the sialic acid binding pocket of HA. Although antigenic drift will not likely result in severe influenza pandemics, different vaccines are required each season. Although there have been attempts to develop a universal influenza vaccine (**discussed in section 1.6.1**) to combat antigenic drift, some studies have suggested that live attenuated vaccines may be more effective than inactivated influenza vaccines at inducing cross-protective immunity (Carrat & Flahault, 2007).

Antigenic shift occurs due to the reassortment of influenza genomic RNA and has resulted in the most severe pandemics. For antigenic shift to occur, multiple influenza virus types must infect a single cell, which relies on a common host as a “mixing pot” (Zambon, 2001). When multiple influenza viruses infect the same host, RNA segments from each may be packaged into progeny virions, resulting in recombinant virus types. Antigenic shift has only been observed in *Influenza A* since *Influenza B* and *C* do not have persistent animal reservoirs (Zambon, 2001). Often, pandemic influenzas are reassortants of avian and human specific influenza strains; however, each of these virus types recognize a distinct sialic acid moiety, and it remains unlikely that these hosts act as a mixing pot. Since

swine have both SA α 2,6Gal and SA α 2,3Gal present on tracheal cells, it has previously been predicted that they serve as the common host that these viruses could infect (Ito et al., 1998). This theory was supported in 2009 when a triple reassortant virus was identified that had been previously circulating in swine (Neumann et al., 2009). There are typically 3 – 4 pandemics of influenza each century due to antigenic shift (Taubenberger & Morens, 2010). The surveillance of animals for influenza strains with zoonotic potential is severely under-developed; therefore, novel reassortant viruses will continue to enter our population due to antigenic shift (Von Dobschuetz et al., 2015). These reassortant viruses have the potential to cause serious pandemics if not detected in a timely fashion.

1.8 The Influenza RNA-Dependent RNA Polymerase Complex as a Drug Target

The influenza RdRp complex is an interesting drug target since it is required for transcription and replication of the influenza genome. The heterotrimeric complex is one of the largest RNA virus polymerases at approximately 250 kDa and consists of three components: PA, PB1, and PB2 (Stubbs & Te Velhuis, 2014). The binding domains between the three subunits have been well characterized, with PB1 being the central core of the complex and PA and PB2 binding to its N- and C-terminus, respectively (**Fig 1.3**) (Ohtsu et al., 2002). Formation of the heterotrimeric complex is required for full influenza virulence, and disruption of this complex will inhibit the production of progeny virions (Ohtsu et al., 2002).

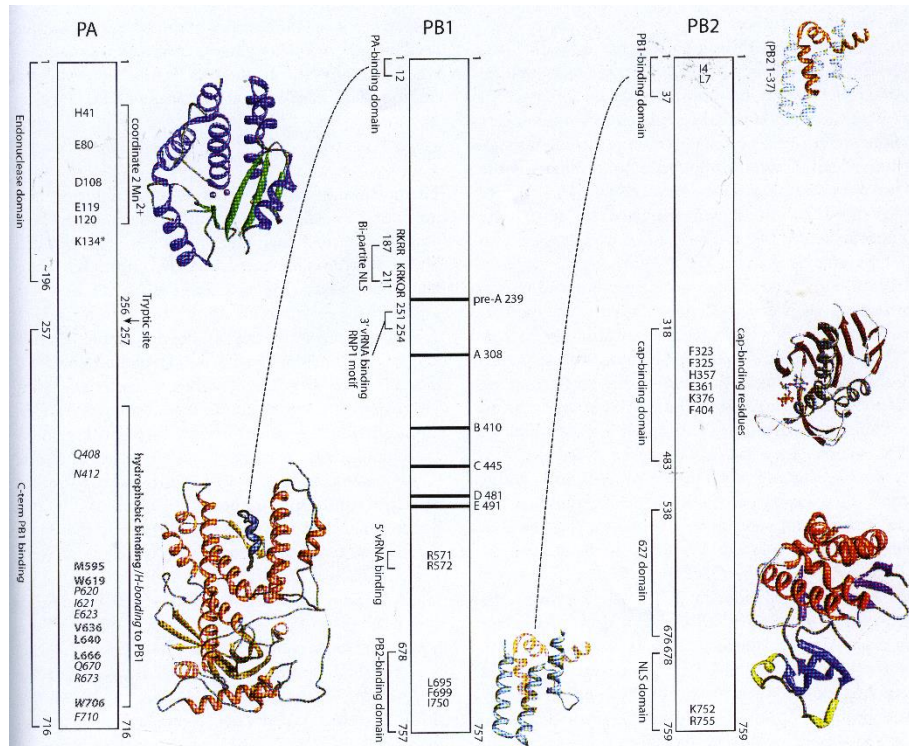


FIGURE 1.3 Overview of the Influenza Heterotrimeric RNA-Dependent RNA Polymerase and Key Interactions

The Influenza RdRp is a heterotrimer consisting of three proteins: PA, PB1, and PB2. Interactions between the subunits are represented with dashed lines. Residues important for interaction are outlined and protein structures of these interactions are indicated. Various domains and essential amino acids are labelled. All protein structures are taken from the protein database. Image taken from the *Textbook of Influenza* (Mehle & McCullers, 2013).

Each subunit of the RdRp complex has important active domains essential for its function. The PA subunit contains an endonuclease domain that is necessary for cap-snatching (Dias et al., 2009). The active site of the endonuclease domain is structurally homologous with the PD-(D/E)XK nuclease superfamily, which is present in multiple restriction enzymes (Crepin et al., 2010). The PA subunit has one or two divalent metal ion binding sites that are believed to bind either Mn^{2+} or Mg^{2+} and are required for its endonuclease activity (Crepin et al., 2010). Interestingly, the cap-binding domain is attributed to the PB2 subunit rather than the PA subunit. Residues 318-483 of PB2 are

required for cap-binding with Phe363 and Phe404 being essential (Guilligay et al., 2008). The PB2 subunit also has a 627 domain containing a conserved P(F/P)AAAPP sequence. This 627 domain appears to play a critical role in the regulation of polymerase activity (Kirui, Bucci, Poole, & Mehle, 2014). The PB1 subunit performs the actual polymerase function and is responsible for catalyzing the addition of new nucleotides to the 3' end of the growing nucleotide chain (Braam et al., 1983). The influenza virus RdRp was the first negative sense RNA virus polymerase to have its structure completely elucidated (Pflug, Guilligay, Reich, & Cusack, 2014)

The 12 N-terminal amino acids of PB1 are all that is required for the interaction with PA (Perez & Donis, 2001) Of the 12 amino acids required for PA binding, 5 are completely essential: Pro5, Leu7, Leu8, Phe9, and Leu10 (Obayashi et al., 2008). Residues 657-716 of PA form a deep hydrophobic groove resembling a “dragon’s head”, which surrounds and binds the N-terminus of PB1 (**Fig 1.4**) (He et al., 2008; Obayashi et al., 2008). Binding between PA and PB1 requires hydrogen bonds and hydrophobic interactions. Residues 2 to 4 of PB1 interact with residues 621 to 623 of PA in a β -sheet-like manner, while residues 2, 3, 4, 8, 9, 10, 12, and 14 of PB1 form hydrogen bonds with residues 623, 408, 621, 620, 706, 670, 673, and 670 of PA, respectively (Obayashi et al., 2008). Important hydrophobic interactions include residue 5 of PB1 packing between residues 411 and 706 of PA, and residue 8 of PB1 interacting with residues 595, 619, 636, and 640 of PA (Obayashi et al., 2008).

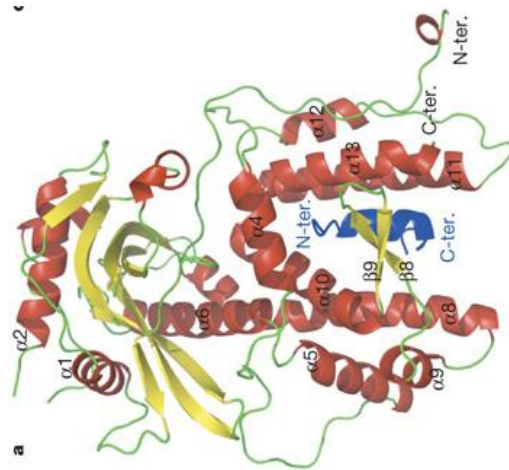


FIGURE 1.4 Interaction Between the RdRp PA C-terminus and the PB1 N-terminus
Ribbon diagram of the interaction between the C-terminus (residues 239–716) of PA and the N-terminus (residues 1–81) of PB1. The PA protein forms a hydrophobic “dragon jaw-like” pocket which surrounds the N terminus of PB1. All PB1 residues are depicted in dark blue. The interaction is mediated through hydrogen bonds and hydrophobic interactions. Figure taken from Obayashi et al. (2008)

The interaction between the PB1 C-terminus and the PB2 N-terminus also involves hydrogen bonds and hydrophobic interactions. In addition, the PB1-PB2 interface is dependent on four salt bridges between Glu2 and Lys698, Arg3 and Asp725, Arg3 and Lys698, and Glu6 and Lys698 of PB2 and PB1, respectively (Sugiyama et al., 2009). Residues 712-746 of PB1 can bind to PB2; however, residues on either side of this interaction strengthen the binding (Poole, Medcalf, Elton, & Digard, 2007). The domain on PB2 responsible for binding PB1 resides within the first 37 N-terminal residues, which is composed of three alpha-helices (Sugiyama et al., 2009). Interestingly, mutating the PB1 Val715 decreases polymerase activity but does not inhibit binding between the two subunits, suggesting that communication between the subunits is essential (Sugiyama et al., 2009).

The influenza RdRp has a high rate of mutation due to its lack of proofreading ability; this results in an average of 1 mutation per genome replication (Drake, 1993). This high mutation rate allows the virus to escape pre-formed host immunity, as discussed in **section 1.7**. Despite the high mutation rate, the domains important for protein interactions remain highly conserved (**Fig 1.5**), indicating mutations are not well tolerated in these areas. Mutations within the binding domains of the polymerase proteins often disrupt formation of the RdRp *in vitro*; therefore, influenza resistance should develop slowly (Obayashi et al., 2008; Poole et al., 2007; Sugiyama et al., 2009). Since the RdRp is essential for influenza virulence, a drug that inhibits the interaction between its subunits should disrupt influenza replication.

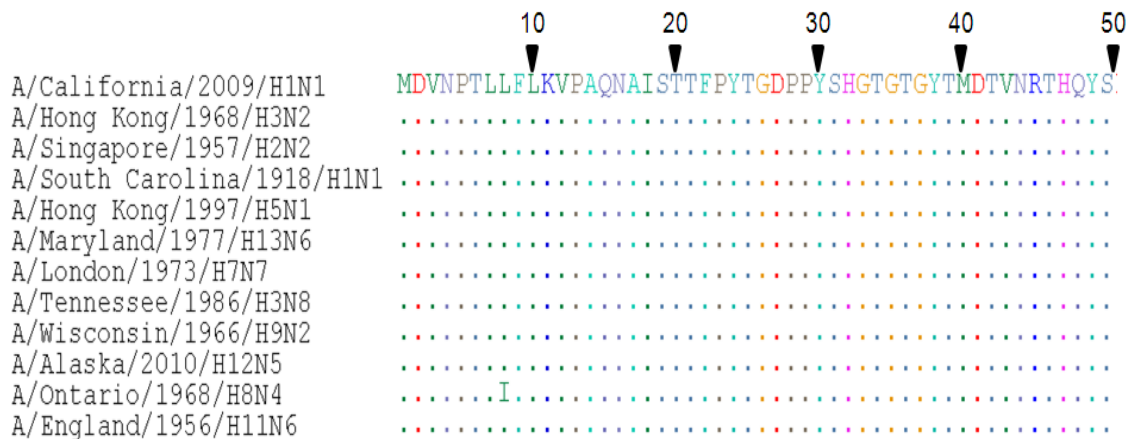


FIGURE 1.5 ClustalW Alignment of the First 50 Amino Acids of PB1 of Various Influenza A Strains

The first 50 amino acids of PB1 in 12 different strains of Influenza were compared using ClustalW alignment. The binding domain is contained within the first 12 amino acids. Dots indicate conserved amino acids. All sequences are 100% identical except for A/Ontario/1968/H8N4 which has a conserved amino acid substitution of leucine to isoleucine. Data and figure courtesy of Kenneth A. Mwachasi

1.9 Small Peptides as Dominant Negative Therapeutics

Peptide mimetics are small sequences of amino acids, often derived from larger protein sequences, that can inhibit crucial protein interactions. The short peptide sequences mimic the binding domain of a protein and thus retain the ability to interact with their target partner (Vagner, Qu, & Hruby, 2008). Since peptide mimetics are a short portion of a protein and lack effector domains, their interaction with the target protein does not induce downstream effects (Mason, 2010). Thus, peptide mimetics have a dominant-negative effect and disrupt the normal function of wild-type proteins. For peptide mimetics to be effective, the target must preferentially interact with the mimetic and not the wild-type protein. To accomplish this, the mimetic must be present at concentrations higher than the wild-type protein. Alternatively, the binding affinity of the mimetic to the target can be increased by modifying the peptide sequence, creating a stronger interaction to out-compete the wild-type binding.

Peptide mimetics must be easy to purify and soluble, non-immunogenic, and localize to the correct sub-cellular location. One of the barriers of using peptide mimetics are their stability and availability, because the peptides are often inactive *in vivo* (Goodwin, Simerska, & Toth, 2012). Peptide mimetics can be fused to larger protein molecules, called carrier proteins, to increase solubility and limit breakdown by proteases (Mason, 2010). Two common carrier proteins include human serum albumin (HSA), which can increase a proteins half-life, and maltose-binding protein (MBP), which can increase solubility of non-soluble fusion partners (Douette et al., 2005; Larsen, Kuhlmann, Hvam, & Howard, 2016).

A vast array of carrier proteins are available; however, the ideal carrier protein for each mimetic must be determined through a trial-and-error process.

If a peptide mimetic has an intracellular target, it must penetrate the extracellular membrane and localize correctly within a cell. Cell penetrating peptides (CPP) are commonly used to localize proteins within cells. The original CPP was a 12 amino acid sequence obtained from the transactivator of transcription (Tat) protein of human immunodeficiency virus (Siomi, Shida, Maki, & Hatanaka, 1990). The Tat peptide is a NLS and is commonly used to transport proteins to the nucleus of cells. Other CPPs have since been isolated from natural sources, such as the 16 amino acid penetratin peptide from the *Drosophila melanogaster* antennapedia protein (Derossi, Joliot, Chassaing, & Prochiantz, 1994). In addition, CPPs have been synthetically designed, such as the polyarginine sequence (Futaki et al., 2001). Since the discovery of the Hiv Tat-1 NLS, over 100 different CPPs, with varying properties and lengths, have been described (Koren & Torchilin, 2012). Each CPP type may vary considerably in its uptake mechanism, and one CPP may use multiple mechanisms to gain access to the intracellular environment (Koren & Torchilin, 2012; Madani, Lindberg, Langel, Futaki, & Gräslund, 2011). The majority of CPPs can cross a membrane through direct penetration, endocytosis, or pore formation (Koren & Torchilin, 2012; Madani et al., 2011). Similar to carrier proteins, a CPP must be chosen on a case-to-case basis depending on the desired function and subcellular localization of the target protein.

1.10 The Elastin Like Polypeptide Class of Protein Carriers

A unique class of proteins, the elastin-like polypeptides (ELPs), have emerged as a potential carrier protein for therapeutics. Elastin-like polypeptides are intriguing because they can be easily manipulated, have excellent solubility, and should be fairly non-immunogenic. Elastin-like polypeptides are based on the highly insoluble human tropoelastin protein and consist of variable repeats of the sequence Val-Pro-Gly-Xaa-Gly, where Xaa can be any amino acid except for proline (Meyer & Chilkoti, 1999). This is a common motif in human tropoelastin, where approximately 75% of the sequence consists of the hydrophobic amino acids glycine, valine, alanine, and proline (Vrhovski & Weiss, 1998).

Interestingly, ELP proteins demonstrate the unique property of temperature-dependent solubility. Elastin-like polypeptides are soluble below a defined transition temperature (T_t); however, when raised above the T_t , ELPs form insoluble aggregates (Meyer & Chilkoti, 1999). Below the T_t , ELPs are intrinsically disordered and fully hydrated, whereas above the T_t , the ELPs form an insoluble β -spiral structure with one β -turn per every three repeats (Herrero-Vanrell et al., 2005; Reiersen, Clarke, & Rees, 1998). The insoluble structure is primarily stabilized through hydrophobic interactions (Kowalczyk, Hnatuszko-Konka, Gerszberg, & Kononowicz, 2014). The T_t of an ELP construct is often at an extremely sharp temperature (2-3 °C) and ELP aggregation is completely reversible when the temperature is reduced below the T_t (Hassouneh, MacEwan, & Chilkoti, 2012). This property of ELPs allows them to be purified using inverse transition cycling (ITC), a process unique to ELPs. To perform ITC, aggregated

ELP can be pelleted by centrifugation, thus separating them from other soluble proteins, and subsequently resolubilized in cold buffer. Proteins fused to ELP constructs can be purified at high levels and to high purity, making it an ideal carrier protein for peptide based drugs (Hassouneh et al., 2012; Meyer & Chilkoti, 1999). Recently, recombinant ELP proteins were purified from tobacco plant leaves, which may act as a system to scale-up the production of ELPs and achieve pharmaceutically relevant yields (J. Patel et al., 2007).

The T_t of ELPs can be fine tuned so that ELP proteins can be designed to meet specific needs. Three main factors affect the T_t of ELP fusion constructs; namely, the number of ELP repeats, the composition of the guest residues, and the concentration of ELP in solution. Increasing the length of the ELP protein decreases the T_t due to the greater availability of hydrophobic residues available for hydrophobic interactions (Meyer & Chilkoti, 2004). An increase in the concentration of ELP proteins in solution also results in a decreased T_t due to the increased availability of intermolecular hydrophobic interactions (Meyer & Chilkoti, 2004). The identity of the guest residue (Xaa) will also affect the T_t , with the general pattern that hydrophobic residues lower the T_t while hydrophilic residues increase T_t (Urry et al., 1991). When cargo proteins are fused to ELPs, the construct will typically retain the thermal transition property, however this will result in a modified T_t . The modified T_t is primarily dependent on the fusion proteins surface hydrophobicity and is referred to as the “fusion ΔT_t effect” (Trabicc-Carlson et al., 2004).

Predicting an ELP's T_t allows the construct to be bioengineered to meet specific needs; because of this, various models have been designed to accurately predict the T_t of fusion proteins (Christensen, Hassouneh, Trabicc-Carlson, & Chilkoti, 2013). If an ELP

protein is bioengineered to have a T_t slightly above body temperature, the construct can be localized to a specific area of the body by heating the affected tissue. Increased accumulation of ELP fusion constructs to solid tumors using localized heating has been demonstrated previously using a mouse model (Ryu & Raucher, 2015). Elastin-like polypeptides have also been used to encapsulate drugs, resulting in slow release of drug for up to 30 days (Herrero-Vanrell et al., 2005).

Elastin has a high level of sequence homology across mammalian species, making it a potentially non-immunogenic carrier protein (Vrhovski & Weiss, 1998). Elastin-like polypeptides tested *in vivo* have demonstrated minimal toxicity and have been relatively immunotolerant (Rincon et al., 2006; Ryu & Raucher, 2015). To further limit immunogenicity, exact sequences from human tropoelastin can be used. Human elastin-like polymers (HELPS), composed of exon 24 of human tropoelastin, retain the thermal transition property characteristic of ELP constructs (Bandiera et al., 2005). Since this sequence is directly identical to human tropoelastin it is expected to have a low immunogenic potential. Similarly, a series of immune-tolerant elastin-like polypeptides (iTEPs) have been designed that maintain the thermal transition property but have no epitopes capable of binding to human and mouse B- or T-cell receptors (Cho, Dong, Parent, & Chen, 2016). The iTEP sequences are non-immunogenic in mice and could boost a cytotoxic T lymphocyte mediated vaccine response (Cho et al., 2016). Elastin-like polypeptides are an intriguing class of carrier protein based on their high yields, manipulability, and potentially low immunogenic and cytotoxic effects.

1.11 Thesis Objectives

Previously, our lab has used peptide mimetics to inhibit the *Chlamydia pneumoniae* Type III secretion system (Stone et al., 2011). By inhibiting the ATPase-CdsL interaction, a crucial interaction in *C. pneumoniae* life cycle, *C. pneumoniae* replication could be inhibited *in vitro*. In 2007, Ghanem et al. (2007) demonstrated that a synthetically synthesized, 25 amino acid long, PB1 derived peptide linked to an NLS was able to impede the replication of influenza *in vitro*. Our lab has expanded on this by attaching a similar construct to the C-terminus of the HisMBP carrier protein. For our construct, we used the first 21 amino acids of PB1 to inhibit influenza replication because the N-terminus of PB1 is highly conserved (**Fig 1.5**), and this portion is sufficient for PA binding. This sequence was linked to the His-MBP carrier protein and the HIV-1 Tat NLS to increase protein solubility and cellular uptake of the peptide, respectively. This recombinant protein could gain intracellular access to MDCK cells and inhibit the replication of influenza *in vitro* (Unpublished data). To determine whether the binding interaction could be enhanced, the sequence was analyzed using Zhorov Molecular Modelling to determine the free energy of binding of various mutations (**Sup. Fig 6.1**). Interestingly, this analysis predicted that a threonine to arginine mutation at position 6 would have less free energy of binding and therefore have a higher binding energy. The T6R peptide was also analyzed and showed greater antiviral activity when compared to the wild-type PB1 peptide (Unpublished data).

The anti-influenza protein used previously by our lab was attached to the *E. coli* derived His-MBP carrier which would be unfavourable for use in humans. This study focused on the design of the anti-influenza peptide linked to a human carrier protein and its

activity. For this purpose, we used the ELP carrier, which is easy to manipulate, purifies to large-scales in a cost-effective manner, and should be relatively non-immunogenic. The ELP carrier was designed to be small, to limit bulkiness, and have a physiologically compatible T_t . To initiate uptake of our protein in to cells, it was also linked to the HIV-1 Tat NLS sequence. The PB1-T6R peptide mimetic was used due to its high degree of anti-influenza activity. We hypothesized that influenza replication will still be attenuated when the anti-influenza peptide attached to the HisMBP carrier protein is instead attached to the human ELP scaffold.

Chapter 2 – Materials and Methods

MATERIALS AND METHODS

2.1.1 Genetic Cloning and Design of Expression Constructs Using the Invitrogen Gateway Cloning System

All protein constructs using HisMBP or GST tags were cloned using the Invitrogen Gateway® Cloning System. Starting materials were ordered as gBlocks® Gene Fragments from Integrated DNA Technologies and contained *attB* sites for cloning into the Gateway® pDonr201 entry vector. To perform the BP reaction, 25 ng of the gBlocks® Gene Fragment was incubated with the pDonr™201 entry vector, the Gateway® BP clonase enzyme mix, and TE buffer (10 mM Tris-HCl pH 8.0, 1 mM EDTA) as per the manufacturer's protocol. After 1 or 24 hours, the reaction was stopped by adding 4 µg of proteinase K and incubating the sample at 37°C for 10 minutes. The BP reaction was transformed into chemically competent *Escherichia coli* Turbo cells (New England Biolabs), as per section 2.2.2, and plated on Luria Bertani (LB) agar plates (1% w/v tryptone, 0.5% w/v yeast extract, 1% w/v NaCl, 1.5% w/v agar) supplemented with 30 µg/mL kanamycin. Plasmids were extracted from transformed colonies, as per section 2.1.4, and a successful BP reaction that produced an entry clone was confirmed using agarose gel electrophoresis.

To construct expression vectors, plasmids from successful BP reactions were used in a Gateway® LR reaction. The desired construct was cloned into pDest™-HisMBP or pDest™15 to produce HisMBP or GST fusion constructs, respectively. To perform the LR reactions, the entry clone was incubated with the pDest plasmid, Gateway® LR clonase, and TE buffer for 1 or 24 hours as per the manufacturer's protocol. The reaction was terminated by incubation with 4 µg of proteinase K at 37°C for 10 minutes. LR reactions were transformed into chemically competent *E. coli* Turbo cells and plated on LB agar

plates containing 100 µg/mL ampicillin. To ensure the transformants contained the proper insert, purified plasmids were verified using agarose gel electrophoresis. Plasmids believed to contain insert were verified by sequencing from the MOBIX sequencing facility (McMaster University, Hamilton ON). Plasmids containing proper insert were ultimately transformed in to chemically competent *E. coli* BL21 (DE3) or *E. coli* Rosetta (DE3) (Life Technologies) for expression purposes.

2.1.2 Genetic Cloning and Design of Expression Constructs Using Recursive Directional Ligation

For cloning of all elastin-like polypeptide sequences, recursive directional ligation (RDL) was utilized as described by McDaniel et al. (2010). An overview of one round of RDL can be found in **Sup. Fig 6.2**. The ELP sequence was cloned as a library of various repeats. The initial construct consisted of five repeats of the motif VPGXG, where the guest residue, X, was alanine in one of the repeats and valine in the other four. To generate this construct, two overlapping oligonucleotides were purchased (Sigma-Aldrich) and amplified by polymerase chain reaction (PCR), as per section 2.1.3. The PCR amplicon was gel extracted from a 3% agarose gel using the Geneaid™ gel/PCR DNA Fragments Extraction Kit as per manufacturers protocol. The extracted amplicon and purified pUC19 cloning plasmid (New England Biolabs) were each digested with both EcoRI-HF (New England Biolabs) and HindIII-HF (New England Biolabs), as per the manufacturer's protocol. The digested constructs were ligated overnight using T4 DNA ligase (Invitrogen) as per manufacturers protocol, transformed into chemically competent *E. coli* TURBO cells, and plated on LB agar plates containing 100 µg/mL ampicillin.

To perform RDL, pUC19 containing ELP insert was digested with PflMI (New England Biolabs) alone or digested with both PflMI and BglII (New England Biolabs), as per the manufacturer's protocol. The digested products were purified using the Geneaid™ gel/PCR DNA Fragments Extraction Kit and ligated using T4 DNA ligase to double the insertion size. This was repeated two more times to yield ELPs with twofold increasing sizes after each round. Each round of RDL was confirmed by PCR and agarose gel electrophoresis. To clone the desired insert on to the ELP construct, overlapping primers corresponding to the desired fusion sequence were purchased (Sigma-Aldrich) and amplified by PCR, as per section 2.1.3. Gel extracted amplicon and pET-25b(+) vector (graciously donated by Dr. Drazen Raucher) were each digested with both NdeI (New England Biolabs) and EcoRI-HF before being ligated with T4 DNA ligase. The resulting pET-25b(+) vector containing insert was digested with SfiI (New England Biolabs) while pUC19 plasmid containing ELP of desired length was digested with both PflMI and BglII. The ELP sequence was gel extracted and ligated in to the digested pET-25b(+) plasmid using T4 DNA ligase. The resulting construct was transformed in to *E. coli* BL21 (DE3) for expression. All constructs were verified by the MOBIX sequencing facility (McMaster University, Hamilton ON).

2.1.3 Primer Resuspension and Polymerase Chain Reaction

All primers used in this study were shipped as lyophilized stocks. To make a master stock, primers were resuspended in UltraPure™ DNase/RNase-Free Distilled Water (Invitrogen) to a final concentration of 100 µM. To make a working stock for PCR, primers were diluted to 10 µM. For all genetic cloning using PCR, Platinum® Pfx DNA Polymerase

(Thermo Fisher) was used as per the manufacturer's protocol. For overlapping primer PCR, 1 μ M of each primer was used. When using PCR to confirm the identity of a plasmid, Platinum® Taq DNA Polymerase (Thermo Fisher) was used as per the manufacturer's protocol. In all instances of PCR performed in this work, an annealing temperature of 55°C and 30 cycles was sufficient to generate amplicon. An overview of all PCR primers used in this study can be found in **Sup. Table 6.1**.

2.1.4 Quantification and Agarose Gel Electrophoresis of DNA

Plasmid DNA was isolated from *E. coli* using the Geneaid™ High-Speed Plasmid Mini Kit as per the manufacturer's protocol. Briefly, an overnight culture of bacteria was grown at 37°C with shaking (250 RPM) for 16 hours. The plasmid mini kit uses a modified protocol for the alkaline lysis method of extracting bacterial plasmids (Bimboim & Doly, 1979). Plasmids were eluted in UltraPure™ DNase/RNase-Free Distilled Water for use in all downstream applications. DNA samples were quantified using a NanoDrop® Spectrophotometer ND-1000 with the ND-1000 data viewer program.

DNA samples to be analyzed by electrophoresis were mixed at a 4:1 ratio with 5X loading dye (50% w/v sucrose, 0.05 M EDTA, 0.1% w/v Bromophenol Blue, 4 M Urea, pH 7.0). Agarose gels were prepared in varying concentrations by heating agarose (0.4% to 4% (w/v)) with 1X TAE buffer (40 mM Tris, 20 mM Acetate, 1 mM EDTA) and adding ethidium bromide to a final concentration of 5 μ g/mL. After loading DNA samples, DNA was electrophoresed through the gel for 60 minutes at 120 V using the PowerPac Basic Power Supply (Bio-Rad) with 1X TAE as running buffer. The gel was imaged under UV light using the GelDoc™ XR+ (Bio-Rad) system with the quantity one software.

2.2.1 Preparation of Chemically Competent *E. coli*

The *E. coli* strains used in this study were BL21 (DE3), Rosetta (DE3), and TURBO. To induce chemical competency, *E. coli* was grown with vigorous shaking (250 RPM) at 37°C in LB broth (1% w/v tryptone, 0.5% w/v yeast extract, 1% w/v NaCl) overnight. The overnight culture was inoculated in to fresh LB broth at a ratio of 1:100 and grown to an OD₆₀₀ of approximately 0.5. The cells were then chilled on ice for 15 minutes and pelleted by centrifuging them at 3000 RPM for 10 minutes at 4°C. The cell pellet was resuspended in ice cold 10 mM MgSO₄ and incubated on ice for 30 minutes before being pelleted, as described previously. Pelleted cells were resuspended in ice cold 50 mM CaCl₂ and chilled on ice for an additional 30 minutes before being pelleted. Finally, the cells were resuspended in ice cold 50 mM CaCl₂ containing 15% (v/v) glycerol, divided in to 100 µL aliquots, flash frozen, and stored at -80°C for subsequent use.

2.2.2 Transformation of Chemically Competent *E. coli*

To transform *E. coli*, an aliquot of chemically competent *E. coli* was thawed on ice and approximately 10 ng of plasmid DNA was added to the cells. Cells were mixed by gentle swirling with a pipette tip, after which they were incubated on ice for an additional 30 minutes. Cells were then heat shocked by incubating the tube in a 42°C water bath for 45 seconds followed by another incubation on ice for three minutes. After adding 500 µL of SOC media (2% w/v tryptone, 0.5% w/v yeast extract, 0.05% w/v NaCl, 5 mM KCl, 10 mM MgCl₂, 4 mM glucose), cells were incubated at 37°C with shaking (250 RPM) for an additional one hour. Afterwards, 100 µL of the transformed cells were plated on LB agar

plates containing either 100 µg/ml ampicillin or 30 µg/ml kanamycin using sterile glass beads. The remaining transformed cells were pelleted for one minute at 13,000 RPM, resuspended in 100 µL of SOC media, and plated. Plates were incubated at 37°C overnight and individual colonies were selected, grown overnight in LB broth, and screened. Stocks of *E. coli* were made by mixing a confluent overnight culture with sterile 50% glycerol at a 1:1 dilution and storing at -80°C for subsequent use.

2.3.1 Hexa-histidine Tagged Recombinant Protein Expression and Affinity Purification

Escherichia coli BL21 (DE3) or Rosetta (DE3) containing recombinant plasmid was grown overnight in LB broth with 100 µg/mL ampicillin at 37°C with vigorous shaking (250 RPM). Stationary phase cells were inoculated in 6 L of pre-warmed LB containing 100 µg/mL ampicillin at a 1:60 ratio. The cells were grown under identical conditions until an optical density (OD₆₀₀) of approximately 0.6 was achieved. Expression of recombinant proteins was induced by the addition of isopropyl β-D-1-thiogalactopyranoside (IPTG) to a final concentration of 0.2 mM. Cells were grown for an additional 2.5-3 hours at 37°C with shaking. Cells were pelleted by centrifugation at 16,000 x g for 6 minutes (4°C) and resuspended in 30 mL of Nickel Buffer A (20 mM Tris-HCl pH 7.0, 0.03% v/v LDAO, 0.02% v/v β-mercaptoethanol, 500 mM KCl, 10% v/v glycerol, 10 mM imidazole) adjusted to a pH of 7.0. To inhibit the action of proteases in the cell lysate, 2 Pierce™ Protease Inhibitor Mini Tablets (EDTA-Free) (Thermo Fisher) were dissolved in the cell suspension. To lyse cells, the cell suspension was pulse sonicated six times at approximately 20 watts

on ice (Fisher Scientific Sonic Dismembrator – Model 100). Sonication was performed in 20 second intervals with a 30 second rest period between each pulse. To separate the soluble portion from the insoluble portion, the cell suspension was centrifuged at 46,000 x *g* for 45 minutes (4°C). The supernatant was vacuum filtered through a 0.22 µM GP Millipore Express® bottle filter and kept on ice prior to purification.

To separate hexa-histidine tagged proteins from the rest of the cell lysate, affinity chromatography, utilizing the ÄKTA Protein Purification System (GE Healthcare), was used. Filtered cell lysates were loaded into a Superloop (GE Healthcare) and passed over a HisTrap™ HP column pre-loaded with Ni Sepharose™ (GE Healthcare). The column was then washed with Nickel Buffer A. Non-specifically bound proteins were removed by washing with a stepwise increasing concentration of Nickel Buffer B (20 mM Tris-HCl pH 7.0, 0.03% v/v LDAO, 0.02% v/v β-mercaptoethanol, 500 mM KCl, 10% v/v glycerol, 300 mM imidazole) and bound proteins were eluted with 100% Nickel Buffer B. Eluted protein was collected and exchanged into 1X PBS (Lonza) containing 10% (v/v) glycerol using a HiPrep™ 26/10 Desalting Column (GE Healthcare). The buffer exchanged protein was filtered through an Acrodisc® Low-Protein Binding 0.2 µM Supor® Syringe Filter (Pall) and concentrated using an Amicon® Ultra-15 Centrifugal Filter Device (Millipore) at 2,000 x *g* for 45 to 60 minutes (4°C). Protein aliquots were stored at -80°C for future use. To strip and store the HisTrap™ HP column, 20 column volumes each of 50 mM EDTA, ddH₂O, and 20% ethanol were washed through the column, and it was capped at both ends. The column was re-charged by washing with 20 column volumes of 100 mM Nickel(II) chloride.

2.3.2 Purification of Elastin-Like Polypeptide Fusion Constructs

To purify ELP fusion constructs a unique mechanism, inverse transition cycling (ITC), was used as described by Hassouneh et al. (2012). *Escherichia coli* BL21 (DE3) containing recombinant plasmid was grown overnight in LB broth with 100 µg/mL ampicillin at 37°C with vigorous shaking (250 RPM). Stationary phase cells were inoculated in 1 L of pre-warmed terrific broth (1.2% w/v tryptone, 2.4% w/v yeast extract, 0.4% v/v glycerol, 17 mM potassium phosphate monobasic, 72 mM potassium phosphate dibasic) with 100 µg/mL ampicillin at a ratio of 1:1000. Cells were grown for 24 hours at 37°C (250 RPM) without IPTG induction. After 24 hours, cells were harvested by centrifugation at 16,000 x g for six minutes (4°C) and cell pellets were resuspended in 70 ml of PBS. Cells were pulse sonicated on ice at approximately 45 watts for nine minutes by sonicating in cycles of 10 seconds followed by 20 seconds of rest. To precipitate DNA contaminants, polyethylimine (MP Biomedicals) was added to a final concentration of 0.5% v/v. The lysate was centrifuged at 16,000 x g for 20 minutes (4°C) and the supernatant was added to 50 ml canonical tubes (Greiner Bio-One). To oligomerize ELP protein, NaCl salt was added step-wise to the harvested supernatant until it appeared cloudy and turbid. The oligomerized protein was harvested by centrifugation at 16,000 x g for 10 minutes (room temperature) and the protein pellet was resuspended in 10 ml of PBS.

To perform one round of ITC, NaCl was added to the solubilized protein in a step-wise fashion until it appeared turbid. This sample was aliquoted in to 1.5 mL centrifuge tubes and pelleted at 16,000 x g (room temperature) for 10 minutes. The supernatant, containing soluble contaminants, was discarded while the pellet was resuspended in half

the volume of PBS. To remove insoluble contaminants, this solution was spun at 16,000 x *g* for 10 minutes (4°C) and the supernatant was retained. Typically, three to five rounds of ITC are performed to obtain a pure product. To determine how many rounds of ITC should be performed, an aliquot of protein was saved after each round of ITC and analyzed using zinc staining, as per section 2.4.2, to determine the purity of the protein sample. For each ELP fusion protein used in this study, four rounds of ITC were performed. On the final round of ITC, the protein was resuspended in PBS to the final desired volume. Purified protein was filtered through an Acrodisc® Low-Protein Binding 0.2 µM Supor® Syringe Filter and stored at -20°C for future use. An overview of the ITC process is outlined in **Sup. Fig. 6.3**. All expression strains used in this study can be found in **Sup. Table 6.2**.

2.4.1 Gel Electrophoresis of Protein Samples

To prepare protein samples for electrophoresis, protein was mixed at a 1:4 ratio with 5X laemmli loading buffer (4% v/v SDS, 100 mM Tris pH 7.0, 2 mM EDTA, 10% v/v glycerol, 0.002% w/v bromophenol blue, 12.5% v/v β-mercaptoethanol) and placed in a heat block at 100°C for 10 – 30 minutes. Protein samples were electrophoresed on polyacrylamide gels ranging from 8–15%. Polyacrylamide gels were prepared with both a resolving gel (375 mM Tris-HCl pH 6.8, 0.1% v/v SDS, 0.4% v/v TEMED, 8-15% v/v Acryl/Bis-Acryl, and 0.1% v/v APS) and stacking gel. The stacking gel was identical to the resolving gel, but composed of 5% (v/v) Acryl/Bis-Acryl. The solidified gels were loaded into the mini-PROTEAN Tetra Cell (Bio-Rad) vertical polyacrylamide apparatus and the protein samples were loaded in the wells of the polyacrylamide gel. The protein samples were electrophoresed through the stacking gel at 80 V for 20 minutes using the PowerPac

Basic Power Supply (Bio-Rad) before being separated for an additional 80 minutes at 120 V. Proteins were electrophoresed in SDS-PAGE running buffer (25 mM Tris, 192 mM Glycine, 0.1% w/v SDS). To transfer the separated proteins samples to a nitrocellulose membrane, the iBlot Gel Transfer Device (Invitrogen) was used as per manufacturers protocol. To determine the approximate size of the electrophoresed proteins, an aliquot of BLUelf Prestained Protein Ladder (FroggaBio) was loaded on to each gel. The approximate size of a protein was determined by comparing its size to the closest band size of the protein ladder.

2.4.2 Assessment of Protein Purity Using Coomassie, Zinc Sulphate, and Ponceau S Red Staining

To non-specifically detect protein separated on a polyacrylamide gel, three different techniques were used: Coomassie staining, Ponceau S red staining, and zinc sulphate staining. Each of these techniques has various advantages and sensitivities, and were used for different applications. For Coomassie staining of polyacrylamide gels, the gel was first incubated with a Coomassie stain solution (0.25% w/v Coomassie R-250, 45% v/v methanol, 10% v/v glacial acetic acid) for one hour with rocking. To eliminate background staining, the gel was then incubated in destaining solution (45% v/v methanol, 10% v/v glacial acetic acid) and banding patterns were analyzed.

To detect proteins using zinc sulphate negative staining, the polyacrylamide gel was incubated in zinc staining solution 1 (0.2 M imidazole, 0.1% w/v SDS) for 15 minutes. Following this, the gel was transferred in to zinc stain solution 2 (0.3 M ZnSO₄) for 30 seconds to two minutes until sufficient staining was observed. To stop the staining reaction,

the gel was rinsed and stored in ddH₂O. When necessary, the gel was destained with zinc destain solution (0.1% w/v SDS, 75 mM Tris-HCl, 0.2 M glycine) for 30 minutes and subsequently transferred to a nitrocellulose membrane, as per section **2.4.1**, for downstream applications.

To visualize proteins via Ponceau S Red staining, the polyacrylamide gel was first transferred to a nitrocellulose membrane. The nitrocellulose membrane was then stained by incubating it with Ponceau S stain solution (BioShop) for 2 minutes. To visualize protein bands, the membrane was destained using three short ddH₂O washes. After staining, the membrane could be used for all downstream applications.

2.4.3 Western Blotting

To visualize tagged proteins separated by polyacrylamide gel electrophoresis, Western blot analysis was used. After being separated by electrophoresis, proteins were transferred to a nitrocellulose membrane as per section **2.4.1**. Membranes were blocked with 20 mL of blocking buffer (PBS, 0.1% v/v Tween-20, 5% w/v skim milk powder) for one hour at room temperature with rocking. The membranes were then incubated with primary antibodies, diluted in 20 mL of blocking buffer, for one hour (room temperature) or overnight (4°C) with rocking. The primary antibodies were used at the following concentrations: mouse anti-polyhistidine (Sigma-Aldrich) (1:10,000), mouse anti-GST (Sigma-Aldrich) (1:5,000), mouse anti- α -Tubulin (GenScript) (1:10,000), and rabbit anti-laminin (BioLegend) (1:500). To wash away non-specifically bound antibodies, the membrane was washed three times for five minutes with PBS + 0.1% v/v Tween-20. Following the wash, the membranes were incubated with goat anti-mouse (Sigma-Aldrich)

(1:5,000) or goat anti-rabbit (Sigma-Aldrich) (1:5,000) antibody conjugated to horse radish peroxidase, diluted in 20 mL of blocking buffer. After incubating for one hour at room temperature with rocking, the membranes were washed three times, as before. To detect a signal, enhanced chemiluminescence solution (ECL) (Pierce) was washed over the membrane, and membranes were exposed to CL-XPosure™ (ThermoFisher) film paper in the dark. Film was developed using the Konica SRX-101A Tabletop Photo Processor.

2.4.4 Quantification of Protein Samples

To quantify purified protein, a modified version of the standard Lowry procedure was performed (Lowry, Rosebrough, Farr, & Randall, 1951). Briefly, protein standards of various concentrations were made by dissolving bovine serum albumin (BSA) in the same buffer as the purified protein. An aliquot of protein sample and all standards were mixed with 127.5 μ L of DC™ Protein Reagent A (BioRad), containing alkaline copper tartrate, followed by 1 mL of DC™ Protein Reagent B (BioRad), containing folin, as per the manufacturer's protocol. Each sample absorbance was read at an OD of 750 nm on a spectrophotometer (Ultrospec 4300 Pro), and a standard curve was established using the BSA standards. Based on the absorbance of the unknown protein, its concentration was calculated using the line of best fit from the standard curve as a reference.

2.4.5 Protein Sample Concentration using TCA Precipitation

When necessary, protein samples were concentrated using Trichloroacetic acid (TCA) precipitation. To perform a TCA precipitation, TCA was added to a final concentration of 10% (v/v) to the protein sample and the sample was incubated on ice for 60 minutes. Precipitated protein was pelleted by centrifugation at 16,000 x *g* for five

minutes at 4°C. The supernatant was discarded while the pellet was washed three times in ice cold acetone for 1 hour at -80°C, with centrifugation at 16,000 x g for five minutes (4°C) after each incubation. The supernatant was discarded and the pellet was dried on a heat block at 100°C for 10 minutes. The pelleted protein was resuspended in 5X laemmli buffer to run on a polyacrylamide gel.

2.4.6 Thermal Characterization of ELP Fusion Constructs

To measure the transition temperature of ELP fusion constructs, a sample of ELP protein was diluted to 50 µM in DMEM containing 10% FBS. The sample was loaded into two quartz cuvettes (Beckman). One cuvette was left at room temperature and used as a reference blank while the other was subjected to an increase in temperature. To increase the temperature of the ELP solution, the quartz cuvette was incubated in a water bath for 10 minutes at various increasing temperatures. After it was equilibrated with the water bath, the cuvette was immediately dried and placed in a spectrophotometer. To determine the degree of turbidity the OD was measured at 350 nm, using the room temperature sample as a reference blank.

2.5.1 Cell Culture Seeding and Passaging

The following cell types were obtained from ATCC and used in this study: Madin-Darby Canine Kidney (MDCK) (canine kidney), LLC-MK2 (rhesus monkey kidney), and A549 (human lung carcinoma). All cell lines were grown in Dulbecco's Modified Eagle Medium (DMEM) (ThermoFisher) supplemented with 10 % v/v fetal bovine serum (FBS). All cells were maintained in an incubator at 37°C with 5% CO₂ in 25 cm², 75 cm², or 175

cm² sterile tissue culture flasks (Greiner Bio-One). Cells were passaged every two to five days, as necessary, at a ratio of 1:2 to 1:10. To passage cells, existing media was aspirated and monolayers were washed with 1 mL of 0.05% Trypsin-EDTA (Invitrogen) to remove any residual FBS. The wash media was aspirated and 4 mL of Trypsin-EDTA was added to the flask. The cells were incubated at 37°C with 5% CO₂ for up to 10 minutes or until cells had visually dissociated from the monolayer. The cells were resuspended in DMEM with 10% FBS, to inhibit trypsinization, and added to the appropriate tissue culture flask at the desired ratio.

For experiments involving six-well plates, 24-well plates, or coverslips in shell vials, cells were trypsinized, as described previously. After resuspending the cells in DMEM with 10% FBS, the cells were harvested by centrifugation at 500 x g for five minutes. Media was aspirated off the pelleted cells and they were resuspended in 10 mL of DMEM with 10% FBS. An aliquot of cells was mixed at a 1:1 ratio with 0.4% Trypan Blue, and 10 µL of this was added to a chamber of a Bright-Line Hemacytometer (Hausser Scientific) by capillary action. Cells were counted and cell numbers were calculated by averaging the counts on four squares of the hemacytometer, as per the manufacturer's protocol. Cells were seeded on to plates or coverslips, based on a previously established cell density, to achieve confluency after 24 or 48 hours.

2.5.2 Cell Culture Cryopreservation and Thawing

For long term storage of cells, a confluent 75 cm² cell culture flask was trypsinized, as per section 2.5.1, and cells were harvested by centrifugation at 500 x g for five minutes. The supernatant was aspirated off the harvested cells and cells were resuspended in 5 mL

of DMEM with 10% v/v FBS and 10% v/v DMSO. Resuspended cells were dispensed in 1 mL aliquots into 2 mL cryopreservation vials (Argos Technologies) and the cells were frozen at -80°C. After 24 hours, the cells were placed in liquid nitrogen storage for long term preservation. To restore frozen cells, an aliquot was taken from liquid nitrogen and thawed rapidly in a 37°C water bath. Thawed cells were added dropwise to 10 mL of DMEM with 10% FBS and pelleted by centrifugation at 500 x *g* for five minutes. The supernatant was aspirated and cells were resuspended in 5 mL of DMEM with 10% FBS and grown in a 25 cm² cell culture flask at 37°C with 5% CO₂. After 24 hours, the culture media was replaced to remove any unattached cells.

2.6.1 Influenza Propagation

All propagation of influenza was performed using the MDCK cell line. Aliquots of unknown concentration of pandemic *Influenza A* virus H1N1 (A/California-like/04/2009(H1N1)) or *Influenza A* virus H3N2 (A/Victoria/3/1975(H3N2)) were obtained from clinical specimens at the St. Joseph's Hospital virology laboratory. To culture virus, a confluent 75 cm² flask of MDCK cells was prepared, as per section 2.5.1. Before infecting the flask, it was washed three times with DMEM to remove any residual FBS. The virus was diluted 1:500 in 10 mL of DMEM containing 100 units/ml of penicillin and 100 µg/mL of streptomycin (ThermoFisher) and 1 µg/ml TPCK-treated trypsin (Sigma-aldrich). The diluted virus was added to the 75 cm² flask containing MDCK cells and incubated at 37°C with 5% CO₂. Every 24 hours, infected cells were visualized under a light microscope and compared to a no-virus control for signs of cytopathic effect. Virus was harvested when the cells displayed 50 – 80% cytopathic effect, which typically

occurred after two to four days. To harvest virus, the supernatant was collected and transferred to a 50 mL conical tube. To disrupt membranes of floating cells, the supernatant was vortexed with glass beads twice for 30 seconds before being centrifuged at 500 x g for five minutes. The supernatant was collected, filtered using a 0.2 µM Supor® Syringe Filter (Pall), and stored at -20°C in 100 µL aliquots.

2.6.2 – Influenza Titering Using Plaque Assays

All plaque assays were performed using the MDCK cell line and were performed based on a modified protocol from Szretter et al. (2006). MDCK cells were seeded in a 6-well plate, as per section 2.5.1, and allowed to fully attach to the plate for three days. To perform the plaque assay, monolayers were washed three times with DMEM and 100 µL of influenza virus, at various (diluted ten-fold in DMEM) concentrations, was added to the monolayers. The plate was incubated at 37°C with 5% CO₂ for 45 minutes. During the incubation, a solution of 1.6% w/v agarose was mixed at a 1:1 ratio with 2X DMEM containing 2 µg/ml TPCK-treated trypsin (Sigma-Aldrich) and stored at 44°C. After washing each well twice with DMEM, 2 mL of the agarose solution was applied to each well. The plates were incubated at 37°C with 5% CO₂ and observed for plaque formation each day. After three days, the monolayers were fixed by adding 2 mL of 10% buffered formalin (10% v/v formalin, 33 mM sodium phosphate monobasic, and 46 mM sodium phosphate dibasic) directly to each agar plug and incubating the plate for 30 minutes at room temperature. After fixing, the agar plugs were removed and the monolayer was stained with 0.5% w/v crystal violet for 30 minutes. Crystal violet was washed away with ddH₂O and circular areas devoid of staining were counted as plaques. Based on the number

of plaques and the dilution factor, virus was quantified in plaque forming units per mL (PFU/mL).

2.7.1 Assessing Protein Toxicity with A549 Growth Assays

To assess the toxicity of the protein constructs used in this study, the growth of A549 cells was monitored in the presence of protein. A549 cells were seeded to under-confluency on a 6-well plate, as per section 2.5.1. Purified recombinant protein or cycloheximide (Sigma-Aldrich) was diluted to the desired concentration in DMEM containing 10% FBS. Next, 1 mL of media containing no protein, protein (at various concentrations), or cycloheximide was added to the under-confluent monolayers and cells were incubated for up to 48 hours. To assess cell growth, cell density was measured at defined time points and compared to the no-peptide control. To measure cell density, wells were first washed with 500 μ L PBS to remove detached cells and then treated with 1 mL of trypsin for five minutes or until all cells had dissociated from the plate. To ensure that all cells had properly dissociated from the plate, each well was visualized using light microscopy. The trypsinized cells were loaded into cuvettes and absorbance was read at 800 nm on a spectrophotometer (Ultrospec 4300 Pro), using trypsin alone as a reference blank. The OD₈₀₀ reading can be used to accurately measure cell density regardless of media the cells are contained in (Mohler, Charlton, & Blau, 1996). Cyclohexamide was used as an inhibitor of eukaryotic translation (Ennis & Lubin, 1964) and thus was a positive control.

2.7.2 Assessing Protein Uptake Using Nuclear Localization Assays

Protein uptake in cell culture was assessed using both the LLC-MK2 and MDCK cell lines. To assess uptake, cells were seeded to confluency in 6-well tissue culture plates, as per section **2.5.1**. Recombinant proteins were diluted to 50 μ M in DMEM alone, 1 mL of which was added to each monolayer. After 24 hours, DMEM was removed and cells were washed twice in PBS. The cells were then incubated with an ice-cold acid wash buffer (0.2 M glycine buffer; 0.15M NaCl; pH 3.0) for one minute before being washed once more with PBS. Acid wash buffer was used to remove cell-surface bound proteins (Kameyama et al., 2007). Following the acid wash, 500 μ L of ice cold nuclear localization buffer (10 mM HEPES buffer pH 7.5; 10 mM KCl; 0.1 mM EDTA; 0.4% v/v IGEPAL; 0.5 mM PMSF; 1 Pierce™ Protease Inhibitor Mini Tablet (EDTA-Free)) was added to the cells, and incubated at room temperature for 10 minutes. After 10 minutes, cells were dissociated from the monolayer using a cell scraper and the supernatant was transferred to a 1.5 mL tube and incubated on ice for an additional 10 minutes. To ensure all cells were properly dissociated from the monolayer, each well was observed using light microscopy. The nuclear extraction buffer containing the lysed cells was spun at 16000 x g for three minutes to separate the nuclear and cytoplasmic fraction. The pelleted nuclear portion was washed three times in nuclear extraction buffer and resuspended in 5X laemmli buffer. The cytoplasmic supernatant portion was TCA precipitated, as per section **2.4.5**, before being resuspended in 5x laemmli buffer. The resuspended samples were boiled on a heat block for 10 minutes and separated on a polyacrylamide gel, as per section **2.4.1**. A Western blot

of the gel was performed to detect hexa-histidine tagged proteins, α -Tubulin, and laminin A, as per section 2.4.3.

2.7.3 Assessing Protein Interaction Using GST Pull-Down Assays

GST pull-down assays were used to explore whether two proteins interacted. *Escherichia coli* containing recombinant GST plasmids were grown and protein was overexpressed using IPTG. Lysates were obtained as per section 2.3.1, with the sole exception that the bacterial pellet was resuspended in 1x PBS instead of Nickel A Buffer. Lysates containing GST proteins (bait) were incubated with Glutathione High Capacity Magnetic Agarose Beads (Sigma-Aldrich) at 4°C for one hour with shaking. After one hour, the beads were pelleted by centrifuging them at 500 x g for five minutes and the supernatant was aspirated. The beads were resuspended in 50 mL of blocking buffer (PBS, 0.1% v/v Tween-20, 5% w/v BSA) and again incubated for one hour at 4°C with shaking. The beads were pelleted as before and the supernatant was removed until 5 mL remained. The beads were resuspended in the remaining blocking buffer and 500 μ L of beads were added to a 1.5 mL tube for each sample. Purified proteins containing hexahistidine tags (prey) were diluted to approximately 1 mg/mL in blocking buffer and 500 μ L was added to each condition. The beads were incubated overnight at 4°C with shaking.

The 1.5 mL tubes containing beads were placed into the NucliSENS miniMag® and the supernatants were removed, using the magnet to ensure minimal bead loss. To wash the beads, 1 mL of PBS was added to each tube and the NucliSENS miniMag® was run for one minute with one second spin intervals. This process was repeated seven times to ensure the beads were sufficiently washed. After the seventh wash, the beads were resuspended in

laemmli buffer and boiled for 10 minutes before proteins were separated on a polyacrylamide gel, as per section 2.4.1. Western blot of the gels was performed to detect hexa-histidine tagged proteins and GST-tagged proteins, as per section 2.4.3.

2.8 Viral Inhibition Assay Using Fluorescence Microscopy

To determine whether the proteins could inhibit influenza replication, viral inhibition was assessed using fluorescence microscopy. To perform the assays, confluent monolayers of MDCK cells were established in 24-well plates, 96-well plates, or on shell vials with coverslips, as per section 2.5.1. To perform the inhibition assay, the MDCK monolayers were washed twice with DMEM, protein was diluted in DMEM to the desired concentration, and 100 μ L or 500 μ L of the protein was added to the monolayers. The cells were incubated at 37°C with 5% CO₂ for 60 minutes. After incubating the cells with protein, the cells were infected with *Influenza A* H3N2 or H1N1 virus using centrifuge-assisted infection. To perform this, the virus was diluted to a pre-determined dilution factor in DMEM and 500 μ L or 100 μ L (96-well plates) was added to each monolayer. The cells were centrifuged at 1,500 x *g* for 30 minutes and were then incubated at 37°C with 5% CO₂ for an additional 30 minutes. The virus media was removed from the monolayers and the cells were treated with another round of protein in DMEM and incubated at 37°C with 5% CO₂ for an additional 12-24 hours.

To view infected cells, coverslips were fixed using ice cold acetone, while 24-well or 96-well plates were fixed with the addition of ice cold methanol for 30 minutes. After fixing, cells were washed with PBS + 0.1% v/v Tween-20 and blocked using a blocking solution (50 mg/ml BSA; PBS; 0.1% v/v Tween-20) for one hour at room temperature.

After blocking, mouse anti-Influenza A virus nucleoprotein 1 antibody (Abcam) was diluted 1:5,000 in blocking solution and applied to each condition. Cells were incubated for one hour at 37°C with shaking before being washed three times with PBS + 0.1% v/v Tween-20.

A goat anti-mouse antibody conjugated to FITC (Cedar Lane) was diluted 1:200 in blocking solution and was applied to each condition; this and all following steps were performed in the dark. The secondary antibody was incubated at 37°C for one hour with shaking before being washed three times with PBS + 0.1% v/v Tween-20. To counter stain cells, 0.04% w/v Evans Blue was applied to each condition and incubated on cells for 30 minutes at room temperature. After washing three times with PBS + 0.1% v/v Tween-20, shell vials were mounted on glass slides using mounting solution (PBS with 50% v/v glycerol) and visualized. Alternatively, 24-well and 96-well plates were directly visualized using fluorescence microscopy. To visualize stained cells, the EVOS FL Cell Imaging System was used. Evans Blue stained cells were visualized using the texas red lens and FITC was visualized using the gfp lens.

2.9 – Statistical Methods

All statistics were performed using the GraphPad Prism 7.0 software. Error bars in figures **3.7**, **3.10**, and **3.11** were calculated as plus or minus one standard deviation from the mean. For figures **3.10** and **3.11** the P-values were calculated using a two-way ANOVA with the Dunnett test for multiple comparisons to a virus only control (ns $P > 0.05$; * $P < 0.05$; ** $P < 0.01$; *** $P < 0.001$; **** $P < 0.0001$).

Chapter 3 – Results

RESULTS

3.1.1 Design of Recombinant Proteins

The HisMBP construct was previously designed and cloned by Kenneth A. Mwawasi. All work done with this construct used his bacterial stock containing the cloned plasmid. The HisMBP carrier was chosen for its ability to increase solubility and its stability (Douette et al., 2005). The construct was cloned using the Gateway® cloning system with pDestHisMBP as the final cloning vector. The HIV-1 Tat CPP was used to ensure the protein construct could efficiently localize to the cell nucleus. The first 21 N-terminal amino acids of the wildtype PB1 sequence were used to inhibit the PB1-PA interaction. Since the plasmid cloning site is on the C-terminal end of the HisMBP carrier, the NLS and PB1 sequences were attached to the C-terminus of HisMBP. To ensure the 21-amino acid PB1 peptide was in the proper orientation, the sequence was flipped so that the methionine amino acid previously in position 1 of PB1 was now the final amino acid. The final fusion order of the expression construct was HisMBP-NLS-PB1 and an overview of the construct, including the lengths of each portion, is detailed in **Fig 3.1a**.

Elastin-like polypeptides were used as a carrier protein due to their high levels of expression and their similarity to human elastin. The ELP composition was chosen based on two main criteria; namely, the size of the construct and its predicted T_t . It was not necessary that the ELP carrier had a strictly defined T_t ; however, it was designed to be above 37 °C to limit any toxicity or negative effects due to aggregation. Additionally, the length of the ELP protein was limited to facilitate protein entry and limit any potential

shielding affects from the carrier due to its size. To achieve these criteria, an ELP construct was selected from a previously established library (McDaniel, Radford, & Chilkoti, 2013). We used an ELP construct (ELP[A0.2]₄₀) that was 40 repeats long and had a 1:4 ratio of alanine to valine at the guest residue (Xaa). The ELP[A0.2]₄₀ construct had a T_t of 50 °C at 50 μ M (McDaniel et al., 2013). Any changes to the T_t due to the fusion ΔT_t effect should still result in the construct being above physiological temperature.

The HIV-1 Tat CPP was again used to induce uptake into cells, as Tat-ELP constructs have demonstrated up to 70% cell internalization in 24 hours (Massodi, Bidwell, & Raucher, 2005). The PB1-T6R peptide mimetic was chosen instead of wildtype PB1, as it had previously been shown to inhibit the replication of influenza to a greater degree than wild-type PB1 (**unpublished data**). Although the HisMBP fusion protein was designed to have the fusion peptide on the C-terminus, the fusion peptide was placed on the N-terminus of the ELP construct. The fusion order of a protein can affect the expression, yield, solubility, and degradation rate of a protein; therefore, it must be assessed on a case-to-case basis. The effect of fusion order on ELP constructs has previously been examined and, in most cases, N-terminal peptide-ELP fusion proteins are expressed to higher levels than C-terminally fused peptides (Christensen et al., 2009). Two ELP constructs were designed; one containing a hexahistidine tag and Tev site for detection using Western blot, while the other had no fusion tags. The final constructs were T6R-NLS-His-Tev-ELP[A0.2]₄₀, where the His-Tev sequence is only present in one of the constructs. An overview of the ELP fusion constructs, including the lengths of each portion, is seen in **Fig 3.1b**.

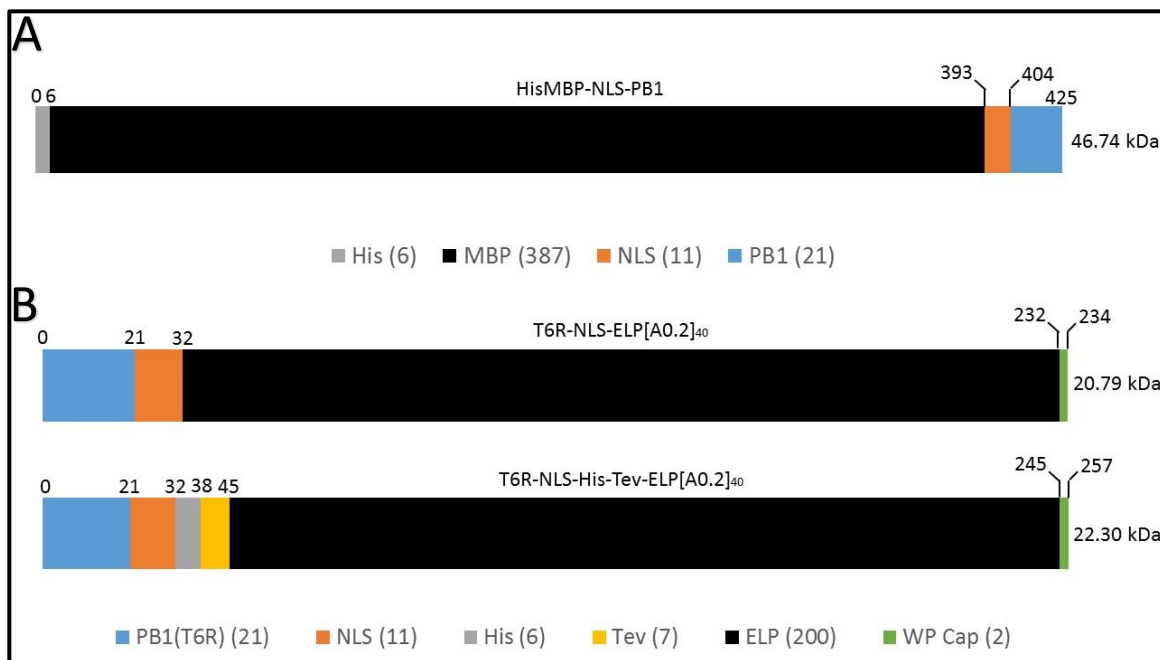


FIGURE 3.1 Structure of Recombinant Proteins Used in This Study

Boxcar diagram of the (a) HisMBP and (b) ELP recombinant proteins used in this study. Numbers in brackets indicate the amino acid length of that portion of the protein construct. Numbers on the diagram indicate the cumulative length of the protein construct in amino acids. Calculation of protein molecular weight was performed using the online ExPASy Compute pI/Mw tool and are therefore just a prediction of molecular weight.

3.1.2 Cloning of the PB1-Elastin-like Polypeptide Fusion Protein Using RDL

To clone the recombinant ELP, an ELP gene library consisting of ELP[A0.2] at varying repeats was first cloned using RDL. An overview of the RDL process is depicted in **Sup. Fig 6.2** and described in detail in section **2.1.2**. In brief, overlapping oligonucleotides corresponding to 5 repeats of ELP[A0.2] were amplified by PCR, and ligated into the pUC19 cloning vector. The ligated insert was doubled in length three times by performing three rounds of RDL. To perform this, the ELP insert was digested out of pUC19 using the BglII and PflMI restriction enzymes. The insert was re-ligated into insert-containing pUC19 plasmid that had been digested with PflMI only. To confirm the presence of a plasmid containing double length ELP insert, the plasmid was digested with restriction

enzymes and the insert size was analyzed using an agarose gel. The produced library had ELP sequences of 5, 10, 20, and 40 repeats (**Fig 3.2**). After cloning the library, overlapping oligonucleotides corresponding to the fusion sequence were amplified using PCR, and ligated in to the pET-25b(+) cloning vector. BglII and PflMI digested ELP insert of desired length was ligated into pET-25b(+) containing the correct fusion sequence. The resulting plasmid was transformed into *E. coli* BL21 for expression.

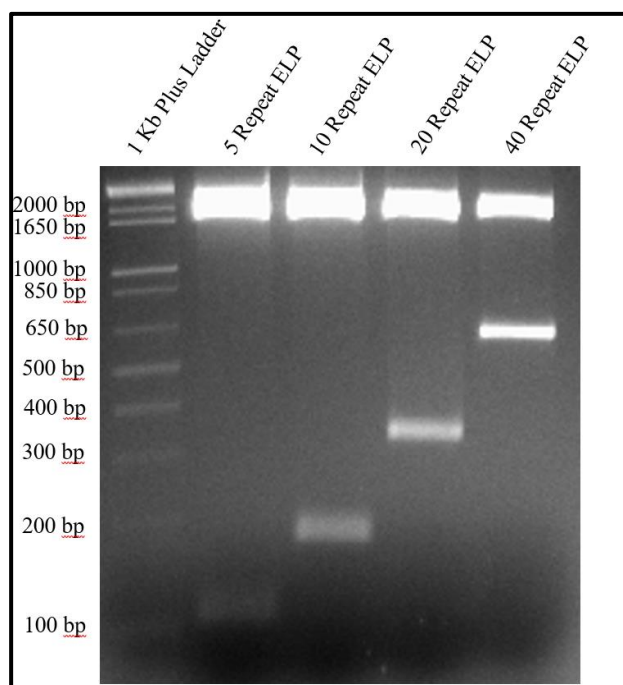


FIGURE 3.2 Library of ELP[A0.2] Containing 5, 10, 20, and 40 Repeats

Agarose gel demonstrating the cloned ELP[A0.2] library contained in the pUC19 plasmid. Plasmids containing various numbers of ELP repeats were digested with EcoRI and HindIII and 1000 ng of each digested plasmid was run on a 3% agarose gel. The gel was analyzed on the Biorad GelDoc™XR+ system using quantity one. Approximate dropout size can be determined by comparison with the 1kb plus ladder (Thermo Fisher). Expected sizes of the dropouts for plasmids containing 5, 10, 20, and 40 repeats are 108, 183, 333, and 633 basepairs respectively.

3.1.3 Expression and Purification of Hexahistidine Tagged Proteins

All hexahistidine tagged proteins were purified using affinity chromatography on the ÄKTA protein purification system (GE Healthcare), as described in section 2.3.1. Using affinity chromatography, HisMBP-NLS-PB1 was purified at yields of approximately 2 mg/L of culture. Protein lysates containing recombinant protein were passed over a HisTrap Ni sepharose column, washed with increasing imidazole concentrations, and eluted using a high concentration of imidazole (**Fig 3.3a**). The eluted protein was exchanged into PBS containing 10% glycerol using a HiPrep desalting column (**Fig 3.3b**). To ensure the previous buffer was not eluted off the column during the buffer exchange, the conductance percentage was monitored. The purification chromatograms were compared to previous protein purifications of the same recombinant protein, to ensure consistency between the protein preparations.

During the purification, the bound protein was washed with increasing amounts of imidazole in nickel B buffer; however, each wash resulted in some degree of protein loss. To analyze how much washing was required to obtain pure protein, samples of each of the 5%, 10%, and 15% wash were run on a polyacrylamide gel and analyzed using Ponceau S Red staining. The fraction eluted during the 15% wash had little breakdown and no contaminating proteins; therefore, only the 5% and 10% washes were performed for all following purifications (**Fig 3.3a**).

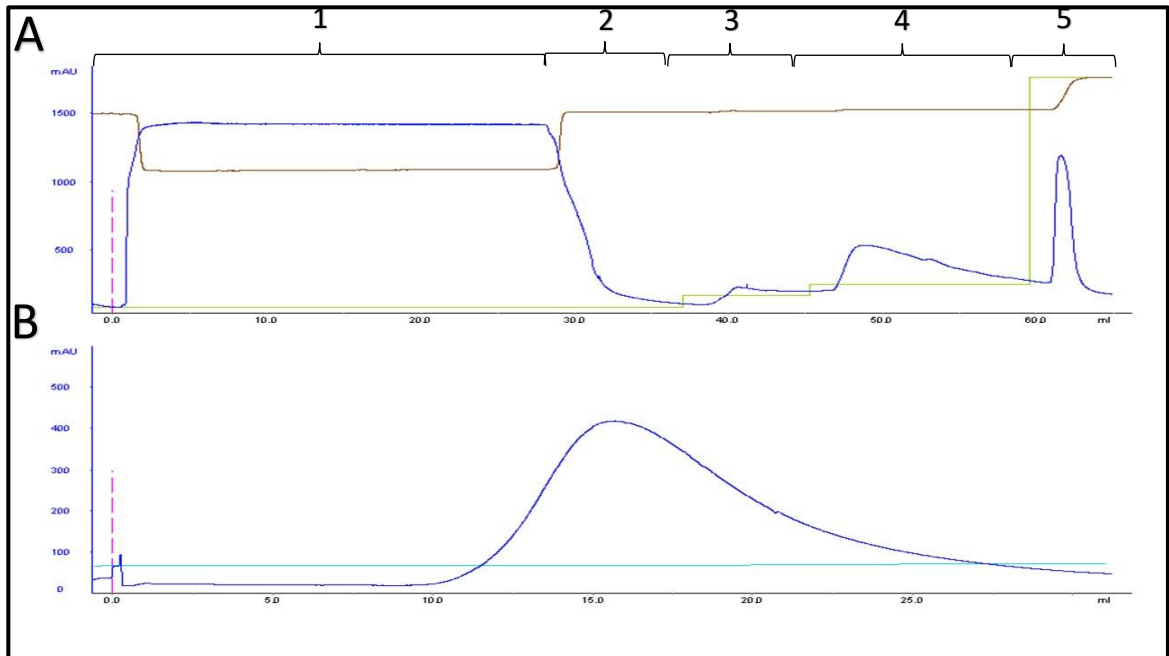


FIGURE 3.3 Purification and Buffer Exchange Chromatogram for HisMBP-NLS-PB1

Hexahistidine tagged proteins were purified by affinity chromatography using the ÄKTA protein purification system with Unicorn 4.11 software. Dark blue lines indicate UV (an indirect measure of protein), yellow is Nickel B percentage, and brown or light blue is conductance percentage (an indirect measure of salt). (a) [1] Cell lysates containing recombinant HisMBP-NLS-PB1 were loaded into a superloop (GE Healthcare) and passed over a HisTrap Column. [2] Non-specifically bound protein was washed away with Nickel A, [3] 5% Nickel B, and [4] 10% Nickel B. [5] Hexahistidine tagged protein was eluted off the column with 100% Nickel B. (b) To exchange the buffer into PBS + 10% glycerol, eluted protein was injected into a HiPrep desalting column. Protein was collected when the UV began to rise and stopped when the UV had leveled out. Percent conductance was monitored to ensure the previous buffer had not yet eluted.

3.1.4 Expression and Purification of Elastin-like Polypeptide Fusion Proteins

The ELP fusion proteins were purified using ITC, as described in section 2.3.2. Purification of ELP fusion proteins using ITC has many advantages over traditional purification methods including it being faster, more cost effective, and requiring few specialized lab instruments. Using ITC, ELP protein purifications could be completed in less than 2 hours after the cell lysate was obtained. The ITC process could be monitored throughout the entire procedure, as coacervation of protein was visually observed each time

the protein was brought above the required T_t through the addition of salt (**Fig 3.4**). Using ITC, the ELP recombinant proteins could be expressed and purified to yields of 30 – 60 mg/L of uninduced culture. This contrasts the purification of hexahistidine tagged proteins in our lab using affinity chromatography, which typically yields 1 – 5 mg/L.

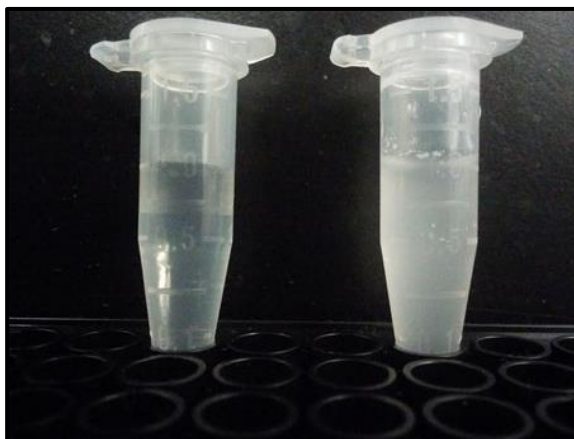


FIGURE 3.4 Precipitation of T6R-NLS-ELP[A0.2]₄₀ Using NaCl During Inverse Transition Cycling Purification

During ELP purification using ITC, soluble recombinant protein (left) is forced to concatamerize (right) with a stepwise addition of NaCl. Sodium chloride, which lowers the proteins apparent T_t , is added until the solution appears turbid. Concatamerized protein can be pelleted and the supernatant is removed to eliminate contaminating soluble protein.

For all downstream applications using ELP proteins, it was critical that purified proteins be pure and contain no contaminants. It was essential that no *E. coli* host proteins were present in the purified sample, as contaminating proteins could result in cellular toxicity. To obtain pure protein, 3 – 5 rounds of ITC are usually performed; however, this must be determined for each ELP construct individually. To determine how many rounds of ITC were required for high protein purity, aliquots of protein were saved after each round of ITC and assessed using ZnSO₄ stained polyacrylamide gels. The ZnSO₄ negative stain must be used to visualize ELP fusion constructs as most other commonly used staining techniques, such as Coomassie and Ponceau S staining, are not able to effectively detect

them (Hassouneh et al., 2012). Although it has been reported that some ELP fusion constructs migrate at an abnormal size on polyacrylamide gels, the T6R-NLS-ELP[A0.2]₄₀ construct had an apparent molecular weight of around 21 kDa, as predicted (**Fig 3.5**). After one round of ITC, the purified protein was approximately 95% pure with minor contaminating proteins present at approximately 35, 40, 48, and 60 kDa (**Fig 3.5**). After the second round of ITC, the purified protein had an apparent purity of 99% with all previously contaminating proteins now absent. For all subsequent purifications of ELP proteins, four rounds of ITC were performed. Four rounds were used to further limit the chance that small amounts of undetectable contaminants were present. Results obtained were similar for the T6R-NLS-His-Tev-ELP[A0.2]₄₀ construct.

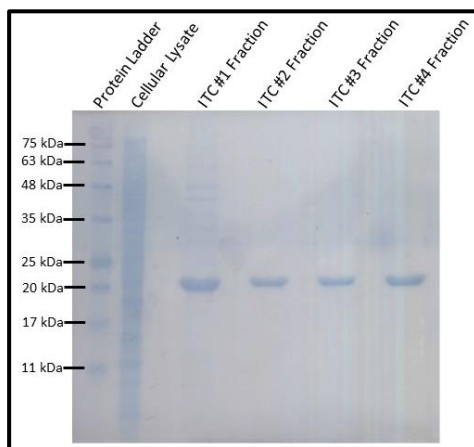


FIGURE 3.5 Purity of the T6R-NLS-ELP[A0.2]₄₀ After Each Round of Inverse Transition Cycling

Aliquots of T6R-NLS-ELP[A0.2]₄₀ were saved after each round of ITC and run on a 15% SDS-PAGE. To visualize protein, the gel was stained using ZnSO₄ staining. Approximate protein size can be estimated by comparing the sizes to the BLUelf Prestained Protein Ladder (FroggaBio). Using the online ExpASY Compute pI/Mw tool the T6R-NLS-ELP[A0.2]₄₀ protein construct is predicted to be 20.79 kDa.

3.1.5 Thermal Characterization of Elastin-like Polypeptide Fusion Proteins

To ensure the ELP fusion proteins did not have a T_t below physiological temperature, the transition temperature of the ELP constructs was measured by analyzing the turbidity of a protein sample at increasing temperatures. The ELP recombinant proteins were designed to have a T_t higher than physiological temperature to ensure its coacervation did not affect its function or nuclear localization. Since the ELP fusion proteins have a modified T_t due to the fusion ΔT_t effect, the modified T_t must be measured using temperature regulated turbidimetry. Below the T_t of the ELP, the fusion constructs are soluble and non-interacting, which results in the majority of light being able to pass through the solution. Once the T_t of the protein is reached, the insoluble proteins interact and oligomerize and less light can pass through the solution due to light scattering. The degree

of light scattering can be measured on a spectrophotometer at 350 nm and a precise T_t can be measured (Hassouneh et al., 2012).

The T_t of an ELP protein is dependent on the buffer composition and its concentration in solution; therefore, the assay was performed in DMEM media with 50 μ M of protein. These conditions mimic what would be used in cell culture experiments (Meyer & Chilkoti, 2004). The T_t of ELP proteins is defined as the temperature where the ELP has reached half its maximum OD_{350} value, which is calculated from the temperature regulated turbidimetry data (Schipperus, Teeuwen, Werten, Eggink, & De Wolf, 2009). The T_t of the T6R-NLS-ELP[A0.2]₄₀ protein at 50 μ M was determined to be 44.85 °C (**Fig 3.6**). Similar results were seen with the T6R-NLS-His-Tev-ELP[A0.2]₄₀ construct. The non-fusion ELP[A0.2]₄₀ reportedly had a T_t of 50 °C; however, the apparent decrease in T_t observed in the fusion constructs was not surprising since the fusion peptide was composed of 35% hydrophobic amino acids (McDaniel et al., 2013). Since the T_t of the constructs were above physiological temperatures, they were used for future cell culture experiments.

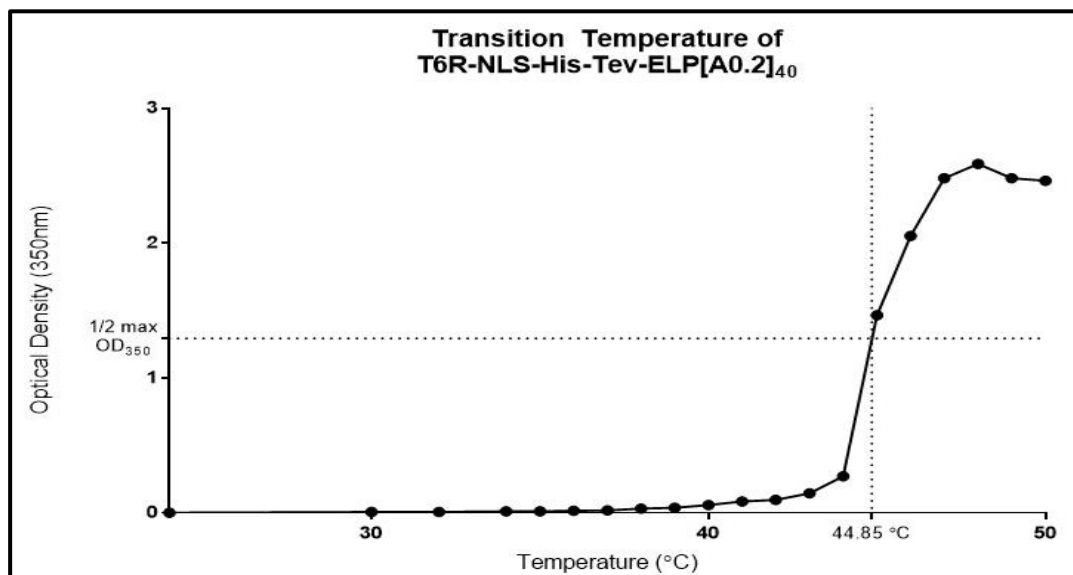


FIGURE 3.6 Thermal Characterization of T6R-NLS- ELP[A0.2]₄₀ Using Temperature Regulated Turbidimetry

The T6R-NLS-ELP[A0.2]₄₀ fusion protein was diluted to 50 μ M in DMEM in a Beckman quartz cuvette. The cuvette was equilibrated to various water bath temperatures for 10 minutes before turbidity was measured at 350 nm on a spectrophotometer (Ultrospec 4300 Pro). A separate sample at room temperature was used as a reference blank. The $\frac{1}{2}$ max OD₃₅₀ was plotted to determine the T_i of the ELP fusion construct.

3.2 The Elastin-like Polypeptide Fusion Protein Does Not Affect A549 Cell Replication

To ensure the recombinant T6R-NLS-ELP[A0.2]₄₀ protein was not toxic to cells, the growth rate of A549 cells, in the presence of protein, was assessed. The A549 cell line was chosen for this assay due to its human lung origin, which closely resembles the influenza virus target tissue. These cells are also susceptible to influenza infection. To assess cell replication, A549 cells were seeded to under-confluency in 6-well plates. Recombinant protein was added to the cells, and at various time cells were harvested and the cell concentration was assessed using spectrophotometry. To harvest cells, individual wells of the 6-well plate were treated with trypsin until all cells had released from the monolayer, which was confirmed using light microscopy. To measure cell density, the

absorbance of the trypsinized cells was measured using a spectrophotometer at a wavelength of 800 nm. The OD₈₀₀ can be used as a direct measurement of total cell number in a solution, regardless of the cell solution (Mohler et al., 1996).

A549 cells were treated with 50 μ M or 10 μ M of T6R-NLS-ELP[A0.2]₄₀ protein diluted in DMEM + 10% FBS, or with PBS diluted in DMEM + 10% FBS as a negative control. As a positive control, cells were also treated with 100 μ g/ml of cycloheximide diluted in DMEM + 10% FBS, which is known to inhibit eukaryotic protein translation and therefore cellular replication (Ennis & Lubin, 1964). Cells were harvested and cell density was assessed at the 0, 24, and 48-hour time points. At each time point, there was no difference in absorbance at OD₈₀₀ between cultures treated with recombinant protein and the PBS control, indicating the rate of cellular replication was similar in each condition (**Fig 3.7a**). At the 24 and 48-hour time points, cells treated with cycloheximide had a lower absorbance at OD₈₀₀ than both the recombinant protein and PBS treated conditions, indicating that replication was inhibited in cycloheximide treated samples (**Fig 3.7a**). Cells treated with cycloheximide had a slight decrease in absorbance at each successive time point, likely due to small amounts of cell death during the metabolically inactive state. Data is also shown as a bar graph to compare the differences between means at each time point (**Fig 3.7b**). Similar results were observed with the T6R-NLS-His-Tev-ELP[A0.2]₄₀ construct. Toxicity was not assessed for the HisMBP-NLS-PB1 construct, as previous members of the lab had already demonstrated the construct was not toxic to MDCK cells (**Sup. Fig 6.4**).

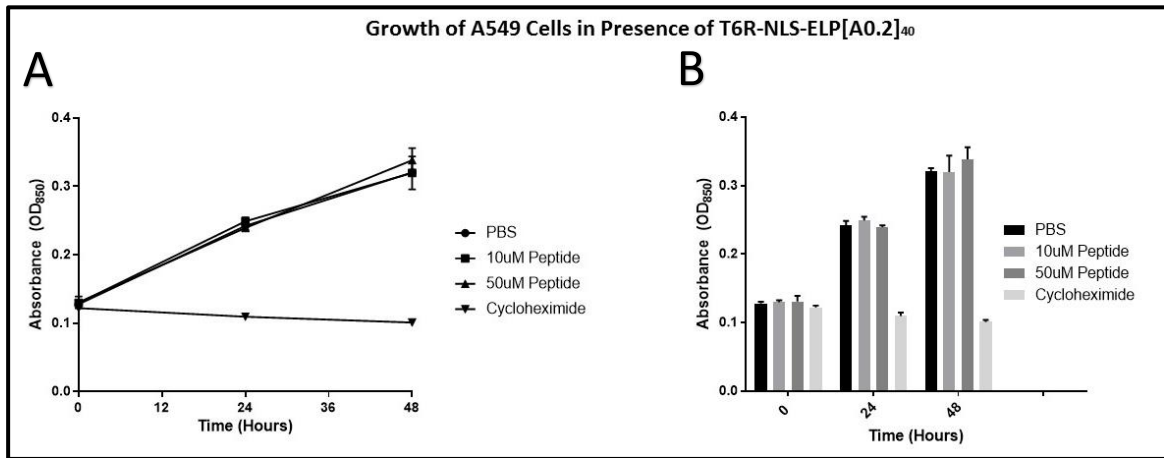


FIGURE 3.7 Growth of A549 cells in presence of T6R-NLS-ELP[A0.2]₄₀

A549 cells were seeded in triplicate into 6 well plates at a density of 250 000 cells per well. After 24 hours, cells were treated with DMEM+10% FBS supplemented with PBS, 100 µg/ml cycloheximide, 10 µM T6R-NLS-ELP[A0.2]₄₀, or 50 µM T6R-NLS-ELP[A0.2]₄₀. At each indicated time point, cells were trypsinized and absorbance of the resuspended cells was read at an optical density of 800 nm on a spectrophotometer (Ultrospec 4300 Pro). (a) Results were plotted as a line graph to display growth over time (b) and as a bar graph to compare differences between means. Error bars represent +/- 1 SD of the mean of three triplicate samples

3.3 The ELP and HisMBP Fusion Proteins Localize Primarily into the Nucleus of Two Different Cell Types

To determine whether the ELP[A0.2]₄₀ or HisMBP recombinant proteins could enter the cell nucleus, a nuclear localization assay was used. The proteins must enter the cell nucleus to inhibit the interaction between the RdRp subunits and ultimately inhibit influenza replication. Since the original T6R-NLS-ELP[A0.2]₄₀ construct had no detection tag, the T6R-NLS-His-Tev-ELP[A0.2]₄₀ construct was used. To assess the ability of the recombinant proteins to penetrate cell membranes, recombinant protein was diluted to 50 µM in DMEM and applied to confluent monolayers of MDCK and LLC-MK2 cells. Protein uptake into two different cell types was analyzed due to the potential cell-type dependency of the HIV Tat-1 CPP (Koppelhus et al., 2002; Zhang et al., 2004). After the recombinant

protein was incubated on cells for 24 hours, the cells were harvested using nuclear extraction media containing NP-40. NP-40 is the most commonly used detergent to extract cell nuclei as it is milder than most other detergents and leaves the cell nuclei intact (Antalis & Godbolt, 1991). The harvested cells were centrifuged at high speeds to separate the nuclear fraction from the cytoplasmic fraction. The pelleted nuclei were resuspended in laemmli buffer while the cytoplasmic supernatant fractions were TCA precipitated and resuspended in laemmli buffer. To detect protein in each fraction, the samples were run on a polyacrylamide gel and hexahistidine tagged proteins were detected using Western blot. To ensure the nuclear and cytoplasmic fractions were properly separated, each fraction was blotted using anti-laminin and anti-tubulin antibodies, which are specific markers for the nuclear and cytoplasmic fractions, respectively.

As a positive control for uptake, a HisMBP-NLS-PB2 construct that had previously been shown to enter LLC-MK2 cells was used. Both the HisMBP-NLS-PB1 and T6R-NLS-His-Tev-ELP[A0.2]₄₀ constructs were localized to the nucleus of LLC-MK2 cells and MDCK cells (**Fig 3.8a**). Although some protein was detected in the cytoplasm of each cell-type, a relatively larger proportion was detected in the nuclei, as expected due to the presence of the NLS sequence. Laminin and tubulin were only detected in the nuclear and cytoplasmic samples, respectively, indicating that the two fractions were properly separated from each other (**Fig 3.8b**). This data suggested that these recombinant proteins localize to the nucleus and therefore should be able to disrupt the interaction between the PB1 and PA subunits of RdRp.

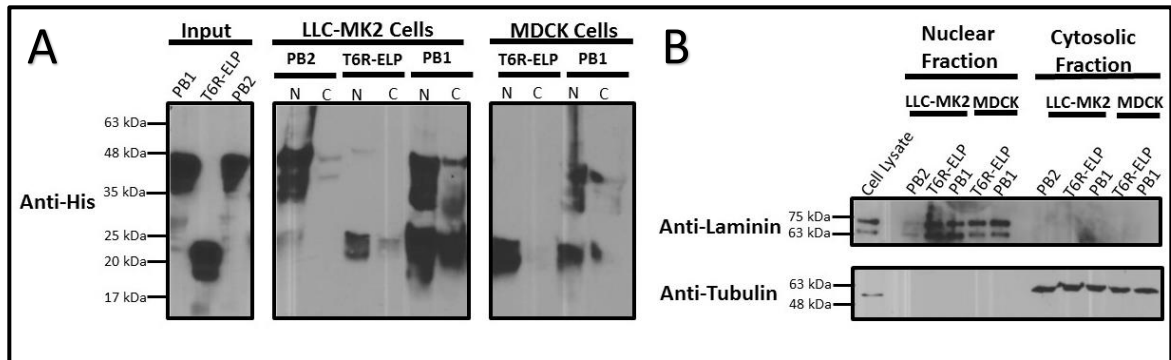


FIGURE 3.8 Nuclear Localization of the HisMBP-NLS-PB1 and T6R-NLS-His-Tev-ELP[A0.2] in LLC-MK2 Cells and MDCK Cells

MDCK and LLC-MK2 cells were seeded to confluency in a 6-well plate. Recombinant protein was diluted to 50 μ M in DMEM and applied to cells for 24 hours. After 24 hours, cells were harvested using nuclear extraction buffer. Pelleted nuclei were resuspended in laemmli buffer and the cytosolic supernatant was TCA precipitated and resuspended in laemmli buffer. Protein samples were run on a 14% polyacrylamide gel and analyzed by western blot using anti-his, anti-laminin, and anti-tubulin antibodies. Protein sizes are indicated using a pre-stained protein ladder as indicated in the materials and methods section. Where it appears, N=nuclear fraction and C=cytosolic fraction. PB2 is HisMBP-NLS-PB2 (positive control), PB1 is HisMBP-NLS-PB1, and T6R-ELP is T6R-NLS-His-Tev-ELP[A0.2]₄₀.

3.4 The ELP and HisMBP Fusion Proteins Interact with the C-terminal Portion of the Influenza PA Protein

To inhibit influenza virus replication, the HisMBP and ELP recombinant proteins must bind to the PA subunit of RdRp. In 2008, the interaction between the two subunits was visualized through a partial crystal structure where the N-terminus of PB1 could interact with the C-terminus of PA through a dragon jaw-like mechanism (**Fig 1.4**). To inhibit the interaction between the polymerase subunits, our peptide mimetic would also have to be able to bind to the C-terminus of PA. The interaction between the C-terminus of PA (amino acids 257-716) and HisMBP-NLS-PB1 or T6R-NLS-His-Tev-ELP[A0.2]₄₀ was assessed using a GST pull-down assay. Cell lysates from *E. coli* expressing either GST-PA_{c(257-716)} or GST alone were bound to Glutathione-Agarose beads and washed to remove

non-specifically bound proteins. Purified recombinant HisMBP-NLS-PB1 or T6R-NLS-His-Tev-ELP[A0.2]₄₀ were incubated with the beads overnight. Weak protein interactions were washed away using seven washes with PBS. The beads were resuspended in laemmli buffer and boiled for 10 minutes to remove bound proteins. Samples were run on a polyacrylamide gel and hexahistidine tagged or GST tagged proteins were analyzed using Western blot. The HisMBP-NLS-PB1 construct was able to interact with the GST-PA_{c(257-716)} but not GST alone, ruling out the possibility of non-specific binding (**Fig 3.9a**). Similar results were obtained with the T6R-NLS-His-Tev-ELP[A0.2]₄₀ construct (**Fig 3.9b**). All GST constructs were properly expressed and bound to glutathione beads (**Fig 3.9**).

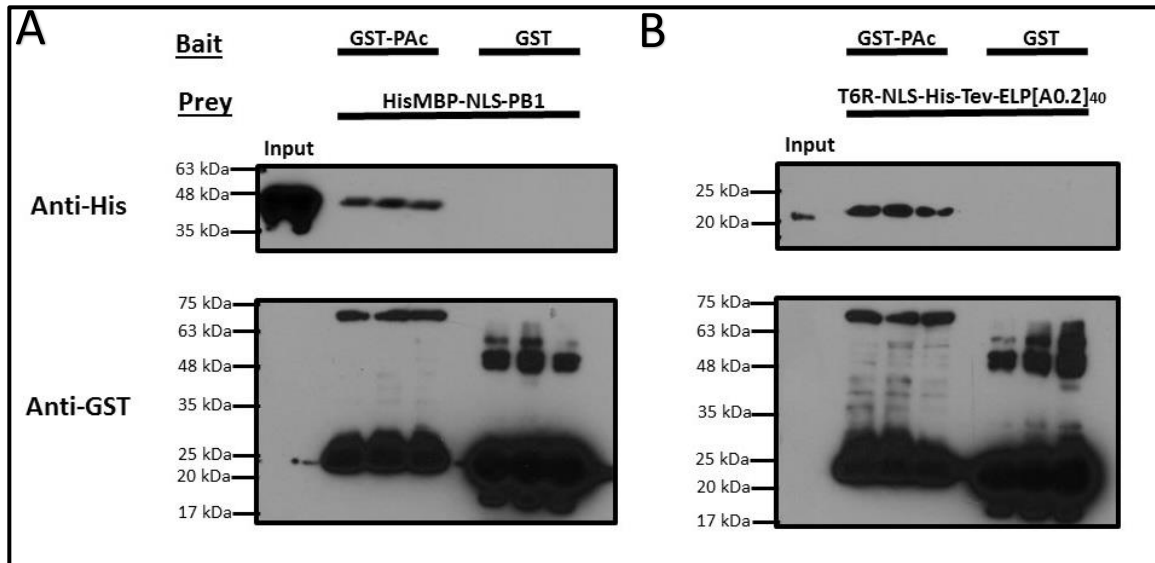


FIGURE 3.9 The HisMBP-NLS-PB1 and T6R-NLS-His-Tev-NLS-ELP[A0.2]₄₀ Proteins Interact with the PA Portion of the Influenza Polymerase Complex

GST or GST-PAc(257-716) (Bait) were overexpressed in recombinant *E. coli*. Cell lysates were bound to glutathione high capacity magnetic agarose beads. Protein-bound beads were incubated in a blocking solution (PBS, 0.1% v/v Tween-20, 5% BSA w/v) for one hour. (a) HisMBP-NLS-PB1 or (b) T6R-NLS-His-Tev-ELP[A0.2]₄₀ purified protein (Prey) was diluted in blocking solution and incubated with beads at 4 °C overnight. Beads were washed in 1x PBS seven times for one minute using the NucliSENS miniMag® with 1 second spin intervals. After the final wash, the beads were re-suspended laemmli buffer and samples were run on a 12% polyacrylamide gel and analyzed by western blot using anti-his and anti-GST antibodies. Protein sizes are indicated using a pre-stained protein ladder as indicated in the materials and methods section. Data is presented as triplicate samples of each condition. Where it appears, PAC represents amino acids 257-716 of the Influenza PA protein.

3.5.1 Inhibition of Influenza A H3N2 Replication by the HisMBP Fusion Protein but Not the ELP Fusion Protein

Since both the HisMBP and ELP fusion proteins were non-toxic, could localize to cell nuclei, and could bind to the C-terminus of PA, these proteins were both tested for anti-influenza activity. To test the protein's ability to inhibit influenza infection, MDCK cells were treated with 200 μM, 100 μM, or 50 μM of either protein for one hour before being infected with *Influenza A H3N2* virus (A/Victoria/3/1975(H3N2)). After one hour of

incubation with virus, the inoculum was removed and cells were treated with another round of protein and incubated for an additional 12 hours. The assay was performed in triplicate.

Influenza infected cells were detected by indirect immunofluorescence microscopy. When visually comparing the amount of infection between the HisMBP-NLS-PB1 treated samples and the virus only treated conditions, the protein treated condition displayed fewer infected cells for all three concentrations of protein (**Fig 3.10a**). The inhibition was most apparent when cells were treated with 200 μ M protein. To confirm the observational data, the number of infected cells was counted for each monolayer and the triplicate data was averaged (**Fig 3.10b**). As the concentration of the HisMBP-NLS-PB1 construct was increased, there was increased inhibition in a dose-dependent fashion. In contrast, no reduction in virus levels was observed when using the T6R-NLS-His-Tev-ELP[A0.2]₄₀ recombinant protein at any concentration. The percent inhibition elicited from each protein treated sample was also calculated using the formula $(\frac{x-y}{x}) * 100\%$, where x is the number of viruses per monolayer on the virus only control and y is the number of viruses per monolayer on the protein treated samples. The percent inhibition data confirms that the HisMBP-NLS-PB1 construct could inhibit H3N2 virus to nearly 40% at 200 μ M whereas the T6R-NLS-His-Tev-ELP[A0.2]₄₀ construct resulted in little or no inhibition (**Fig 3.10c**).

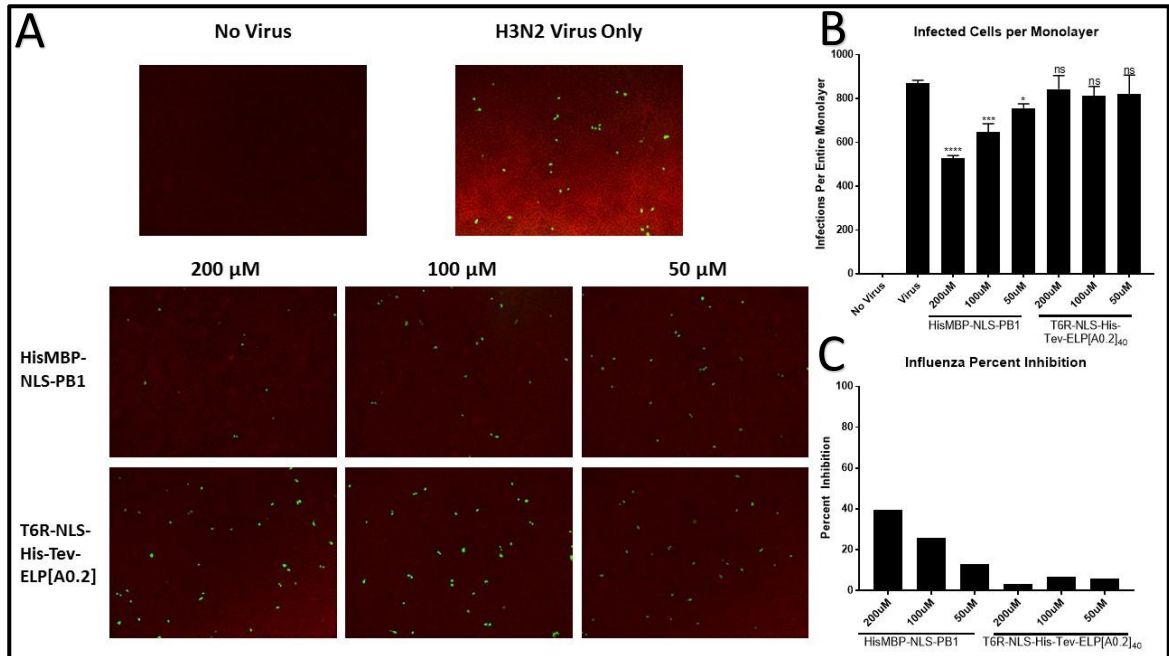


FIGURE 3.10 Inhibition of Influenza H3N2 Replication Using the HisMBP-NLS-PB1 and T6R-NLS-His-Tev-ELP[A0.2]₄₀ Proteins

MDCK cells were treated for 1 hour with purified protein in DMEM, challenged with influenza H3N2, and treated with another round of protein in DMEM for 12 hours. (a) After 12 hours, cells in each well were fixed, stained, and visualized using immunofluorescence microscopy as described in the materials and methods section. Mouse anti-NP1 was used as a primary antibody to detect influenza proteins. Infected cells appear green due to viral nucleoprotein. (b) Total number of infected cells were counted on each monolayer and averaged. (c) Percent Inhibition was calculated for each condition and expressed as percent inhibition. Error bars represent +/- 1 SD of the mean of three triplicate samples. HisMBP-NLS-PB1 protein concentrations of 50, 100, and 200 μM were statistically significantly different from the no peptide control; *= $p < 0.05$, ***= $p < 0.001$, ****= $p < 0.0001$. ns= $p > 0.05$.

3.5.2 Inhibition of Influenza A H1N1 Replication by the HisMBP Fusion Protein but Not the ELP Fusion Protein

Since the PA and PB1 subunit of the RdRP are highly conserved (Fig 1.5), the recombinant proteins should be able to inhibit a variety of *Influenza A* subtypes. To confirm that the protein was active against another *Influenza A* strain, the proteins were tested against 2009 pandemic influenza H1N1. MDCK cells grown to confluency in a 96 well plate, and were treated with 200 μM, 100 μM, or 50 μM of either protein for one hour

before being infected with *Influenza A H1N1* virus (A/California-like/04/2009(H1N1)). After one hour of viral incubation time, cells were treated with another round of protein and allowed to incubate for an additional 12 hours. The assay was performed in triplicate.

Using fluorescence microscopy, we observed a decrease in infection in the HisMBP-NLS-PB1 protein treated condition compared to the virus only control (**Fig 3.11a**). This effect was most apparent when cells were treated with 200 μ M protein. This pattern was again concentration-dependent, as there were less infected cells on each monolayer as the concentration of HisMBP-NLS-PB1 increased. These results were confirmed by averaging the number of infected cells on five separate fields of view (**Fig 3.11b**). Again, there were only minimal differences in infection between any of the T6R-NLS-His-Tev-ELP[A0.2]₄₀ samples and the virus only control. The percent inhibition elicited from each protein treated sample was also calculated using the formula $(\frac{x-y}{x}) \times 100\%$, where x is the number of viruses per monolayer on the virus only control and y is the number of viruses per monolayer on the protein treated samples. The percent inhibition data confirms that the HisMBP-NLS-PB1 construct could inhibit influenza H1N1 virus to nearly 45% at 200 μ M whereas the T6R-NLS-His-Tev-ELP[A0.2]₄₀ construct resulted in very little inhibition (**Fig 3.11c**).

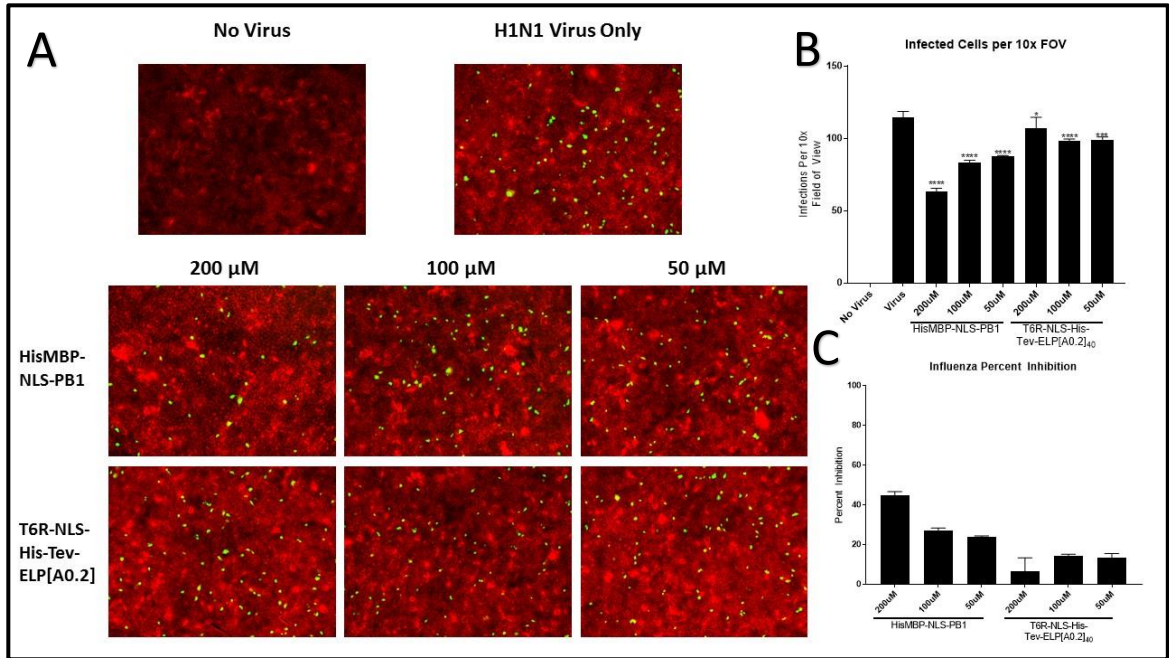


FIGURE 3.11 Inhibition of Influenza H1N1 Replication Using the HisMBP-NLS-PB1 and T6R-NLS-His-Tev-ELP[A0.2]₄₀ Proteins

MDCK cells were treated for 1 hour with purified protein in DMEM, challenged with influenza H1N1, and treated with another round of protein in DMEM for 12 hours. (a) After 12 hours, cells in each well were fixed, stained, and visualized using immunofluorescence microscopy as described in the materials and methods section. Mouse anti-NP1 was used as a primary antibody to detect influenza proteins. Infected cells appear green due to viral nucleoprotein. (b) Total number of infected cells were counted on five fields of view and averaged. (c) Percent Inhibition was calculated for each condition and expressed as percent inhibition. Error bars represent \pm 1 SD of the mean determined by testing triplicate samples. Levels of virus infection with various concentrations of peptide were statistically significantly different from the no virus control: $*=p<0.05$, $***=p<0.001$, $****=p<0.0001$

Chapter 4 – Discussion and Future Directions

Discussion and Future Directions

4.1.1 Design, Synthesis, and Purification of Elastin-like Polypeptide Proteins

Previously, our lab used the first 21 amino acids of the influenza PB1 protein as a novel peptide mimetic by attaching it to the His-MBP protein carrier. Although this carrier is ideal for inducing solubility of foreign constructs and is expressed to high levels, this carrier would likely not be suitable for use in humans. The foreign nature of the carrier may elicit an immune response and could therefore be immunogenic. For this reason, a new carrier suitable for humans is required. There are a variety of human compatible carriers and often the ideal carrier protein for a given peptide must be chosen on a case-by-case basis. Our lab has explored various carrier proteins including: designed-ankyrin repeats (DARPin) (Stumpp, Binz, & Amstutz, 2008), albumin binding domains, monomeric IgG1 Fc (Ying, Gong, Ju, Prabakaran, & Dimitrov, 2014), and most recently elastin-like polypeptides.

The ELP class of protein carriers has many advantages over other previously used carriers. Notably, ELPs can be finely tuned and adapted to a variety of specific uses. Since ELP proteins are multiple repeated units, they can be synthesized from small nucleotides to form a library. They also show modularity, and multiple repeat types can be combined to create unique ELP sequences (Meyer & Chilkoti, 2002). In this study, two 75 base pair long oligonucleotides were used to create an ELP library of 5, 10, 20, and 40 repeats. Doubling the ELP size was completed using simple restriction digestion methods and each doubling reaction could be completed within 2 days. The generation of an ELP library is

advantageous since the T_t and properties of ELP fusion proteins can not always be accurately predicted. The availability of an ELP library allows for rapid generation of ELP fusion constructs with different repeat lengths; thus, the T_t can be finely tuned. Additionally, once the library is established, any nucleotide sequence can be efficiently fused to the ELP so that multiple fusion constructs can be generated in quick succession.

Elastin-like polypeptides can also be tuned by changing the composition of their guest residue. Every fifth residue in the repeat sequence is the guest residue, which can be any amino acid except proline (Meyer & Chilkoti, 1999). This variable composition allows for even more control over the T_t of the ELP. Although T_t generally decreases with increased ELP length, it is possible to develop a short ELP with a low T_t through guest residue manipulation. The ELP used in this study was composed of a 1:4 alanine to valine composition at the guest residue spot. At 50 μM , a 40-repeat unit of this ELP construct has a T_t of 50 °C. However, a 40 repeat unit of an ELP composed of only alanine in the guest residue spot has a T_t of 100 °C, supporting the significant effect of the guest residue (McDaniel et al., 2013). Because of the fusion ΔT_t effect, having a variety of ways to manipulate the T_t is an important tool when designing ELP-based constructs.

The purification of ELP fusion proteins is a streamlined process, and very little specialized equipment is required, making it fast and cost-effective. High yields of protein could be obtained by expressing the recombinant protein in *E. coli*, grown for 24 hours in terrific broth. Terrific broth allows bacteria to grow to a higher OD and maintains the plasmid at high copy number, which increases the yield of protein (Tartof & Hobbs, 1987).

The use of terrific broth allowed purification of large amounts of protein from only one litre of culture, compared to standard purification procedures which use six litres of bacterial culture. Additionally, the pET-25b(+) uses the T7 promoter system, which is known to have leaky expression (Mertens, Remaut, & Fiers, 1995). This leaky expression is sufficient for protein expression and no IPTG was required to induce protein expression. Once a soluble lysate was obtained, protein purification by ITC took under two hours and was completed using only 1.5 mL centrifuge tubes, NaCl, PBS, and a benchtop centrifuge. The colour of the pellet and turbidity of the resuspended supernatants were a good indication of protein purity and yields. Visually, protein appeared pure after two rounds of ITC, which was confirmed using polyacrylamide gel electrophoresis. Since the protein was pelleted and could be resuspended in any buffer, no dialysis was required. Overall, this streamlined purification technique resulted in high yields (up to 60 mg/L) of pure (~99%) recombinant protein.

4.1.2 The Transition Temperature of the Recombinant Elastin-like Polypeptides

For use in cell culture, the T_t of our ELP fusion constructs should be above the physiological temperature of 37 °C. When a protein is fused to an ELP sequence, the T_t is often modified due to the fusion ΔT_t effect (Trabacchi-Carlson et al., 2004). The T_t of the ELP[A0.2] construct alone was previously determined to be 50 °C; however, due to the fusion ΔT_t effect, we expected the recombinant proteins used in this study to vary from this temperature. Generally, if the fusion construct is composed of hydrophobic amino acids, the T_t will decrease and vice versa. The T_t of the T6R-NLS-ELP[A0.2]₄₀ construct was

approximately 45 °C, above the physiological range necessary for our experiments. Since the T_t of the ELP[A0.2]₄₀ construct without the attached peptide was not directly compared to the T6R-NLS-ELP[A0.2]₄₀, no distinct value can be provided for the fusion ΔT_t effect after addition of the N-terminal fusion peptide. However, it does appear that the N-terminal fusion sequence lowers the T_t of the ELP[A0.2]₄₀ protein to some degree. Using the peptide 2.0 software, the fusion construct was determined to have a hydrophobicity of 37.5%, therefore a lowered T_t was not surprising. Since the recombinant protein was soluble in cell culture media at physiological temperature, it was used for downstream experiments.

4.1.3 Assessing the Recombinant Elastin like Polypeptide Proteins Toxicity

The cellular toxicity of all recombinant protein constructs must be minimal to ensure their compatibility *in vivo*. For the scope of this study, toxicity was only measured *in vitro* using cell culture. The toxicity of the HisMBP-NLS-PB1 construct had previously been assessed; therefore, only the T6R-NLS-ELP[A0.2]₄₀ was analyzed in this study (**Sup. Fig 6.4**). Since *Influenza A* is primarily a respiratory pathogen, the cell line chosen for toxicity assays should mimic respiratory tissues, to best represent the drugs primary target tissue. Although there is no perfect *in vitro* model to mimic the respiratory tissue, the A549 cell line is commonly used to test drug toxicity (Steimer, Haltner, & Lehr, 2005). The A549 cell line is a continuous cell line and was first isolated from an alveolar epithelial adenocarcinoma in 1973 (Giard et al., 1973). The A549 cell line is also highly susceptible to influenza infection due to the high density of sialic acid receptors on the cell membrane (Zou et al., 2011).

The toxicity of the T6R-NLS-ELP[A0.2]₄₀ recombinant protein was assessed by monitoring the growth rate of A549 cells. The growth of A549 cells in the presence of recombinant protein was monitored for 2 days and compared to cells maintained in growth media with PBS. No inhibition of A549 cell growth was seen in protein treated samples after 48 hours, indicating the protein did not have any adverse effects on the cells. A drug that is toxic would be expected to modify the metabolic activity and proliferation of cells, resulting in a decreased growth rate. Cells treated with cycloheximide, which disrupts protein translation, demonstrated a decreased growth rate.

A notable characteristic of ELP constructs are their similarity to human tropoelastin, which suggests that they are relatively non-toxic. Compared to other foreign synthesized drugs, ELP molecules are thought to induce less cytotoxicity, immunotoxicity, and inflammatory responses (Ryu & Raucher, 2015). Previous studies demonstrated that minimal toxicity was attributed to ELP protein both *in vitro* and *in vivo* (Rincon et al., 2006). Elastin-like polypeptides conjugated to anti-cancer drugs have been tested in mouse models, where recombinant proteins were able to accumulate in tumor tissue while causing minimal adverse systemic effects (Ryu & Raucher, 2015). Two different ELP conjugant drugs, produced by PhaseBio Inc., have entered clinical trials for human safety (Despanie, Dhandhukia, Hamm-Alvarez, & MacKay, 2016). Glymera™, used to treat hyperglycemia, and Vasomera™, used to treat arterial hypertension, have entered phase II B and phase I clinical trials, respectively. Glymera appeared to perform well in clinical trials and had very few adverse effects, with only one individual developing a non-neutralizing antibody

response (Christiansen et al., 2012). Elastin-like polypeptide proteins are relatively non-immunogenic, which makes them an intriguing carrier protein.

4.2.1 Recombinant Proteins Mechanism of Inhibition – CPPs

For recombinant proteins to properly inhibit influenza in cell culture, they must localize to the correct subcellular area and interact with their intended target. To determine whether the recombinant proteins entered cells, we used a nuclear localization assay. Cells were incubated with the recombinant proteins diluted in DMEM to induce uptake. To detect the presence of intracellular protein, extracellular proteins were first degraded using an ice-cold acid wash buffer to disrupt the interaction between the CPP and the cell membrane (Kameyama et al., 2007). This was to ensure only intracellular proteins were being detected. The outer membrane was lysed using a mild detergent (NP-40) which left the nuclear membrane intact. To detect protein, the nuclear and cytoplasmic fractions were separated, run on a polyacrylamide gel, and analyzed using Western blot. Since protein uptake can be cell-type specific, two separate cell lines were used for this study: MDCK and LLC-MK2. Both HisMBP-NLS-PB1 and T6R-NLS-His-Tev-ELP[A0.2]₄₀ recombinant proteins entered the cell nuclei of both cell types. Under each condition, there was more protein in the cell nuclei compared to the cytoplasmic portion, as expected. Since the proteins are found primarily in the cell nuclei, they should be in the correct location to interact with the RdRp.

Although CPP's have been researched extensively since their discovery, the uptake of proteins with a CPP is still a poorly understood process. The exact mechanism through

which CPPs internalize proteins remains unclear; however, the two prevailing theories are direct membrane penetration and endocytosis (Madani et al., 2011). Models of direct penetration are supported by the fact that positively charged CPPs can directly interact with the negatively charged cell membrane (Deshayes, Morris, Divita, & Heitz, 2006). Direct penetration may be dependent on membrane associated heparin sulfate; however, this is highly debated (Madani et al., 2011). Direct translocation of protein across a cell membrane is likely energy- and temperature- independent (Bechara & Sagan, 2013). For the most accepted mechanism of direct penetration, protein aggregates on the outside of cell membranes. Once reaching a threshold of extracellular protein concentration, CPPs are attracted to the distal side of the membrane and subsequently traverse the membrane (Herc & Garcia, 2007). Although this is the most common theory of direct penetration, other theories have been proposed.

Cell penetrating peptides may also take an endocytic route that is generally considered an energy-dependent process (Madani et al., 2011). Endocytic uptake is typically believed to occur through one of three mechanisms: macropinocytosis, endocytosis with clathrin coated pits, and endocytosis independent of clathrin (Koren & Torchilin, 2012). The HIV-1 Tat peptide may interact with actin, which can induce macropinocytosis through cytoskeletal remodelling (Mishra et al., 2011). Alternatively, the peptides may induce activation of a Rac1 GTPase, which can initiate cytoskeletal remodelling resulting in macropinocytosis (Gerbai-Chaloin et al., 2007). Use of clathrin-dependent endocytosis inhibitors partially inhibits uptake of some CPP conjugated proteins, suggesting clathrin-mediated endocytosis is involved in protein uptake (Richard

et al., 2005). However, endocytosis of some CPP-containing peptides is also likely due to clathrin-independent mechanisms, which have been less characterized. To transverse the extracellular membrane, CPPs likely utilize a combination of the various mechanisms that may depend on different factors such as: cell type, pH, temperature, salt concentration, and energy availability. Additionally, the cargo attached to the CPP plays an important role in the ability of a protein to penetrate the cell membrane (Koren & Torchilin, 2012). This study focused solely on whether the protein was internalized; thus, any of the proposed mechanisms of protein uptake can not be ruled out.

In our study, CPP internalized both recombinant proteins in the MDCK and LLC-MK2 cell types. Although we did not directly compare the amount of protein that was internalized into each cell type, this could be an important step to determine the appropriate CPP for use with various cargo. Cell type seems to be an important factor in CPP uptake as well. In a study by Koppelhus et al. (2002), Tat conjugated peptides were only poorly taken up into five cell types, suggestive of a more complex uptake pattern. Interestingly, it has previously been reported that Tat-conjugated peptides are not efficiently internalized into MDCK cells (Krämer & Wunderli-Allenspach, 2003; Violini, Sharma, Prior, Dyszlewski, & Piwnica-Worms, 2002). This is surprising since both recombinant proteins used in this study localized to the MDCK cell nuclei. Certain epithelial cell types, such as MDCK cells, seem to have an inherent ‘barrier’ preventing the uptake of some CPP fused constructs; however, this was not observed in our results (Zhang et al., 2004). Although the uptake patterns of CPP conjugated proteins can change depending on their cargo and the cell type, all recombinant proteins in this study could efficiently localize to the nucleus of

MDCK and LLC-MK2 cells. Based on this, the recombinant proteins should be in the correct location to disrupt the critical PB1-PA interaction of the RdRp.

4.2.2 Recombinant Proteins Mechanism of Inhibition – PA and PB1 Subunit Interaction

To inhibit the function of the RdRp, our recombinant proteins must interact with the PA subunit to prevent RdRp complex formation. To assess this, GST pulldowns were performed where the PA protein was used as bait to interact with recombinant proteins. Since full length PA protein is difficult to express and purify, only residues 257-716 of the PA protein were attached to the GST protein. These residues were chosen since they had previously been purified when attached to GST and were still capable of binding residues 1-25 of PB1 (He et al., 2008). After the GST-PA₂₅₇₋₇₁₆ or GST alone was bound to glutathione beads, aliquots of HisMBP-NLS-PB1 or T6R-NLS-His-Tev-ELP[A0.2]₄₀ were incubated with the beads. To remove non-specific binding, the beads were washed seven times with PBS. By using a PBS buffer, the stringency of the wash conditions was physiologically relevant. Samples were analyzed for interaction by Western blot detection.

When analyzed by Western blot, both HisMBP-NLS-PB1 and T6R-NLS-His-Tev-ELP[A0.2]₄₀ interacted with GST-PA₂₅₇₋₇₁₆. Neither of the two constructs appeared to interact with GST alone, suggesting that the interaction was specific and taking place between PA₂₅₇₋₇₁₆ and our recombinant proteins. Although the two proteins interacted, the strength of the interaction is not known. The assay had to be optimized for washing conditions and when a high salt wash buffer was used, only a weak interaction could be

detected (data not shown). However, since the construct binds to its target partner in PBS, the construct should block formation of the RdRp complex.

Based on the nuclear localization result, the proteins can traverse the cell's outer membrane using the NLS CPP. The exact mechanism through which the CPP functions remains unclear, but it is likely a combination of multiple mechanisms. Once inside the cells, the CPP directs the proteins through nuclear pores and to the nucleus. Based on the GST pulldown data, we believe the proteins interact with the PA portion of the RdRp. Once the proteins are inside the nucleus, they should interact with PA and therefore inhibit the natural interaction between PA and viral PB1 protein.

4.2.3 Influenza Inhibition Using the Recombinant Proteins

To test the ability of the recombinant proteins to inhibit influenza infection, the proteins were tested *in vitro* using the MDCK cell line. The MDCK cell line is highly susceptible to influenza infection, making it an ideal cell line for influenza inhibition assays (Lugovtsev, Melnyk, & Weir, 2013). To perform the assay, MDCK cells were incubated with varying concentrations of recombinant proteins for one hour, infected with influenza for one hour, and incubated with a second round of protein for 12 hours. Following infection, cells were stained by indirect immunofluorescence, the number of infected cells were counted, and percent inhibition was calculated.

The HisMBP-NLS-PB1 construct inhibited *Influenza A H3N2* in a dose-dependent manner. As the concentration of recombinant protein applied to the cells increased, higher levels of inhibition were observed. At 200 μ M, there was 40% inhibition when compared

to the no protein control. Surprisingly, no inhibition was observed when the T6R-NLS-His-Tev-ELP[A0.2]₄₀ protein was used; there are several possible explanations for this result. Although the construct could bind to the PA protein outside of the cell, the conditions inside the nucleus could vary and change the conformation of the ELP or associated peptide. Alternatively, the protein may show low stability in cells and be prone to N-terminal degradation, which would abolish its ability to bind to its target.

To confirm that the peptides were not influenza strain specific, they were also tested against *Influenza A H1N1*. Again, the HisMBP-NLS-PB1 protein (but not the T6R-NLS-His-Tev-ELP[A0.2]₄₀ protein) inhibited influenza H1N1. Inhibition using the HisMBP-NLS-PB1 construct was again dose-dependent and showed a 45% decrease in infected cells compared to the no protein control. This indicated that the HisMBP-NLS-PB1 construct inhibited two separate strains of influenza to approximately equal degrees, as expected.

The HisMBP carrier protein seemingly did not inhibit the function of the PB1 peptide. Although the peptide attached to the HisMBP carrier was not directly compared to the synthetic peptide, similar amounts of synthetic peptides were reportedly used for influenza virus inhibition. Using a plaque reduction assay, which measures the amount of viral progeny, Wunderlich et al. (2009) observed roughly 40 – 75% viral inhibition, depending on the strain, when using a synthetic peptide at 200 µM. To explore the effect that the carrier protein has on the peptide's ability to inhibit influenza, a future study should directly compare the HisMBP-NLS-PB1 construct to synthetic peptide. Despite both recombinant proteins seemingly entering the nucleus of MDCK cells and interacting directly with the influenza PA protein, the ELP conjugated peptide did not inhibit influenza.

4.3.1 Future Objective: Modification of the ELP Carrier

Although the PB1 peptide did not inhibit influenza when attached to the ELP carrier, there are many modifications that can be made to the carrier to enhance its effectiveness. Previously, other labs have attached fusion proteins to ELP and maintained biological activity, suggesting that the ELP carrier used in this study may require optimization (Bidwell & Raucher, 2010; Floss et al., 2009). The ELP class of protein carriers are highly variable and modifications to its length, T_t , fusion order, and guest residue composition could change how the carrier interacts with attached proteins or the cellular environment. Since the ELP constructs are intrinsically disordered, length may affect their function within the cell. To test the effect of length on the activity of the recombinant protein, different length fusion constructs can be cloned using the already established ELP library (**Fig 3.2**) and tested for anti-influenza activity. To date, most studies using ELP fusion proteins have fused the recombinant protein to an ELP with over 100 repeats. This study used an ELP containing only 40 repeats to attempt to limit protein size related toxicity; however, the larger ELP may be more biologically stable resulting in enhanced activity.

The fusion construct sequence could also affect how the peptide interacts with the PA protein. Although it is generally believed that fusion proteins should be attached to the N-terminus of ELP proteins, they can be attached to the C-terminus with varying effects (Christensen et al., 2009). The HisMBP construct has a C-terminal peptide fusion, supporting that the C-terminus is an effective fusion location. Additionally, our lab has observed that a neighbouring sequence can strongly affect a peptide, due to various charge

differences. In particular, a positively charged CPP sequence was hindered when next to a negatively charged peptide sequence (unpublished data). Thus, the order of the ELP sequence could be modified to ensure that all domains are functional. Alternatively, a linker sequence could be included between the PB1 protein and the remainder of the construct. Linker proteins have been shown to increase the bioavailability of fused constructs, with many different types available including: flexible, rigid, and cleavable (X. Chen, Zaro, & Shen, 2013).

Finally, to modify the ELP construct, the composition of the guest residues could be changed. The ELP used in this study has a 1:4 alanine to valine ratio which was chosen to maintain the T_t above 37 °C while keeping its size small. By using an ELP which more closely mimics human tropoelastin, such as iTEPs, the protein may be more stable and active. Changing the guest residues would also change the associated T_t of the ELP construct. Although the peptide fused to the ELP carrier protein did not effectively inhibit influenza infection, the ELP carrier can be modified in a variety of ways to make the peptide more biologically active and stable.

4.3.2 Future Objective: CPP-Induced Cellular Uptake of the Recombinant Proteins

This study exclusively used an NLS CPP because the interaction between PA and PB1 was believed to occur within the nucleus. However, it has been proposed that some or all of the components of the polymerase may associate within the cytoplasm before entering the nucleus (Fodor & Smith, 2004) (**Fig 4.1**). Recently, a study was performed using cross-correlation spectroscopy, that suggested the PB1 and PA subunits associate in the

cytoplasm before entering the nucleus (Huet et al., 2010). This study also suggested that the PB2 protein entered the nucleus prior to binding with the PB1-PA complex, consistent with proposed model B in Figure 4.1.

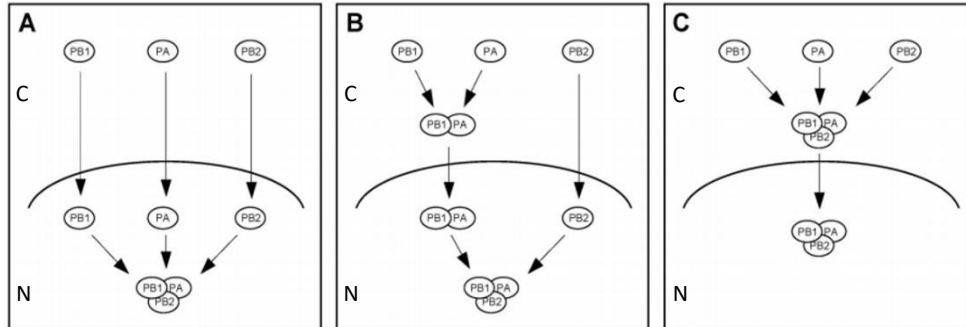


FIGURE 4.1 Proposed Models of the Interaction Between the Influenza RdRp

Three proposed models of where the interaction between the influenza PB1, PB2, and PA take place. N is the nuclear portion; C is cytoplasmic. In model A, all three components of the polymerase enter the nucleus before associating with each other. In model B, the PB1 and PA proteins interact in the cytoplasm and enter the nucleus as a complex where they interact with PB2. In model C, all three components of the polymerase associate in the cytoplasm before being transported to the nucleus. Figure taken from Fodor & Smith (2004)

If the PA and PB1 are interacting within the cytoplasm, then the NLS may not be the most ideal CPP to use for inhibition. Ideally, the recombinant protein would be localized to the same area where the interaction is believed to occur. To determine whether the CPP has any effect on the inhibiting properties of the recombinant proteins, other CPP types could be used. A variety of CPPs exist each with their own unique properties and different localization patterns (Bechara & Sagan, 2013). The *Drosophila* derived penetratin peptide has previously been used to localize ELP constructs to the cytoplasm of cells and could be tested with both the HisMBP and ELP construct (Bidwell & Raucher, 2010). Ideally, a CPP that localizes to both the cytoplasm and nucleus would be chosen so that any transient interactions between PA and PB1 in the nucleus could also be inhibited. Using a different

CPP may increase the effectiveness of the HisMBP-NLS-PB1 construct and allow the T6R-NLS-His-Tev-ELP[A0.2]₄₀ construct to properly inhibit.

4.3.3 Future Objective: Other Human Specific Carriers

Although the ELP sequence is an intriguing human carrier due to its similarity to human tropoelastin and ease of purification, other carriers could be analyzed that would potentially be non-immunogenic. One interesting carrier is the Fc domain of human IgG1, which has a long half-life and is highly soluble (Ying, Chen, Gong, Feng, & Dimitrov, 2012). Fusion proteins using the monomeric Fc domain have been shown to retain binding ability to the neonatal Fc receptor (FcRn), which protects antibodies from degradation in the blood stream (Roopenian & Akilesh, 2007). Additionally, if a smaller carrier is desired, the Fc domain can be broken-down to its component parts, CH2 or CH3, which can both bind to the FcRn and increase the half-life (Ying et al., 2014).

Another protein commonly used as a carrier protein is human serum albumin (HSA), which is the most common carrier protein found in the human bloodstream (Varshney et al., 2010). The native HSA protein is believed to have a half-life of approximately 19 days, which is maintained through its interaction with FcRn, similar to the human IgG protein (Larsen et al., 2016). To be effective, the HSA protein must fold correctly; therefore, the protein is typically expressed in a yeast system and a proper linker must be chosen (Larsen et al., 2016). Albiglutide, the first HSA fusion drug, fuses human GLP-1 to HSA in an attempt to control diabetes. It has performed well in phase III clinical trials for long-term safety (Ahrén et al., 2017).

Our lab is currently testing another carrier based on the human thioredoxin (hTrx) protein that is conjugated with an RSV peptide. Thioredoxin proteins act as disulfide reductases and have been found in every type of organism known (Arnér & Holmgren, 2000). Since thioredoxin is ubiquitous in nature, it is expected to be relatively non-immunogenic. Previously, hTrx constructs have been difficult to purify using a bacterial system because they form insoluble aggregates. Recent work done by Borghouts et al. (2008) have improved the solubility of hTrx by mutating five cysteine residues, that are required for protein-protein interactions, to ensure it is expressed as a monomeric product. This protein, when attached to a CPP, could penetrate the extracellular membrane and enter cells. Additionally, when treating cells with the protein, an attached anti-cancer peptide was active and inhibited cell proliferation. A variety of human specific carriers exist, each with their own unique functions and characteristics.

4.3.4 Future Objective: Delivery of the Recombinant Proteins

Currently, one of the largest obstacles to protein therapeutics is their delivery to the target tissue (Mason, 2010). If the peptides are linked to a human carrier protein and can inhibit influenza, their delivery to the target tissue must be optimized. Protein delivery can be limited due to enzymatic degradation and low epithelial permeability when delivered orally (Mitragotri, Burke, & Langer, 2014). One approach to these issues includes using microparticles that surround the protein drug and facilitate slow delivery. If the ELP construct was redesigned to be more effective at combating influenza, insoluble ELPs demonstrate microparticle-like traits and can form drug depots for slow drug release (Liu et al., 2010). Nebulizers, which can aerosolize proteins, have also been used to deliver

peptides to target tissues, with varying degrees of success. Recently, more efficient nebulizers have been designed that could result in increased pulmonary delivery of protein constructs (Y. Wang, Rezk, Khara, Yeo, & Ee, 2016). After being nebulized, the protein should be tested for efficacy and the distribution of the peptides must be measured to determine whether this approach is viable for drug delivery.

A unique method of protein drug delivery our lab is currently exploring involves the use of commensal bacteria. By genetically modifying commensal bacteria to produce and secrete the recombinant proteins, we believe that we could induce long-lasting protection without the need for an invasive delivery method. Previous studies using an HIV peptide demonstrated that live microbial systems can produce stable antiviral peptides and secrete them extracellularly (Rao et al., 2005). Our lab has previously developed recombinant *Streptococcus anginosus* that was able to secrete a short peptide sequence (**unpublished data**). *Streptococcus anginosus* is generally considered to be a non-pathogenic bacteria that is a commensal of many humans (Tan & File, n.d.). Other members of the lab have also attempted to clone constructs in to *Streptococcus gorodonii*, which has previously been mutated to be less immunogenic (Andrian, Qi, Wang, Halperin, & Lee, 2012). We have also explored using *Streptococcus salivarius*, a commensal commonly found in the mouth that is already being used as a probiotic, delivered through chewing gum or lozenges (Burton, Chilcott, Moore, Speiser, & Tagg, 2006). A stable commensal bacteria producing the therapeutic protein would allow for long-lasting protection of its host.

4.4 Influenza Global Burden, the Need for New Therapeutics, and Closing Remarks

Despite the influenza vaccine being available since the early 1940s, influenza continues to affect many people each year and is responsible for serious outbreaks. The influenza vaccine must be administered each year as influenza can develop resistance to the previous season's vaccine through antigenic drift and shift. Due to the high mutation rate of the polymerase, influenza can rapidly evolve and gain resistance to commonly used antivirals. For these reasons, antivirals are used sparingly and there is a need for novel antivirals that do not induce rapid resistance. The influenza polymerase is a trimeric complex required for influenza virulence. The polymerase is an ideal drug target since the interactions between the three components are highly conserved. In this thesis, we used a small peptide mimetic that blocks the PB1 and PA interaction. The mimetic was attached to an NLS sequence and one of two carriers; namely, the solubility inducing MBP carrier or a human specific ELP carrier. Both recombinant proteins could localize to cell nuclei and interact with the C-terminal portion of the PA protein. However, only the peptide attached to the MBP carrier could inhibit influenza replication *in vitro*. Although the peptide mimetic attached to the ELP protein was not effective, ELP proteins can be manipulated and a different construct may be more effective. Peptide mimetics are an intriguing strategy to inhibit specific protein-protein interactions, but their success is dependent on overcoming key obstacles. A carrier protein must be chosen which retains the biological activity of the peptide, increases the proteins half life, and is non-immunogenic. Although significant strides have been made in the field of protein therapeutics, further studies are required.

Chapter 5 – References

- Ahrén, B., Carr, M. C., Murphy, K., Perkins, C., Rendell, M., Mallory, J., ... Johnson, S. (2017). Albiglutide for the treatment of type 2 diabetes mellitus: An integrated safety analysis of the HARMONY phase 3 trials. *Diabetes Research and Clinical Practice*, *126*, 230–239.
- Alexander, D. J. (2007). An overview of the epidemiology of avian influenza. *Vaccine*, *25*(30), 5637–5644.
- Andrian, E., Qi, G., Wang, J., Halperin, S. A., & Lee, S. F. (2012). Role of surface proteins SspA and SspB of *Streptococcus gordonii* in innate immunity. *Microbiology*, *158*(8), 2099–2106.
- Antalis, T. M., & Godbolt, D. (1991). Isolation of intact nuclei from hematopoietic cell types. *Nucleic Acids Research*, *19*(15), 4301.
- Arnér, E. S. J., & Holmgren, A. (2000). Physiological functions of thioredoxin and thioredoxin reductase. *European Journal of Biochemistry*, *267*(20), 6102–6109.
- Arranz, R., Coloma, R., Chichón, F. J., Conesa, J. J., Carrascosa, J. L., Valpuesta, J. M., ... Martín-Benito, J. (2012). The structure of native influenza virion ribonucleoproteins. *Science*, *338*(6114), 1634–1637.
- Atsmon, J., Caraco, Y., Ziv-Sefer, S., Shaikevich, D., Abramov, E., Volokhov, I., ... Ben-Yedidia, T. (2014). Priming by a novel universal influenza vaccine (Multimeric-001)-A gateway for improving immune response in the elderly population. *Vaccine*, *32*(44), 5816–5823.
- Bandiera, A., Taglienti, A., Micali, F., Pani, B., Tamaro, M., Crescenzi, V., & Manzini, G. (2005). Expression and characterization of human-elastin-repeat-based temperature-responsive protein polymers for biotechnological purposes. *Biotechnology and Applied Biochemistry*, *42*(3), 247–256.
- Barry, J. M. (2004). The site of origin of the 1918 influenza pandemic and its public health implications. *Journal of Translational Medicine*, *2*(1), 3.
- Batishchev, O. V., Shilova, L. A., Kachala, M. V., Tashkin, V. Y., Sokolov, V. S., Fedorova, N. V., ... Chizmadzhev, Y. A. (2015). pH-Dependent Formation and Disintegration of the Influenza A Virus Protein Scaffold To Provide Tension for Membrane Fusion. *Journal of Virology*, *90*(1), 575–585.
- Bechara, C., & Sagan, S. (2013). Cell-penetrating peptides: 20 years later, where do we stand? *FEBS Letters*, *587*(12), 1693–1702.
- Belshe, R. B., Edwards, K. M., Vesikari, T., Black, S. V., Walker, R. E., Hultquist, M., ... Connor, E. M. (2007). Live attenuated versus inactivated influenza vaccine in infants and young children. *The New England Journal of Medicine*, *356*(7), 685–696.
- Bidwell, G. L., & Raucher, D. (2010). Cell penetrating elastin-like polypeptides for therapeutic peptide delivery. *Advanced Drug Delivery Reviews*, *62*(15), 1486–1496.

- Bimboim, H. C., & Doly, J. (1979). A rapid alkaline extraction procedure for screening recombinant plasmid DNA. *Nucleic Acids Research*, 7(6), 1513–1523.
- Bloom, J. D., Gong, L. I., & Baltimore, D. (2010). Permissive secondary mutations enable the evolution of influenza oseltamivir resistance. *Science*, 328(5983), 1272–1275.
- Boivin, S., Cusack, S., Ruigrok, R. W. H., & Hart, D. J. (2010). Influenza A virus polymerase: Structural insights into replication and host adaptation mechanisms. *Journal of Biological Chemistry*, 285(37), 28411–28417.
- Borghouts, C., Kunz, C., Delis, N., & Groner, B. (2008). Monomeric recombinant peptide aptamers are required for efficient intracellular uptake and target inhibition. *Molecular Cancer Research*, 6(2), 267–281.
- Böttcher-Friebertshäuser, E., Freuer, C., Sielaff, F., Schmidt, S., Eickmann, M., Uhlendorff, J., ... Garten, W. (2010). Cleavage of influenza virus hemagglutinin by airway proteases TMPRSS2 and HAT differs in subcellular localization and susceptibility to protease inhibitors. *Journal of Virology*, 84(11), 5605–5614.
- Braam, J., Ulmanen, I., & Krug, R. M. (1983). Molecular model of a eucaryotic transcription complex: Functions and movements of influenza P proteins during capped RNA-primed transcription. *Cell*, 34(2), 611–618.
- Browne, M. J., Moss, M. Y., & Boyd, M. R. (1983). Comparative activity of amantadine and ribavirin against influenza virus in vitro: Possible clinical relevance. *Antimicrobial Agents and Chemotherapy*, 23(3), 503–505.
- Bui, M., Whittaker, G., & Helenius, A. (1996). Effect of M1 protein and low pH on nuclear transport of influenza virus ribonucleoproteins. *Journal of Virology*, 70(12), 8391–8401.
- Burton, J. P., Chilcott, C. N., Moore, C. J., Speiser, G., & Tagg, J. R. (2006). A preliminary study of the effect of probiotic *Streptococcus salivarius* K12 on oral malodour parameters. *Journal of Applied Microbiology*, 100(4), 754–764.
- Bush, R. M., Bender, C. A., Subbarao, K., Cox, N. J., & Fitch, W. M. (1999). Predicting the evolution of human influenza A. *Science*, 286(5446), 1921–1925.
- Carrat, F., & Flahault, A. (2007). Influenza vaccine: The challenge of antigenic drift. *Vaccine*, 25(40), 6852–6862.
- Carrat, F., Vergu, E., Ferguson, N. M., Lemaître, M., Cauchemez, S., Leach, S., & Valleron, A. J. (2008). Time lines of infection and disease in human influenza: A review of volunteer challenge studies. *American Journal of Epidemiology*, 167(7), 775–785.
- Centers for Disease Control and Prevention. (2009). Oseltamivir-resistant novel influenza A (H1N1) virus infection in two immunosuppressed patients --- Seattle, Washington,

2009. *Morbidity and Mortality Weekly Report*, 58(32), 893. Retrieved from <http://www.cdc.gov/mmwr/preview/mmwrhtml/mm5832a3.htm>
- Centers for Disease Control and Prevention. (2012). First global estimates of 2009 H1N1 pandemic mortality released by CDC-led collaboration. Retrieved from <https://www.cdc.gov/flu/spotlights/pandemic-global-estimates.htm>
- Centers for Disease Control and Prevention. (2015). Influenza activity — United States, 2014–15 season and composition of the 2015–16 influenza vaccine. *Morbidity and Mortality Weekly Report*, 64(21), 583–590.
- Centers for Disease Control and Prevention. (2016a). Flu symptoms & complications. Retrieved April 27, 2017, from <https://www.cdc.gov/flu/about/disease/complications.htm>
- Centers for Disease Control and Prevention. (2016b). Flu vaccine nearly 60 percent effective. Retrieved from <http://www.cdc.gov/media/releases/2016/flu-vaccine-60-percent.html>
- Centers for Disease Control and Prevention. (2016c). Selecting viruses for the seasonal influenza vaccine. Retrieved from <http://www.cdc.gov/flu/about/season/vaccine-selection.htm>
- Chan-Tack, K. M., Murray, J. S., & Birnkrant, D. B. (2009). Use of Ribavirin to Treat Influenza. *New England Journal of Medicine*, 361(17), 1713–1714.
- Chen, B. J., Leser, G. P., Jackson, D., & Lamb, R. A. (2008). The influenza virus M2 protein cytoplasmic tail interacts with the M1 protein and influences virus assembly at the site of virus budding. *Journal of Virology*, 82(20), 10059–10070.
- Chen, X., Zaro, J. L., & Shen, W. C. (2013). Fusion protein linkers: Property, design and functionality. *Advanced Drug Delivery Reviews*, 65(10), 1357–1369.
- Cho, S., Dong, S., Parent, K. N., & Chen, M. (2016). Immune-tolerant elastin-like polypeptides (iTEPs) and their application as CTL vaccine carriers. *Journal of Drug Targeting*, 24(4), 328–339.
- Christensen, T., Amiram, M., Dagher, S., Trabbic-Carlson, K., Shamji, M. F., Setton, L. A., & Chilkoti, A. (2009). Fusion order controls expression level and activity of elastin-like polypeptide fusion proteins. *Protein Science*, 18(7), 1377–1387.
- Christensen, T., Hassouneh, W., Trabbic-Carlson, K., & Chilkoti, A. (2013). Predicting transition temperatures of elastin-like polypeptide fusion proteins. *Biomacromolecules*, 14(5), 1514–1519.
- Christiansen, M., Matson, M., Brazg, R., Georgopoulos, L., Arnold, S., Kramer, W., ... Strange, P. (2012). Weekly subcutaneous doses of Glymera (PB1023), a novel GLP-1 analogue reduces glucose exposure dose dependently. In *American Diabetes Association 72nd Scientific Sessions*.

- Connor, R. J., Kawaoka, Y., Webster, R. G., & Paulson, J. C. (1994). Receptor specificity in human, avian, and equine H2 and H3 influenza virus isolates. *Virology*, *205*(1), 17–23.
- Cowling, B. J., Ip, D. K. M., Fang, V. J., Suntarattiwong, P., Olsen, S. J., Levy, J., ... Mark Simmerman, J. (2013). Aerosol transmission is an important mode of influenza A virus spread. *Nature Communications*, *4*, 1935.
- Cox, N. J., & Subbarao, K. (2000). Global epidemiology of influenza: past and present. *Annual Review of Medicine*, *51*(1), 407–421.
- Crepin, T., Dias, A., Palencia, A., Swale, C., Cusack, S., & Ruigrok, R. W. (2010). Mutational and metal binding analysis of the endonuclease domain of the influenza virus polymerase PA subunit. *Journal of Virology*, *84*(18), 9096–9104.
- Cros, J. F., & Palese, P. (2003). Trafficking of viral genomic RNA into and out of the nucleus: Influenza, Thogoto and Borna disease viruses. *Virus Research*, *95*(1), 3–12.
- Cross, K. J., Burleigh, L. M., & Steinhauer, D. a. (2001). Mechanisms of cell entry by influenza virus. *Expert Reviews in Molecular Medicine*, *3*(21), 1–18.
- Das, K., Aramini, J. M., Ma, L.-C., Krug, R. M., & Arnold, E. (2010). Structures of influenza A proteins and insights into antiviral drug targets. *Nature Structural & Molecular Biology*, *17*(5), 530–538.
- De Filette, M., Jou, W. M., Birkett, A., Lyons, K., Schultz, B., Tonkyro, A., ... Fiers, W. (2005). Universal influenza A vaccine: Optimization of M2-based constructs. *Virology*, *337*(1), 149–161.
- de Wit, E., Bestebroer, T. M., Spronken, M. I. J., Rimmelzwaan, G. F., Osterhaus, A. D. M. E., & Fouchier, R. A. M. (2007). Rapid sequencing of the non-coding regions of influenza A virus. *Journal of Virological Methods*, *139*(1), 85–89.
- Derossi, D., Joliot, A. H., Chassaing, G., & Prochiantz, A. (1994). The third helix of the Antennapedia homeodomain translocates through biological membranes. *Journal of Biological Chemistry*, *269*(14), 10444–10450.
- Deshayes, S., Morris, M. C., Divita, G., & Heitz, F. (2006). Interactions of amphipathic CPPs with model membranes. *Biochimica et Biophysica Acta - Biomembranes*, *1758*(3), 328–335.
- Despanie, J., Dhandhukia, J. P., Hamm-Alvarez, S. F., & MacKay, J. A. (2016). Elastin-like polypeptides: Therapeutic applications for an emerging class of nanomedicines. *Journal of Controlled Release*, *240*, 93–108.
- Dias, A., Bouvier, D., Crépin, T., McCarthy, A. a, Hart, D. J., Baudin, F., ... Ruigrok, R. W. H. (2009). The cap-snatching endonuclease of influenza virus polymerase resides in the PA subunit. *Nature*, *458*(7240), 914–918.

- Douette, P., Navet, R., Gerkens, P., Galleni, M., Lévy, D., & Sluse, F. E. (2005). Escherichia coli fusion carrier proteins act as solubilizing agents for recombinant uncoupling protein 1 through interactions with GroEL. *Biochemical and Biophysical Research Communications*, 333(3), 686–693.
- Drake, J. W. (1993). Rates of spontaneous mutation among RNA viruses. *Proceedings of the National Academy of Sciences of the United States of America*, 90(9), 4171–4175.
- Dubois, J., Terrier, O., & Rosa-Calatrava, M. (2014). Influenza viruses and mRNA splicing: doing more with less. *mBio*, 5(3).
- Earn, D. J. D., Dushoff, J., & Levin, S. A. (2002). Ecology and evolution of the flu. *Trends in Ecology and Evolution*, 17(7), 334–340.
- Eggink, D., Goff, P. H., & Palese, P. (2014). Guiding the immune response against influenza virus hemagglutinin toward the conserved stalk domain by hyperglycosylation of the globular head domain. *Journal of Virology*, 88(1), 699–704.
- Ennis, H. L., & Lubin, M. (1964). Cycloheximide: Aspects of Inhibition of Protein Synthesis in Mammalian Cells. *Science*, 146(3650), 1474–1476.
- Firth, A. E., Jagger, B. W., Wise, H. M., Nelson, C. C., Parsawar, K., Wills, N. M., ... Atkins, J. F. (2012). Ribosomal frameshifting used in influenza A virus expression occurs within the sequence UCC_UUU_CGU and is in the +1 direction. *Open Biology*, 2(10), 120109.
- Fleming, D. M., Van Der Velden, J., & Paget, W. J. (2003). The evolution of influenza surveillance in Europe and prospects for the next 10 years. *Vaccine*, 21(16), 1749–1753.
- Floss, D. M., Sack, M., Arcalis, E., Stadlmann, J., Quendler, H., Rademacher, T., ... Conrad, U. (2009). Influence of elastin-like peptide fusions on the quantity and quality of a tobacco-derived human immunodeficiency virus-neutralizing antibody. *Plant Biotechnology Journal*, 7(9), 899–913.
- Fodor, E., & Smith, M. (2004). The PA subunit is required for efficient nuclear accumulation of the PB1 subunit of the influenza A virus RNA polymerase complex. *Journal of Virology*, 78(17), 9144–9153.
- Fontana, J., Cardone, G., Heymann, J. B., Winkler, D. C., & Steven, A. C. (2012). Structural changes in influenza virus at low pH characterized by cryo-electron tomography. *Journal of Virology*, 86(6), 2919–2929.
- Francis, J. N., Bunce, C. J., Horlock, C., Watson, J. M., Warrington, S. J., Georges, B., & Brown, C. B. (2015). A novel peptide-based pan-influenza A vaccine: A double blind, randomised clinical trial of immunogenicity and safety. *Vaccine*, 33(2), 396–402.

- Furuta, Y., Gowen, B. B., Takahashi, K., Shiraki, K., Smee, D. F., & Barnard, D. L. (2013). Favipiravir (T-705), a novel viral RNA polymerase inhibitor. *Antiviral Research*, *100*(2), 446–454.
- Futaki, S., Suzuki, T., Ohashi, W., Yagami, T., Tanaka, S., Ueda, K., & Sugiura, Y. (2001). Arginine-rich peptides. An abundant source of membrane-permeable peptides having potential as carriers for intracellular protein delivery. *Journal of Biological Chemistry*, *276*(8), 5836–5840.
- Gamblin, S. J., & Skehel, J. J. (2010). Influenza hemagglutinin and neuraminidase membrane glycoproteins. *The Journal of Biological Chemistry*, *285*(37), 28403–28409.
- Garten, R. J., Davis, C. T., Russell, C. A., Shu, B., Lindstrom, S., Balish, A., ... Cox, N. J. (2009). Antigenic and genetic characteristics of swine-origin 2009 A(H1N1) influenza viruses circulating in humans. *Science*, *325*(5937), 197–201.
- Gatherer, D. (2009). The 2009 H1N1 influenza outbreak in its historical context. *Journal of Clinical Virology*, *45*(3), 174–8.
- Gerbal-Chaloin, S., Gondeau, C., Aldrian-Herrada, G., Heitz, F., Gauthier-Rouvière, C., & Divita, G. (2007). First step of the cell-penetrating peptide mechanism involves Rac1 GTPase-dependent actin-network remodelling. *Biology of the Cell*, *99*(4), 223–238.
- Ghanem, A., Mayer, D., Chase, G., Tegge, W., Frank, R., Kochs, G., ... Schwemmler, M. (2007). Peptide-mediated interference with influenza A virus polymerase. *Journal of Virology*, *81*(14), 7801–7804.
- Ghendon, Y. (1994). Introduction to pandemic influenza through history. *European Journal of Epidemiology*, *10*(4), 451–453.
- Giard, D. J., Aaronson, S. a, Todaro, G. J., Arnstein, P., Kersey, J. H., Dosik, H., & Parks, W. P. (1973). In vitro cultivation of human tumors: establishment of cell lines derived from a series of solid tumors. *Journal of the National Cancer Institute*, *51*(5), 1417–1423.
- Glaser, L., Stevens, J., Zamarin, D., Wilson, I. A., Garcia-Sastre, A., Tumpey, T. M., ... Palese, P. (2005). A single amino acid substitution in 1918 influenza virus hemagglutinin changes receptor binding specificity. *Journal of Virology*, *79*(17), 11533–11536.
- Goodwin, D., Simerska, P., & Toth, I. (2012). Peptides As Therapeutics with Enhanced Bioactivity. *Current Medicinal Chemistry*, *19*(26), 4451–4461.
- Goraya, M. U., Wang, S., Munir, M., & Chen, J. L. (2015). Induction of innate immunity and its perturbation by influenza viruses. *Protein and Cell*, *6*(10), 712–721.
- Government of Canada. (2016). Public Funding for Influenza Vaccination by

- Province/Territory (as of December 2016). Retrieved from <https://www.canada.ca/en/public-health/services/provincial-territorial-immunization-information/public-funding-influenza-vaccination-province-territory.html>
- Green, N., Alexander, H., Olson, A., Alexander, S., Shinnick, T. M., Sutcliffe, J. G., & Lerner, R. A. (1982). Immunogenic structure of the influenza virus hemagglutinin. *Cell*, 28(3), 477–487.
- Gubareva, L. V, Kaiser, L., & Hayden, F. G. (2000). Influenza virus neuraminidase inhibitors. *Lancet*, 355(9206), 827–835.
- Guilligay, D., Tarendeau, F., Resa-Infante, P., Coloma, R., Crepin, T., Sehr, P., ... Cusack, S. (2008). The structural basis for cap binding by influenza virus polymerase subunit PB2. *Nature Structural and Molecular Biology*, 15(5), 500–506.
- Hannoun, C. (2013). The evolving history of influenza viruses and influenza vaccines. *Expert Review of Vaccines*, 12(9), 1085–1094.
- Hassouneh, W., MacEwan, S. R., & Chilkoti, A. (2012). Fusions of elastin-like polypeptides to pharmaceutical proteins. *Methods in Enzymology*, 502, 215–237.
- He, X., Zhou, J., Bartlam, M., Zhang, R., Ma, J., Lou, Z., ... Liu, Y. (2008). Crystal structure of the polymerase PAC–PB1N complex from an avian influenza H5N1 virus. *Nature*, 454(7208), 1123–1126.
- Henderson, D. A., Courtney, B., Inglesby, T. V, Toner, E., & Nuzzo, J. B. (2009). Public health and medical responses to the 1957-58 influenza pandemic. *Biosecurity and Bioterrorism : Biodefense Strategy, Practice, and Science*, 7(3), 265–273.
- Herce, H. D., & Garcia, A. E. (2007). Molecular dynamics simulations suggest a mechanism for translocation of the HIV-1 TAT peptide across lipid membranes. *Proceedings of the National Academy of Sciences of the United States of America*, 104(52), 20805–20810.
- Herrero-Vanrell, R., Rincon, A. C., Alonso, M., Reboto, V., Molina-Martinez, I. T., & Rodriguez-Cabello, J. C. (2005). Self-assembled particles of an elastin-like polymer as vehicles for controlled drug release. *Journal of Controlled Release*, 102(1), 113–122.
- Hilsch, M., Goldenbogen, B., Sieben, C., Höfer, C. T., Rabe, J. P., Klipp, E., ... Chiantia, S. (2014). Influenza A matrix protein M1 multimerizes upon binding to lipid membranes. *Biophysical Journal*, 107(4), 912–923.
- Hoffmann, J., Schneider, C., Heinbockel, L., Brandenburg, K., Reimer, R., & Gabriel, G. (2014). A new class of synthetic anti-lipopolysaccharide peptides inhibits influenza A virus replication by blocking cellular attachment. *Antiviral Research*, 104(1), 23–33.
- Holsinger, L. J., Nichani, D., Pinto, L. H., & Lamb, R. A. (1994). Influenza A virus M2

- ion channel protein: a structure-function analysis. *Journal of Virology*, 68(3), 1551–63.
- Huet, S., Avilov, S. V, Ferbitz, L., Daigle, N., Cusack, S., & Ellenberg, J. (2010). Nuclear import and assembly of influenza A virus RNA polymerase studied in live cells by fluorescence cross-correlation spectroscopy. *Journal of Virology*, 84(3), 1254–1264.
- Huleatt, J. W., Nakaar, V., Desai, P., Huang, Y., Hewitt, D., Jacobs, A., ... Powell, T. J. (2008). Potent immunogenicity and efficacy of a universal influenza vaccine candidate comprising a recombinant fusion protein linking influenza M2e to the TLR5 ligand flagellin. *Vaccine*, 26(2), 201–214.
- Ito, T., Couceiro, J. N., Kelm, S., Baum, L. G., Krauss, S., Castrucci, M. R., ... Kawaoka, Y. (1998). Molecular basis for the generation in pigs of influenza A viruses with pandemic potential. *Journal of Virology*, 72(9), 7367–7373.
- Johnson, N. P. A. S., & Mueller, J. (2002). Updating the accounts: global mortality of the 1918-1920 “Spanish” Influenza Pandemic. *Bulletin of the History of Medicine*, 76(1), 105–115.
- Kameyama, S., Horie, M., Kikuchi, T., Omura, T., Tadokoro, A., Takeuchi, T., ... Futaki, S. (2007). Acid wash in determining cellular uptake of fab/cell-permeating peptide conjugates. *Peptide Science*, 88(2), 98–107.
- Kendal, A. P., Joseph, J. M., Kobayashi, G., Nelson, D., Reyes, C. R., Ross, M. R., ... Dowdle, W. R. (1979). Laboratory-based surveillance of influenza virus in the United States during the winter of 1977-1978: I periods of prevalence of H1N1 and H3N2 influenza A strains, their relative rates of isolation in different age groups, and detection of antigenic varia. *American Journal of Epidemiology*, 110(4), 449–461.
- Kilbourne, E. D., Smith, C., Brett, I., Pokorny, B. A., Johansson, B., & Cox, N. (2002). The total influenza vaccine failure of 1947 revisited: major intrasubtypic antigenic change can explain failure of vaccine in a post-World War II epidemic. *Proceedings of the National Academy of Sciences of the United States of America*, 99(16), 10748–10752.
- Kim, J. I., & Park, M. S. (2012). N-linked glycosylation in the hemagglutinin of influenza A viruses. *Yonsei Medical Journal*, 53(5), 886–893.
- King, A. M. Q., Adams, M. J., Carsten, E. B., & Lefkowitz, E. J. (2012). *Virus Taxonomy: Classification and Nomenclature of Viruses. Ninth Report of the International Committee on Taxonomy of Viruses. Elsevier Inc. Elsevier.*
- Kirui, J., Bucci, M. D., Poole, D. S., & Mehle, A. (2014). Conserved features of the PB2 627 domain impact influenza virus polymerase function and replication. *Journal of Virology*, 88(11), 5977–86.
- Kiso, M., Takahashi, K., Sakai-Tagawa, Y., Shinya, K., Sakabe, S., Le, Q. M., ... Kawaoka, Y. (2010). T-705 (favipiravir) activity against lethal H5N1 influenza A

- viruses. *Proceedings of the National Academy of Sciences of the United States of America*, 107(2), 882–887.
- Koppelhus, U., Awasthi, S. K., Zachar, V., Holst, H. U., Ebbesen, P., & Nielsen, P. E. (2002). Cell-dependent differential cellular uptake of PNA, peptides, and PNA-peptide conjugates. *Antisense & Nucleic Acid Drug Development*, 12(2), 51–63.
- Koren, E., & Torchilin, V. P. (2012). Cell-penetrating peptides: Breaking through to the other side. *Trends in Molecular Medicine*, 18(7), 385–393.
- Kowalczyk, T., Hnatuszko-Konka, K., Gerszberg, A., & Kononowicz, A. K. (2014). Elastin-like polypeptides as a promising family of genetically-engineered protein based polymers. *World Journal of Microbiology and Biotechnology*, 30(8), 2141–2152.
- Krämer, S. D., & Wunderli-Allenspach, H. (2003). No entry for TAT(44-57) into liposomes and intact MDCK cells: Novel approach to study membrane permeation of cell-penetrating peptides. *Biochimica et Biophysica Acta - Biomembranes*, 1609(2), 161–169.
- Krammer, F., & Palese, P. (2013). Influenza virus hemagglutinin stalk-based antibodies and vaccines. *Current Opinion in Virology*, 3(5), 521–530.
- Krilov, L. R. (2011). Respiratory syncytial virus disease: update on treatment and prevention. *Expert Review of Anti-Infective Therapy*, 9(1), 27–32.
- Kumar, A., Zarychanski, R., Pinto, R., Cook, D. J., Marshall, J., Lacroix, J., ... Fowler, R. a. (2009). Critically ill patients with 2009 influenza A(H1N1) infection in Canada. *The Journal of the American Medical Association*, 302(17), 1872–1879.
- Larsen, M. T., Kuhlmann, M., Hvam, M. L., & Howard, K. A. (2016). Albumin-based drug delivery: harnessing nature to cure disease. *Molecular and Cellular Therapies*, 4(1), 3.
- Leekha, S., Zitterkopf, N. L., Espy, M. J., Smith, T. F., Thompson, R. L., & Sampathkumar, P. (2007). Duration of influenza A virus shedding in hospitalized patients and implications for infection control. *Infection Control and Hospital Epidemiology*, 28(9), 1071–1076.
- Li, F. C. K., Choi, B. C. K., Sly, T., & Pak, A. W. P. (2008). Finding the real case-fatality rate of H5N1 avian influenza. *Journal of Epidemiology and Community Health*, 62(6), 555–559.
- Lindstrom, S. E., Cox, N. J., & Klimov, A. (2004). Genetic analysis of human H2N2 and early H3N2 influenza viruses, 1957-1972: Evidence for genetic divergence and multiple reassortment events. *Virology*, 328(1), 101–119.
- Liu, W., MacKay, J. A., Dreher, M. R., Chen, M., McDaniel, J. R., Simnick, A. J., ... Chilkoti, A. (2010). Injectable intratumoral depot of thermally responsive

- polypeptide–radionuclide conjugates delays tumor progression in a mouse model. *Journal of Controlled Release*, 144(1), 2–9.
- Lowry, O. H., Rosebrough, N. J., Farr, A. L., & Randall, R. J. (1951). Protein measurement with the Folin phenol reagent. *The Journal of Biological Chemistry*, 193(1), 265–275.
- Lugovtsev, V. Y., Melnyk, D., & Weir, J. P. (2013). Heterogeneity of the MDCK cell line and its applicability for influenza virus research. *PLoS ONE*, 8(9), e75014.
- Lupiani, B., & Reddy, S. M. (2009). The history of avian influenza. *Comparative Immunology, Microbiology and Infectious Diseases*, 32(4), 311–323.
- Ma, J.-H., Yang, F.-R., Yu, H., Zhou, Y.-J., Li, G.-X., Huang, M., ... Tong, G. (2013). An M2e-based synthetic peptide vaccine for influenza A virus confers heterosubtypic protection from lethal virus challenge. *Virology Journal*, 10(1), 227.
- Maassab, H. F., & Bryant, M. L. (1999). The development of live attenuated cold-adapted influenza virus vaccine for humans. *Reviews in Medical Virology*, 9(4), 237–244.
- Madani, F., Lindberg, S., Langel, Ü., Futaki, S., & Gräslund, A. (2011). Mechanisms of Cellular Uptake of Cell-Penetrating Peptides. *Journal of Biophysics*, 2011, 1–10.
- Mason, J. M. (2010). Design and development of peptides and peptide mimetics as antagonists for therapeutic intervention. *Future Medicinal Chemistry*, 2(12), 1813–1822.
- Massodi, I., Bidwell, G. L., & Raucher, D. (2005). Evaluation of cell penetrating peptides fused to elastin-like polypeptide for drug delivery. *Journal of Controlled Release*, 108(2), 396–408.
- Matrosovich, M., Tuzikov, A., Bovin, N., Gambaryan, A., Klimov, A., Castrucci, M. R., ... Kawaoka, Y. (2000). Early alterations of the receptor-binding properties of H1, H2, and H3 avian influenza virus hemagglutinins after their introduction into mammals. *Journal of Virology*, 74(18), 8502–8512.
- Matsubara, T. (2012). Potential of Peptides as Inhibitors and Mimotopes: Selection of Carbohydrate-Mimetic Peptides from Phage Display Libraries. *Journal of Nucleic Acids*, 2012, 1–15.
- Matsubara, T., Onishi, A., Saito, T., Shimada, A., Inoue, H., Taki, T., ... Sato, T. (2010). Sialic acid-mimic peptides as hemagglutinin inhibitors for anti-influenza therapy. *Journal of Medicinal Chemistry*, 53(11), 4441–4449.
- McDaniel, J. R., MacKay, J. A., Quiroz, F. G., & Chilkoti, A. (2010). Recursive directional ligation by plasmid reconstruction allows rapid and seamless cloning of oligomeric genes. *Biomacromolecules*, 11(4), 944–952.
- McDaniel, J. R., Radford, D. C., & Chilkoti, A. (2013). A unified model for de novo

- design of elastin-like polypeptides with tunable inverse transition temperatures. *Biomacromolecules*, 14(8), 2866–2872.
- McKimm-Breschkin, J. L. (2013). Influenza neuraminidase inhibitors: antiviral action and mechanisms of resistance. *Influenza and Other Respiratory Viruses*, 7(1), 25–36.
- McMichael, A. J., Gotch, F. M., Noble, G. R., & Beare, P. A. (1983). Cytotoxic T-cell immunity to influenza. *The New England Journal of Medicine*, 309(1), 13–17.
- MDVI, & LLC. (2010). Dose-finding study of favipiravir in the treatment of uncomplicated influenza in: clinicaltrials.gov [internet]. Bethesda (MD): National Library of Medicine (US). 2000-[cited 2017 May 28]. Retrieved from <https://clinicaltrials.gov/ct2/show/NCT01068912>
- Mehle, A., & McCullers, J. A. (2013). Structure and function of the influenza virus replication machinery and PB1-F2. In *Textbook of Influenza* (2nd editio, pp. 133–145). West Sussex, United Kingdom: John Wiley and Sons Ltd.
- Mertens, N., Remaut, E., & Fiers, W. (1995). Tight transcriptional control mechanism ensures stable high-level expression from T7 promoter-based expression plasmids. *Nature Biotechnology*, 13(2), 175–179.
- Meyer, D. E., & Chilkoti, A. (1999). Purification of recombinant proteins by fusion with thermally-responsive polypeptides. *Nature Biotechnology*, 17(11), 1112–1115.
- Meyer, D. E., & Chilkoti, A. (2002). Genetically encoded synthesis of protein-based polymers with precisely specified molecular weight and sequence by recursive directional ligation: Examples from the the elastin-like polypeptide system. *Biomacromolecules*, 3(2), 357–367.
- Meyer, D. E., & Chilkoti, A. (2004). Quantification of the effects of chain length and concentration on the thermal behavior of elastin-like polypeptides. *Biomacromolecules*, 5(3), 846–851.
- Mishra, A., Lai, G. H., Schmidt, N. W., Sun, V. Z., Rodriguez, A. R., Tong, R., ... Wong, G. C. L. (2011). Translocation of HIV TAT peptide and analogues induced by multiplexed membrane and cytoskeletal interactions. *Proceedings of the National Academy of Sciences*, 108(41), 16883–16888.
- Mitragotri, S., Burke, P. A., & Langer, R. (2014). Overcoming the challenges in administering biopharmaceuticals: formulation and delivery strategies. *Nature Reviews Drug Discovery*, 13(9), 655–672.
- Moeller, A., Kirchdoerfer, R. N., Potter, C. S., Carragher, B., & Wilson, I. A. (2012). Organization of the influenza virus replication machinery. *Science*, 338(6114), 1631–1634.
- Mohler, W. A., Charlton, C. A., & Blau, H. M. (1996). Spectrophotometric quantitation of tissue culture cell number in any medium. *BioTechniques*, 21(2), 260–266.

- Molinari, N. A. M., Ortega-Sanchez, I. R., Messonnier, M. L., Thompson, W. W., Wortley, P. M., Weintraub, E., & Bridges, C. B. (2007). The annual impact of seasonal influenza in the US: Measuring disease burden and costs. *Vaccine*, *25*(27), 5086–5096.
- Monto, A. S., Ohmit, S. E., Petrie, J. G., Johnson, E., Truscon, R., Teich, E., ... Victor, J. C. (2009). Comparative efficacy of inactivated and live attenuated influenza vaccines. *The New England Journal of Medicine*, *361*(13), 1260–1267.
- Nachbagauer, R., Miller, M. S., Hai, R., Ryder, A. B., Rose, J. K., Palese, P., ... Albrecht, R. A. (2016). Hemagglutinin stalk immunity reduces influenza virus replication and transmission in ferrets. *Journal of Virology*, *90*(6), 3268–3273.
- Nayak, D. P., Balogun, R. A., Yamada, H., Zhou, Z. H., & Barman, S. (2009). Influenza virus morphogenesis and budding. *Virus Research*, *143*(2), 147–161.
- Nelson, M. I., & Holmes, E. C. (2007). The evolution of epidemic influenza. *Nature Reviews Genetics*, *8*(3), 196–205.
- Neumann, G., Noda, T., & Kawaoka, Y. (2009). Emergence and pandemic potential of swine-origin H1N1 influenza virus. *Nature*, *459*(7249), 931–939.
- Nguyen-Van-Tam, J. (2003). The epidemiology and clinical impact of pandemic influenza. *Vaccine*, *21*(16), 1762–1768.
- Nieto, A., de la Luna, S., Bárcena, J., Portela, A., & Ortín, J. (1994). Complex structure of the nuclear translocation signal of influenza virus polymerase PA subunit. *The Journal of General Virology*, *75*(1), 29–36.
- Noda, T. (2011). Native morphology of influenza virions. *Frontiers in Microbiology*, *2*, 269.
- Obayashi, E., Yoshida, H., Kawai, F., Shibayama, N., Kawaguchi, A., Nagata, K., ... Park, S. Y. (2008). The structural basis for an essential subunit interaction in influenza virus RNA polymerase. *Nature*, *454*(7208), 1127–1131.
- Ohtsu, Y., Honda, Y., Sakata, Y., Kato, H., & Toyoda, T. (2002). Fine mapping of the subunit binding sites of influenza virus RNA polymerase. *Microbiology and Immunology*, *46*(3), 167–175.
- Olitsky, P. K., & Gates, F. L. (1921). Experimental studies of the nasopharyngeal secretions from influenza patients : V. Bacterium pneumosintes and concurrent infections. *Journal of Experimental Medicine*, *34*(1), 1–9.
- Patel, A., & Gorman, S. E. (2009). Stockpiling antiviral drugs for the next influenza pandemic. *Clinical Pharmacology and Therapeutics*, *86*(3), 241–243.
- Patel, J., Zhu, H., Menassa, R., Gyenis, L., Richman, A., & Brandle, J. (2007). Elastin-like polypeptide fusions enhance the accumulation of recombinant proteins in

- tobacco leaves. *Transgenic Research*, 16(2), 239–249.
- Peiris, J. S. M., de Jong, M. D., & Guan, Y. (2007). Avian influenza virus (H5N1): a threat to human health. *Clinical Microbiology Reviews*, 20(2), 243–67.
- Perez, D. R., & Donis, R. O. (2001). Functional analysis of PA binding by influenza A virus PB1: Effects on polymerase activity and viral infectivity. *Journal of Virology*, 75(17), 8127–8136.
- Pflug, A., Guilligay, D., Reich, S., & Cusack, S. (2014). Structure of influenza A polymerase bound to the viral RNA promoter. *Nature*, 516(7531), 355–60.
- Pielak, R. M., Schnell, J. R., & Chou, J. J. (2009). Mechanism of drug inhibition and drug resistance of influenza A M2 channel. *Proceedings of the National Academy of Sciences of the United States of America*, 106(18), 7379–7384.
- Pinto, L. H., Holsinger, L. J., & Lamb, R. A. (1992). Influenza virus M2 protein has ion channel activity. *Cell*, 69(3), 517–528.
- Poole, E. L., Medcalf, L., Elton, D., & Digard, P. (2007). Evidence that the C-terminal PB2-binding region of the influenza A virus PB1 protein is a discrete alpha-helical domain. *FEBS Letters*, 581(27), 5300–5306.
- Poon, L. L., Pritlove, D. C., Fodor, E., & Brownlee, G. G. (1999). Direct evidence that the poly(A) tail of influenza A virus mRNA is synthesized by reiterative copying of a U track in the virion RNA template. *Journal of Virology*, 73(4), 3473–3476.
- Rao, S., Hu, S., McHugh, L., Lueders, K., Henry, K., Zhao, Q., ... Hamer, D. H. (2005). Toward a live microbial microbicide for HIV: commensal bacteria secreting an HIV fusion inhibitor peptide. *Proceedings of the National Academy of Sciences of the United States of America*, 102(34), 11993–11998.
- Read, E. K. C., & Digard, P. (2010). Individual influenza A virus mRNAs show differential dependence on cellular NXF1/TAP for their nuclear export. *The Journal of General Virology*, 91(5), 1290–1301.
- Reich, S., Guilligay, D., Pflug, A., Malet, H., Berger, I., Crépin, T., ... Cusack, S. (2014). Structural insight into cap-snatching and RNA synthesis by influenza polymerase. *Nature*, 516(7531), 361–366.
- Reiersen, H., Clarke, A. R., & Rees, A. R. (1998). Short elastin-like peptides exhibit the same temperature-induced structural transitions as elastin polymers: implications for protein engineering. *Journal of Molecular Biology*, 283(1), 255–264.
- Richard, J. P., Melikov, K., Brooks, H., Prevot, P., Lebleu, B., & Chernomordik, L. V. (2005). Cellular uptake of unconjugated TAT peptide involves clathrin-dependent endocytosis and heparan sulfate receptors. *Journal of Biological Chemistry*, 280(15), 15300–15306.

- Rincon, A. C., Molina-Martinez, I. T., De Las Heras, B., Alonso, M., Bailez, C., Rodriguez-Cabello, J. C., & Herrero-Vanrell, R. (2006). Biocompatibility of elastin-like polymer poly(VPAVG) microparticles: In vitro and in vivo studies. *Journal of Biomedical Materials Research*, 78(2), 343–351.
- Robb, N. C., Jackson, D., Vreede, F. T., & Fodor, E. (2010). Splicing of influenza A virus NS1 mRNA is independent of the viral NS1 protein. *Journal of General Virology*, 91(9), 2331–2340.
- Roopenian, D. C., & Akilesh, S. (2007). FcRn: the neonatal Fc receptor comes of age. *Nature Reviews Immunology*, 7(9), 715–725.
- Rossman, J. S., & Lamb, R. A. (2011). Influenza virus assembly and budding. *Virology*, 411(2), 229–236.
- Rossman, J. S., Leser, G. P., & Lamb, R. A. (2012). Filamentous influenza virus enters cells via macropinocytosis. *Journal of Virology*, 86(20), 10950–10960.
- Rust, M. J., Lakadamyali, M., Zhang, F., & Zhuang, X. (2004). Assembly of endocytic machinery around individual influenza viruses during viral entry. *Nature Structural & Molecular Biology*, 11(6), 567–573.
- Ryu, J. S., & Raucher, D. (2015). Elastin-like polypeptide for improved drug delivery for anticancer therapy: preclinical studies and future applications. *Expert Opinion on Drug Delivery*, 12(4), 653–667.
- Sakaguchi, T., Tu, Q., Pinto, L. H., & Lamb, R. A. (1997). The active oligomeric state of the minimalistic influenza virus M2 ion channel is a tetramer. *Proceedings of the National Academy of Sciences of the United States of America*, 94(10), 5000–5005.
- Salk, J. E., Menke, W. J., & Francis, T. J. (1945). A clinical, epidemiological, and immunological evaluation of vaccination against epidemic influenza. *American Journal of Epidemiology*, 42(1), 57–93.
- Samji, T. (2009). Influenza A: Understanding the viral life cycle. *Journal of Biology and Medicine*, 82(4), 153–159.
- Schipperus, R., Teeuwen, R. L. M., Werten, M. W. T., Eggink, G., & De Wolf, F. A. (2009). Secreted production of an elastin-like polypeptide by *Pichia pastoris*. *Applied Microbiology and Biotechnology*, 85(2), 293–301.
- Schnell, J. R., & Chou, J. J. (2008). Structure and mechanism of the M2 proton channel of influenza A virus. *Nature*, 451(7178), 591–595.
- Shapiro, G. I., Gurney, T., & Krug, R. M. (1987). Influenza virus gene expression: Control mechanisms at early and late times of infection and nuclear-cytoplasmic transport of virus-specific RNAs. *Journal of Virology*, 61(3), 764–773.

- Shimizu, T., Takizawa, N., Watanabe, K., Nagata, K., & Kobayashi, N. (2011). Crucial role of the influenza virus NS2 (NEP) C-terminal domain in M1 binding and nuclear export of vRNP. *FEBS Letters*, 585(1), 41–46.
- Shtyrya, Y. A., Mochalova, L. V., & Bovin, N. V. (2009). Influenza virus neuraminidase: structure and function. *Acta Naturae*, 1(2), 26–32.
- Sidwell, R. W., Bailey, K. W., Wong, M. H., Barnard, D. L., & Smee, D. F. (2005). In vitro and in vivo influenza virus-inhibitory effects of vramidine. *Antiviral Research*, 68(1), 10–17.
- Sieczkarski, S. B., & Whittaker, G. R. (2002). Influenza virus can enter and infect cells in the absence of clathrin-mediated endocytosis. *Journal of Virology*, 76(20), 10455–10464.
- Siomi, H., Shida, H., Maki, M., & Hatanaka, M. (1990). Effects of a highly basic region of human immunodeficiency virus Tat protein on nucleolar localization. *Journal of Virology*, (4), 1803–1807.
- Smith, W., Andrewes, C. H., & Laidlaw, P. P. (1933). A virus obtained from influenza patients. *The Lancet*, 222(5732), 66–68.
- Smorodintseff, A. A., Tushinsky, M. D., Drobyshchanskaya, A. I., Korovin, A. A., & Osteroff, A. I. (1937). Investigation of volunteers infected with the influenza virus. *American Journal of Medical Sciences*, 194(2), 159–170.
- Steimer, A., Haltner, E., & Lehr, C.-M. (2005). Cell culture models of the respiratory tract relevant to pulmonary drug delivery. *Journal of Aerosol Medicine*, 18(2), 137–182.
- Stone, C. B., Bulir, D. C., Emdin, C. A., Pirie, R. M., Porfilio, E. A., Slootstra, J. W., & Mahony, J. B. (2011). Chlamydia pneumoniae CdsL regulates CdsN ATPase activity, and disruption with a peptide mimetic prevents bacterial invasion. *Frontiers in Microbiology*, 2(FEB).
- Stouffer, A. L., Acharya, R., Salom, D., Levine, A. S., Di Costanzo, L., Soto, C. S., ... DeGrado, W. F. (2008). Structural basis for the function and inhibition of an influenza virus proton channel. *Nature*, 451(7178), 596–599.
- Stubbs, T. M., & Te Velhuis, A. J. (2014). The RNA-dependent RNA polymerase of the influenza A virus. *Future Virology*, 9(9), 863–876.
- Stumpp, M. T., Binz, H. K., & Amstutz, P. (2008). DARPins: A new generation of protein therapeutics. *Drug Discovery Today*, 13(15), 695–701.
- Sugiyama, K., Obayashi, E., Kawaguchi, A., Suzuki, Y., Tame, J. R. H., Nagata, K., & Park, S.-Y. (2009). Structural insight into the essential PB1-PB2 subunit contact of the influenza virus RNA polymerase. *The EMBO Journal*, 28(12), 1803–1811.

- Szretter, K. J., Balish, A. L., & Katz, J. M. (2006). Influenza: propagation, quantification, and storage. In *Current protocols in microbiology* (p. 15G.1).
- Tamm, L. K. (2003). Hypothesis: Spring-loaded boomerang mechanism of influenza hemagglutinin-mediated membrane fusion. *Biochimica et Biophysica Acta Biomembranes*, 1614(1), 14–23.
- Tan, J. S., & File, T. M. (n.d.). Streptococcus species (group G and group C Streptococci, viridans group, nutritionally variant Streptococci) - infectious disease and antimicrobial agents. Retrieved from <http://www.antimicrobe.org/b241.asp>
- Tartof, K., & Hobbs, C. (1987). Improved media for growing plasmid and cosmid clones. *Focus*, 9(2), 10.
- Taubenberger, J. K., & Morens, D. M. (2010). Influenza: the once and future pandemic. *Public Health Reports*, 125, 16–26.
- Te, H. S., Randall, G., & Jensen, D. M. (2007). Mechanism of action of ribavirin in the treatment of chronic hepatitis C. *Gastroenterology & Hepatology*, 3(3), 218–225.
- Tellier, R. (2006). Review of aerosol transmission of influenza A virus. *Emerging Infectious Diseases*, 12(11), 1657–62.
- Trabac-Carlson, K., Meyer, D. E., Liu, L., Piervincenzi, R., Nath, N., LaBean, T., & Chilkoti, A. (2004). Effect of protein fusion on the transition temperature of an environmentally responsive elastin-like polypeptide: A role for surface hydrophobicity? *Protein Engineering, Design and Selection*, 17(1), 57–66.
- Treanor, J. (2004). Influenza vaccine-outmaneuvering antigenic shift and drift. *The New England Journal of Medicine*, 350(3), 218–220.
- Trilla, A., Trilla, G., & Daer, C. (2008). The 1918 “Spanish Flu” in Spain. *Clinical Infectious Diseases*, 47(5), 668–673.
- Turk, D. C. (1984). The pathogenicity of Haemophilus influenzae. *Journal of Medical Microbiology*, 18(1), 1–16.
- Urry, D. W., Luan, C. H., Parker, T. M., Gowda, D. C., Prasad, K. U., Reid, M. C., & Safavy, A. (1991). Temperature of polypeptide inverse temperature transition depends on mean residue hydrophobicity. *Journal of the American Chemical Society*, 113(11), 4346–4348.
- Vagner, J., Qu, H., & Hruby, V. J. (2008). Peptidomimetics, a synthetic tool of drug discovery. *Current Opinion in Chemical Biology*, 12(3), 292–296.
- Varshney, A., Sen, P., Ahmad, E., Rehan, M., Subbarao, N., & Khan, R. H. (2010). Ligand binding strategies of human serum albumin: How can the cargo be utilized? *Chirality*, 22(1), 77–87.
- Viboud, C., Grais, R. F., Lafont, B. A. P., Miller, M. A., & Simonsen, L. (2005).

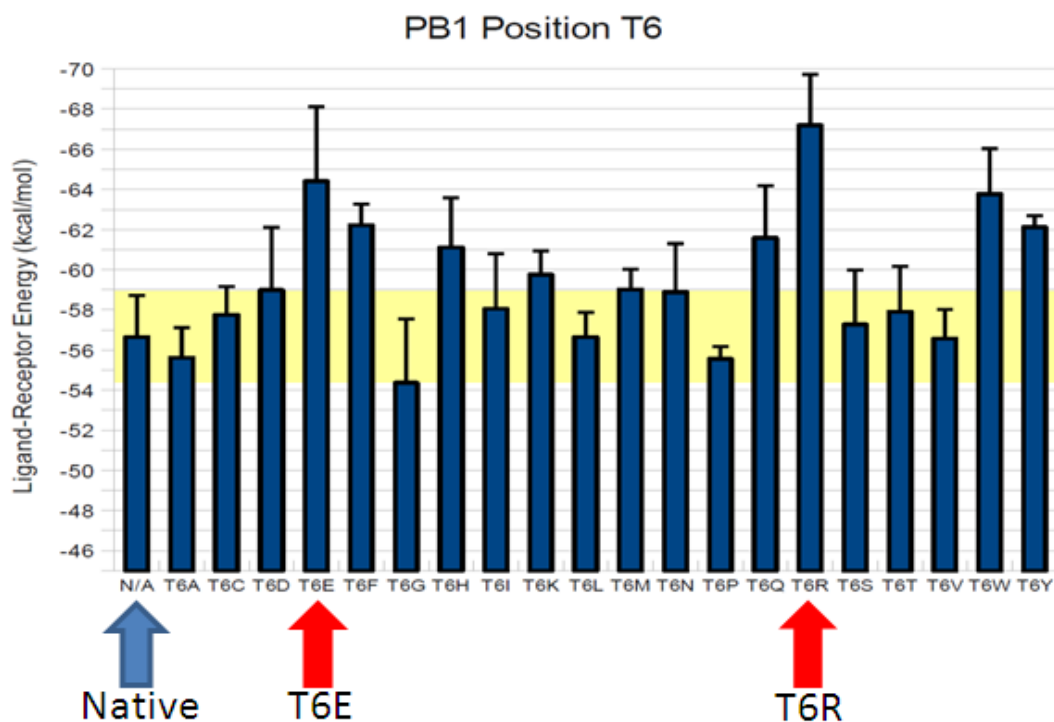
- Multinational impact of the 1968 Hong Kong influenza pandemic: evidence for a smoldering pandemic. *The Journal of Infectious Diseases*, 192, 233–248.
- Viboud, C., Miller, M., Olson, D. R., Osterholm, M., & Simonsen, L. (2010). Preliminary estimates of mortality and years of life lost associated with the 2009 A/H1N1 pandemic in the US and comparison with past influenza seasons. *PLoS Currents Influenza*.
- Violini, S., Sharma, V., Prior, J. L., Dyszlewski, M., & Piwnica-Worms, D. (2002). Evidence for a plasma membrane-mediated permeability barrier to Tat basic domain in well-differentiated epithelial cells: Lack of correlation with heparan sulfate. *Biochemistry*, 41(42), 12652–12661.
- Von Dobschuetz, S., De Nardi, M., Harris, K. A., Munoz, O., Breed, A. C., Wieland, B., ... Stärk, K. D. C. (2015). Influenza surveillance in animals: What is our capacity to detect emerging influenza viruses with zoonotic potential? *Epidemiology and Infection*, 143(10), 2187–2204.
- Vrhovski, B., & Weiss, A. S. (1998). Biochemistry of tropoelastin. *European Journal of Biochemistry*, 258(1), 1–18.
- Wang, T. T., Tan, G. S., Hai, R., Pica, N., Ngai, L., Ekiert, D. C., ... Palese, P. (2010). Vaccination with a synthetic peptide from the influenza virus hemagglutinin provides protection against distinct viral subtypes. *Proceedings of the National Academy of Sciences of the United States of America*, 107(44), 18979–18984.
- Wang, Y., Rezk, A. R., Khara, J. S., Yeo, L. Y., & Ee, P. L. R. (2016). Stability and efficacy of synthetic cationic antimicrobial peptides nebulized using high frequency acoustic waves. *Biomicrofluidics*, 10(3), 34115.
- Webster, R. G., Bean, W. J., Gorman, O. T., Chambers, T. M., & Kawaoka, Y. (1992). Evolution and ecology of influenza A viruses. *Microbiological Reviews*, 56(1), 152–179.
- Wilkinson, T. M. A., Li, C. K., Chui, C. S. C., Huang, A. K. Y., Perkins, M., Liebner, J. C., ... Xu, X.-N. (2012). Preexisting influenza-specific CD4+ T cells correlate with disease protection against influenza challenge in humans. *Nature Medicine*, 18(2), 276–282.
- Wilks, S., de Graaf, M., Smith, D. J., & Burke, D. F. (2012). A review of influenza haemagglutinin receptor binding as it relates to pandemic properties. *Vaccine*, 30(29), 4369–4376.
- World Health Organization. (1980). A revision of the system of nomenclature for influenza viruses: a WHO memorandum. In *Bulletin of the World Health Organization* (Vol. 58, pp. 585–91).
- World Health Organization. (2014). *Global Epidemiological Surveillance Standards for Influenza*. Retrieved from

http://www.who.int/influenza/resources/documents/influenza_surveillance_manual/en/

- World Health Organization. (2016). Influenza (Seasonal) Fact Sheet. Retrieved from <http://www.who.int/mediacentre/factsheets/fs211/en/>
- Worobey, M., Han, G.-Z., & Rambaut, A. (2014). Genesis and pathogenesis of the 1918 pandemic H1N1 influenza A virus. *Proceedings of the National Academy of Sciences of the United States of America*, *111*(22), 8107–12.
- Wu, Y., Wu, Y., Tefsen, B., Shi, Y., & Gao, G. F. (2014). Bat-derived influenza-like viruses H17N10 and H18N11. *Trends in Microbiology*, *22*(4), 183–191.
- Wunderlich, K., Mayer, D., Ranadheera, C., Holler, A. S., Mänz, B., Martin, A., ... Schwemmler, M. (2009). Identification of a PA-binding peptide with inhibitory activity against influenza A and B virus replication. *PLoS ONE*, *4*(10), e7517.
- Ying, T., Chen, W., Gong, R., Feng, Y., & Dimitrov, D. S. (2012). Soluble monomeric IgG1 Fc. *The Journal of Biological Chemistry*, *287*(23), 19399–19408.
- Ying, T., Gong, R., Ju, T. W., Prabakaran, P., & Dimitrov, D. S. (2014). Engineered Fc based antibody domains and fragments as novel scaffolds. *Biochimica et Biophysica Acta - Proteins and Proteomics*, *1844*(11), 1977–1982.
- Zambon, M. C. (2001). The pathogenesis of influenza in humans. *Reviews in Medical Virology*, *11*(4), 227–241.
- Zhang, X., Wan, L., Pooyan, S., Su, Y., Gardner, C. R., Leibowitz, M. J., ... Sinko, P. J. (2004). Quantitative assessment of the cell penetrating properties of RI-Tat-9: evidence for a cell type-specific barrier at the plasma membrane of epithelial cells. *Molecular Pharmaceutics*, *1*(2), 145–155.
- Zheng, W., & Tao, Y. J. (2013). Structure and assembly of the influenza A virus ribonucleoprotein complex. *FEBS Letters*, *587*(8), 1206–1214.
- Zou, S. M., Zhou, J. F., Li, Z., Zhu, W. F., Zhang, Y., Wen, L. Y., ... Shu, Y. L. (2011). The proliferation of H1N1 subtype influenza viruses in A549 and BEAS-2B cells. *Chinese Journal of Experimental and Clinical Virology*, *25*(3), 205–207.

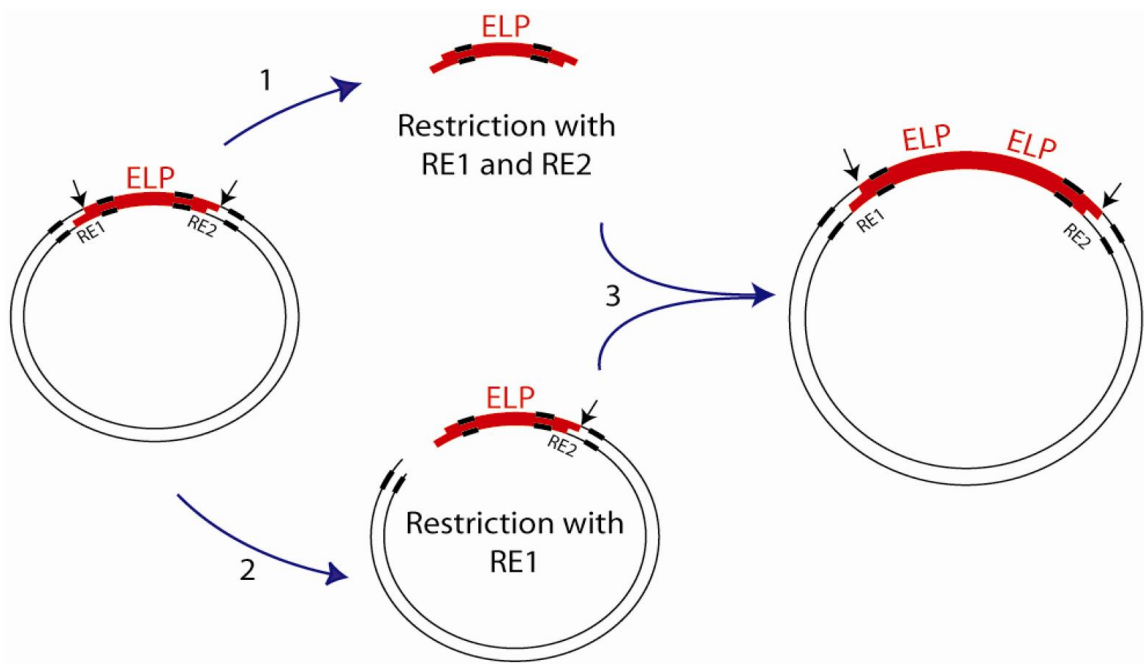
Chapter 6 – Appendix

6.1 Supplementary Figures



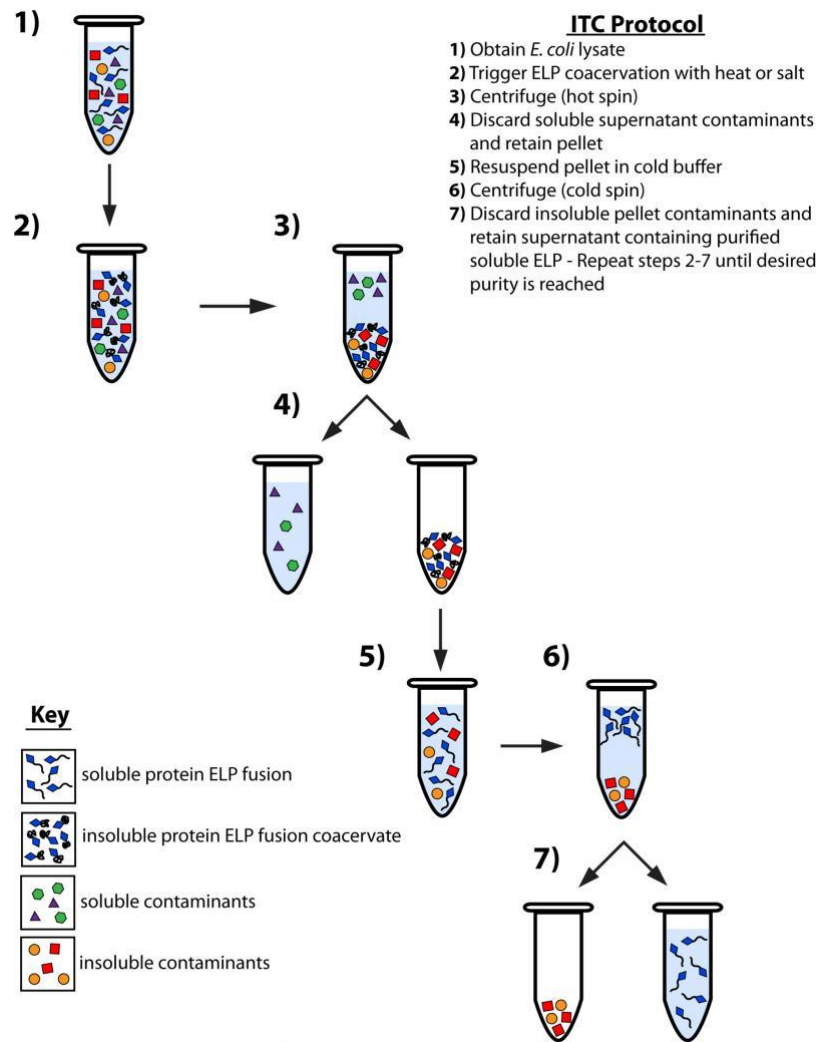
SUPPLEMENTARY FIGURE 6.1 Zhorov Molecular Modelling to Predict Low Energy Binding Mutants at PB1 Position Number 6

To analyze the effect of various mutations at position 6 of PB1 on PA binding, ZMM analysis was used. The crystal structure of the PB1-PA complex was used as a model and the hypothetical free energy of binding was calculated for each possible mutation at position 6. Mutations expected to decrease the free energy of binding and thus bind more readily will have a more negative ligand receptor energy. Two significant mutations which were previously analyzed, T6E and T6R, are outlined on the figure. The modelling was performed by Seji Sugiman-Marangos in 2011 using the McMaster SHARCNET computers. Figure courtesy of Kenneth Mwawasi.



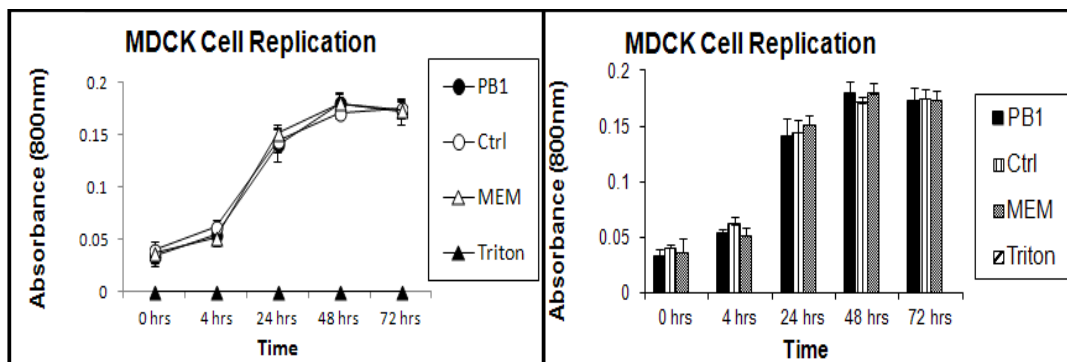
SUPPLEMENTARY FIGURE 6.2 Overview of the Recursive Directional Ligation Process

Recursive directional ligation was used to double the length of ELP repeats. For this thesis, RE1 and RE2 represented the PflMI and BglII restriction sites, respectively. In step 1, plasmid is digested using PflMI and BglII to isolate the insert. In step 2, plasmid is digested with PflMI alone to linearize the plasmid. Finally, in step 3, the two products are ligated together using T4 ligase. Image taken from McDaniel et al. (2010)



SUPPLEMENTARY FIGURE 6.3 Overview of the Inverse Transition Cycling Method to Purify ELP Proteins

To purify the ELP constructs used in this study, ITC was used, which takes advantage of the ELP proteins temperature dependent solubility. To purify the protein, recombinant protein was overexpressed in *E. coli* and a lysate was obtained (1). The soluble ELP in the lysate was forced to oligomerize by the addition of NaCl (2). Oligomerized protein was pelleted via centrifugation (3) and the supernatant containing soluble contaminants was discarded (4). Pelleted protein was resuspended in ice cold PBS (5) and insoluble contaminants were pelleted by centrifugation at 4°C (6). Supernatant containing ELP was retained while the pellet containing contaminants was discarded (7). Steps 2 through 7 represent one round of ITC and this process was repeated 3 – 5 times until pure protein was obtained. Image taken from Hassouneh et al. (2012)



SUPPLEMENTARY FIGURE 6.4 Growth of MDCK cells in presence of HisMBP-NLS-PB1

MDCK cells were seeded to underconfluency into 24 well plates. After 24 hours, cells were treated with MEM, HisMBP-NLS-PB1, a control protein or Triton X-100. At each indicated time point, cells were trypsinized and absorbance of the resuspended cells was read at an optical density of 850nm on a spectrophotometer (Ultrospec 4300 Pro). (a) Results were plotted as a line graph to display growth over time (b) and as a bar graph to compare differences between means. Error bars represent standard error based on three independent experiments. Figure courtesy of Kenneth Mwawasi.

6.2 Supplementary Tables

PCR Product	Forward Primer (5'-3')	Reverse Primer (5'-3')
ELP[A0.2] ₅	ATGCATGCGAATTCATATG GGCCACGGCGTGGGTGTAC CGGGAGTAGGTGTTCCAGG CGCGGGAGTACCGGGGGT	GCATGCATAAGCTTATCAT TTCAGCCCCGCCGGCACGC CTACTCCAGGGACGCCGAC CCCCGGTACTCCCCGCGCC
pUC19 Sequencing	CGTTGTAAAACGACGGCCA GT	AGCTATGACCATGATTACG CC
PB1(T6R)-Tat pET25b(+)	ATGCATGCCATATGGATGT GAATCCGCGGCTTTTATTC CTGAAGGTCCCCGCGCAGA ACGCCATCAGTACAACCTA TGGTC	GCATGCATGAATTCTTATC ACGGCCAGCCCCGGCCCGCT GCGACGGCGTTGACGGCGT TTCTTACGACCATAGGTTG TACTG
PB1(T6R)-Tat- His-Tev pET25b(+)	ATGCATGCCATATGGATGT GAATCCCCGTCTGCTTTTCT TAAAAGTCCCGGCACAGAA CGCGATCAGCACTTAT GGACGTAAAAGCGTCGCC AGCG	GCATGCATGAATTCTTATC ACGGCCAGCCCCGGCCCCGA TTGAAAGTACAGATTTTCG TGATGGTGGTGGTGGTGGG CCCGCCGGCGCTGGCGACG CTTTT

SUPPLEMENTARY TABLE 6.1 List of All Primers Used in This Study

All primers used for cloning in this study are listed. All primers listed except for the pUC19 Sequencing primer are designed as overlapping oligos for overlapping PCR with no template.

<i>E. coli</i> strain	Plasmid Backbone	Gene Insert	Antibiotic Resistance	Recombinant Protein Produced
BL21 (DE3)	pET25b(+)	T6R-NLS-His-Tev-ELP[A0.2] ₄₀	Ampicillin	T6R-NLS-His-Tev-ELP[A0.2] ₄₀
BL21 (DE3)	pET25b(+)	T6R-NLS-ELP[A0.2] ₄₀	Ampicillin	T6R-NLS-ELP[A0.2] ₄₀
BL21 (DE3)	pDestHisMBP	NLS-PB1	Ampicillin	HisMBP-NLS-PB1
BL21 (DE3)	pDestHisMBP	NLS-PB2	Ampicillin	HisMBP-NLS-PB2
Rosetta pLysS	pDest15	PA _{c(257-716)}	Ampicillin	GST-PA _{c(257-716)}
BL21 (DE3)	pGEX-4T-1	None	Ampicillin	GST

SUPPLEMENTARY TABLE 6.2 Expression Strains Used in This Study

All recombinant *E. coli* used in this study was grown in 100 µg/mL ampicillin